2-9-2011

Studies on Group 10 Pincer Carbene Metal Complexes

Agnes Mrutu

Follow this and additional works at: https://digitalrepository.unm.edu/chem_etds
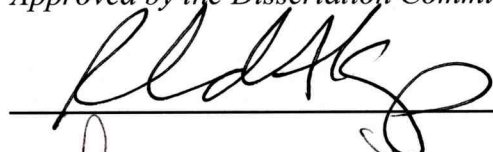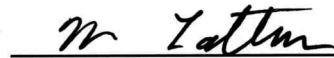
Agnes Mrutu

Candidate

Chemistry and Chemical Biology
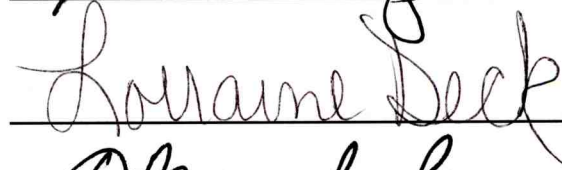
Department

This dissertation is approved, and it is acceptable in quality
and form for publication:

Approved by the Dissertation Committee:

_____, Chairperson

Lorraine Deck

_____

_____

M Tatten

_____

_____

_____

_____

_____

STUDIES ON GROUP 10 PINCER CARBENE METAL COMPLEXES

BY

AGNES MRUTU

B. Sc., Education, University of Dar Es Salaam, 2000

M. Sc., Environmental Science, University of Dar Es Salaam, 2002

DISSERTATION

Submitted for Partial Fulfillment of the

Requirement for the Degree of

Doctor of Philosophy

Chemistry

The University of New Mexico

Albuquerque, New Mexico

December 2010

ACKNOWLEDGEMENT

STUDIES ON GROUP 10 PINCER CARBENE METAL COMPLEXES

BY

AGNES MRUTU

ABSTRACT OF DISSERTATION
Submitted for Partial Fulfillment of the
Requirement for the Degree of

Doctor of Philosophy

Chemistry

The University of New Mexico

Albuquerque, New Mexico

December 2010

Studies On Group 10 Pincer Carbene Metal Complexes

Agnes Mrutu

B.Sc., Education, University of Dar Es Salaam, 2000

M.Sc., Environmental Science, University of Dar Es Salaam, 2002

Ph.D., Chemistry, University of New Mexico, 2010

ABSTRACT

Selective oxidation chemistry is a topic of intense interest worldwide, in particular when using molecular oxygen (O_2) directly as the oxidizing species. The primary reason for using O_2 rather than other oxidants is to take advantage of the inexpensive nature of oxygen; however, the radical ground state of O_2 leads to non-selective reactions with organic substrates. As such, basic knowledge and understanding involving the fundamental reactions of O_2 with organometallic species will be required in order to overcome this lack of selectivity. The work presented in this dissertation has two main research goals to help address this issue. First, we have synthesized and characterized a number of various pincer-carbene containing Ni and Pd hydrides. We have postulated that these species might function as homogeneous catalysts to deliver O atoms to various organic or inorganic substrates. Second, we are interested in demonstrating the reactions of these carbene complexes with O_2. As both the precursors and O_2 reaction products of carbene-pincer complexes have been studied only briefly previously, we anticipated that our studies would add to the fundamental understanding of these complexes.

Specifically, syntheses and characterization of novel pincer carbene Pd-H complexes was achieved. The pincer carbene Pd-H complex proved reactive with O_2; however, the isolation of a discrete Pd-OOH species was unsuccessful. Investigation of

the oxygen transfer ability of these complexes was done through *in situ* reaction of Pd-H species, O_2 and organic substrates. However, there was no evidence indicating oxygen transfer to the organic substrates.

New pincer carbene Pd and Ni complexes were prepared and characterized through alternative routes to M-H or M-OOH. Although none of these routes led to isolation of M-OOH species, ^{Me}CCC-Pd-OTf reacted with H_2O_2/H_2O to form ^{Me}CCC-Pd-OH. Further investigation on this reaction suggested that the desired Pd-OOH species may initially be formed which slowly decomposed to the Pd-OH species.

Attempts to prepare carbene pincer Ni-H complexes and their precursors via a variety of routes resulted in several novel reaction products. We have prepared and structurally-characterized the first example of a unique dinuclear Ni compound containing ^{Me}CNC ligands in both bridging and chelating modes. As well, we have obtained a new 3-dimensional Ag-carbene coordination polymer obtained through a novel reverse transmetallation. This result is only the second case in which carbene transfer from Ni^{2+} to Ag^+ is observed.

TABLE OF CONTENTS

TABLE OF SCHEMES

LIST OF FIGURES

LIST OF TABLES

LIST OF ABBREVIATIONS

MTBE	methyltertiarybutylether
m-CPBA	meta-chloroperoxybenzoic acid
COE	cyclooctene
COD	cyclooctadiene
D*i*PP	2,6-diisopropylphenyl
GC/MS	gas chromatography-mass spectrometry
THF	tetrahydrofuran
M	metal
m	meta
i	ipso
o	ortho
p	para
s	singlet (NMR)
t	triplet (NMR)
ppm	parts per million
*t*Bu	*tert*-butyl, -C(CH$_3$)$_3$
*i*Pr	isopropyl, -CH(CH$_3$)$_2$
cy	cyclohexyl, -C$_6$H$_{11}$
NMR	nuclear magnetic resonance
MMPP	magnesium salt of monoperoxyphthalic acid
PO	propylene oxide
EO	ethylene oxide
BME	butadiene monoepoxide
BDE	butadiene diepoxide
NHC	N-Heterocyclic Carbenes
FW	formula weight
TON	turnover number
AcOH	acetic acid
HOCl	hypochlorous acid
HOBr	hypobromous acid
NaOMe	sodium methoxide
NaO*i*Pr	sodium isopropoxide
R	organic substituent
DMSO	dimethylsulfoxide
D	deuterium
Ph	phenyl

1   CHAPTER ONE

1.1   Introduction

When taking a close look at the process routes for all primary and intermediate products in the chemical industry, one can easily realize that more than 80% of the products involve at least one catalytic reaction step. It is estimated that the application of catalysis is responsible for approximately 18-25% of the gross domestic product of the United States.[1] Therefore, catalysis can be considered as the key enabling technology of chemical industries, and as such is linked to great innovative potentials.[1] It is also noted that while in recent times homogeneous and biocatalysts have become increasingly important, heterogeneous catalysts remain the most dominant in technical production of primary and intermediate chemicals.[1] Even more specifically, despite the fact that epoxidation of alkenes using oxygen is important, there is a major lack of fundamental knowledge on how oxidation catalyst systems, particularly homogeneous ones, function in a mechanistic sense and how molecular oxygen can be effectively utilized in selective partial oxidation.

Simple epoxides, *e.g.*, ethylene- and propylene oxide (EO and PO), are important intermediates in industrial production of various chemicals. Large-scale production of EO is carried out through heterogeneous gas-phase oxidation using a supported silver catalyst. In the case of propylene, the same oxidation reaction parameters result almost entirely in total combustion, giving CO_2 and H_2O. Considering the economical importance of PO and the disadvantages of currently established production routes (chlorohydrin-process, bi-product process involving peroxo-species), the idea of discovering a new method of direct oxidation of propylene has been of high interest in both the industrial and academic communities. Even though many new ideas have been previously suggested, limited progress towards new industrial production routes to PO has been attained. These routes generally do not involve new chemistry, but rather process improvements, such as building a H_2O_2 plant near a PO production facility for safety reasons, as explained in more detail in Section 1.2.1. As of today, epoxidation of alkenes using molecular oxygen via catalytic process remains a challenging subject in the field of oxidation chemistry.[1] The goal of this investigation thus involves an attempt to gain basic knowledge on how partial oxidation catalyst systems, particularly homogeneous ones, function in a fundamental sense. To achieve this goal it was necessary to synthesize a number of possible catalyst precursors. For this reason it appeared reasonable to examine how molecular O_2 can be effectively utilized in selective oxidation of alkenes to form epoxides. Although the ultimate target of the project is concerned with partial oxidation of alkenes to form epoxides, investigation on partial oxidation of other organic substrates was also performed. As has been noted before, homogeneous catalysts are becoming increasingly more important of late, and developing

2

homogeneous catalysts for partial epoxidation of alkenes is one aspect of this dissertation project.

Phosphine pincer ligands have been widely utilized over the past several years since the initial report by Moulton and Shaw in 1976.[2,3] Additionally, nitrogen-stabilized carbenes have attracted considerable attention as possible alternatives for phosphine ligands. Although the potential advantages of carbene ligands over phosphine ligands will be discussed in more detail in Section 1.4, one major advantage of these ligands appears to be that they do not dissociate easily from metal centers and as a result an excess of the ligand is not required in order to prevent aggregation of catalyst molecules.[4] Related to the use of phosphorus or nitrogen donor atoms in pincer chemistry is the use of stabilized N-heterocyclic (NHC) organic carbenes as the donor sites. The use of NHC's or carbene-based pincer ligands will be the primary focus in the synthetic portion of this research.

1.2   Epoxidation of Alkenes

Selective catalytic oxidation of hydrocarbons, including alkenes, using molecular oxygen is exceedingly complex and represents a "Holy Grail" in the field of oxidation chemistry.[5] This moniker not only indicates the difficulty in achieving success but also the paramount importance and benefits if such methodology in selective oxidation is discovered. By selective oxidation, we mean preferential attack by one oxygen atom upon one of the components in an organic material, resulting only in the formation of the desired product and not a number of side products.

1.2.1   Preparation of Epoxides

Three major categories of peroxides used for preparation of epoxides include hydrogen peroxide (H_2O_2), alkyl hydroperoxide (ROOH), and peroxyacids (RC(O)OOH). Peroxides are a source of electrophilic oxygen and react with the nucleophilic π bond of an alkene.[6] It should be noted that most peroxide reactions can also involve homolytic cleavage of the O-O bond, thus generating reactive free radicals.[7] Homolytic cleavage involves the breaking of single bond (two electrons) in which one electron is transferred to each of the atoms.[6] H_2O_2 reacts with alkenes mostly in a concerted or ionic manner.[7] Generally, an alkene (acting as a Lewis base) coordinates with the electrophilic oxygen of a peroxide as in Scheme 1.1, generating a positively-charged dioxygen. This is followed by heterolytic cleavage that transfers that oxygen to the alkene and a proton transfer that liberates the by-product (water from hydrogen peroxide, an alcohol from alkyl hydroperoxide and carboxylic acid from a peroxyacid). This reaction involves an S_N2 process.[7]

Scheme 1.1 Epoxidation using R-OOH
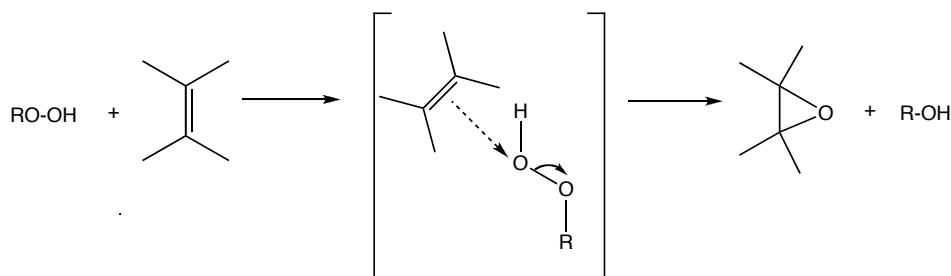
Hydrogen peroxide is largely used as the oxidizing agent for many organic and inorganic compounds. Hydrogen peroxide (H_2O_2) as oxidant on the small-scale is quite appealing, both in terms of atom efficiency and from an environmental point of view. However, the solubility of H_2O_2 in organic solvents hinders its efficiency and ultimate potential. H_2O_2 is used in water or water-miscible solvents. In addition, epoxidation using H_2O_2 is slow unless metal ion catalysts are also used. Common catalysts used together with H_2O_2 include molybdenum trioxide,[8] tungsten trioxide,[9,10] vanadium pentoxide[11] titanium silicate-1 (TS-1),[12] and tungsten oxide-containing titanium silicate (WO_x/TS-1).[13] Thus, H_2O_2 is commonly used in preparation of peroxyacids and alkyl peroxides from carboxylic acids and tertiary peroxides. Unfortunately, on large scales the use of H_2O_2 as oxidants becomes not only expensive due to costs associated with its preparation, but also there are technical safety concerns to be considered. To partially mitigate the costs associated with transportation of H_2O_2, a H_2O_2 plant can be built very close to the production facility of epoxides. A very good example of this approach is a PO facility that has recently been announced to be built in Thailand by Dow and Solvay.[14] Despite these shortcomings, H_2O_2 is still a preferred oxidant in many industries as it does not create hazardous waste forming water as a by-product. Hence, it can be considered environmentally-friendly.

In general, alkyl hydroperoxides can be prepared by reaction of tertiary alcohols or alkenes with H_2O_2 in the presence of sulfuric acid[15] as well as by the autoxidation of alkenes and alkanes (Scheme 1.2) with oxygen (O_2).[16] Tertiary hydroperoxides are used often as oxidizing agents with alkenes because primary or secondary alkyl hydroperoxides are susceptible to rearrangement and decomposition.[6] Another advantage

of alkyl hydroperoxides is that they are relatively soluble in organic solvents, an advantage over H_2O_2.[6] Moreover, the alkylperoxides are easier and safer to handle than hydrogen peroxides.[17] It is worth noting that commercially PO is prepared primarily using this route, as shown in Scheme 1.2. Ethylbenzene can also be used instead of isobutane, and eventually will generate styrene as a co-product. However, in an industrial setting, any process that requires a co-product is less desirable (and less efficient) than one that does not. The *t*-Butyl alcohol produced as the undesired co-product must be utilized to make the process attractive. *t*-Butyl alcohol is primarily used to prepare methyltertiarybutylether (MTBE), a gasoline additive. However, due to environmental problems with MTBE, there is a reduced commercial need for *t*-Butyl alcohol. Thus, it would be very useful commercially, and academically quite interesting, to utilize more atom efficient reactions to produce higher alkene epoxidations. As mentioned above, it is also possible to use ethylbenzene as the starting organic species, eventually generating styrene as a co-product rather than *t*-Butyl alcohol in a process developed by Shell.[18]

Scheme 1.2 Commercial Routes to PO
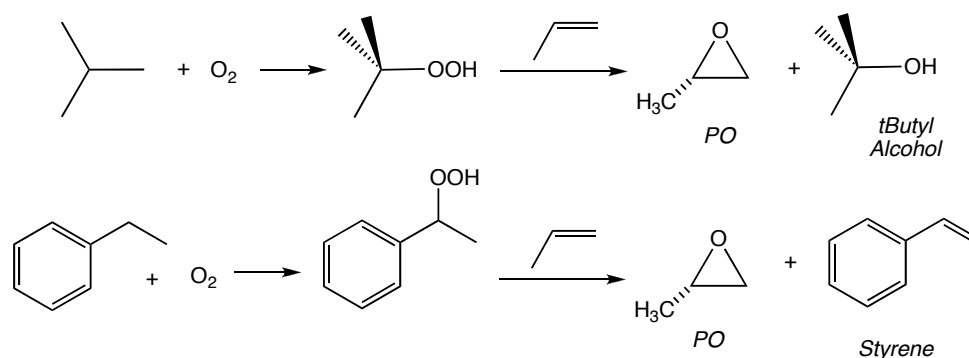
Traditionally, epoxides are prepared in the laboratory by direct oxidation of alkenes with peroxycarboxylic acids. The oxidizing agent in Scheme 1.3, *meta*-chloroperoxybenzoic acid (*m*-CPBA), is an excellent example of a peroxycarboxylic acid. A peroxycarboxylic acid is a carboxylic acid that contains an -OOH (hydroperoxy) group rather than an –OH (hydroxy group).[19,20] While many peroxycarboxylic acids are unstable, they can be generated *in situ* prior to use by mixing the carboxylic acid and H_2O_2. The major advantage of using peroxyacid is the rapid epoxidation of unfunctionalized alkenes in high yields, albeit stoichiometrically rather than catalytically. These alkenes are normally unreactive with H_2O_2 or alkyl peroxide, even in the presence of transition metal catalysts.[21] Although the crystalline solid nature of *m*-CPBA makes it easy to ship commercially and be stored in the laboratory, *m*-CPBA can explode if not handled carefully. Alternatively, the magnesium salt of monoperoxyphthalic acid, MMPP in Figure 1.1 can be used as an oxidant instead of *m*-CPBA as it is less hazardous but has essentially the same reactivity as *m*-CPBA.[20]

Scheme 1.3 Oxidation of Alkenes with Peroxycarboxylic Acids

meta-chloroperoxybenzoic acid   Benzene   *meta*-chlorobenzoic acid
                                          25 °C
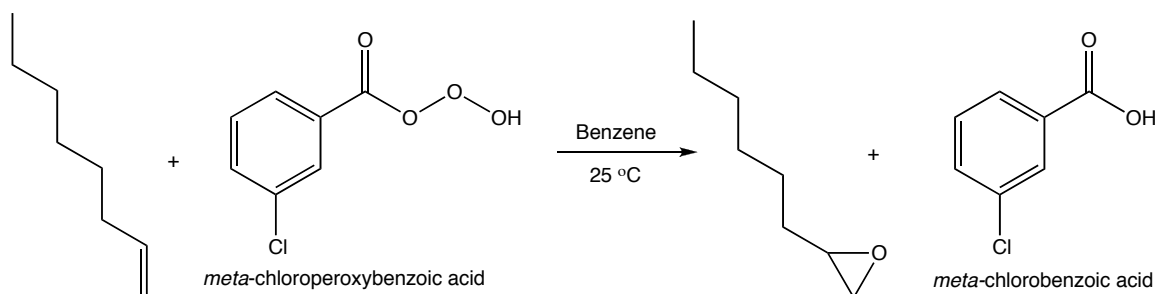
Figure 1.1 Magnesium Monoperoxyphthalate (MMPP)
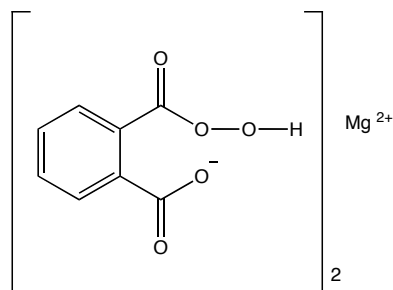
Epoxides can also be prepared by treatment of halohydrins with base (Scheme 1.4). This reaction is an intramolecular variation of the Williamson ether synthesis.[6,20] A halohydrin can be obtained by reaction of an alkene with hypohalous acid (HOCl or HOBr).[6] The halohydrin obtained through this route is *trans*, or anti-halohydrin.[6] Alkoxide anion is formed reversibly by reaction of the alcohol with a base such as NaOH that displaces halide ion from the neighboring carbon. The *anti*-orientation allows displacement of the halide to give an epoxide through an S_N2 mechanism.[6,20] Currently, the chlorohydrin route is a minor production route of PO used by The Dow Chemical Company. There are some environmental implications that limit the utilization of this route, with the primary concerns being the large quantities of acid that are utilized and the large quantities of waste salts that are produced per pound of PO produced.

Scheme 1.4 Cyclization of Halohydrins[20]

1-bromo-2-methylpropan-2-ol   2,2-dimethyloxirane

"A Halohydrin"
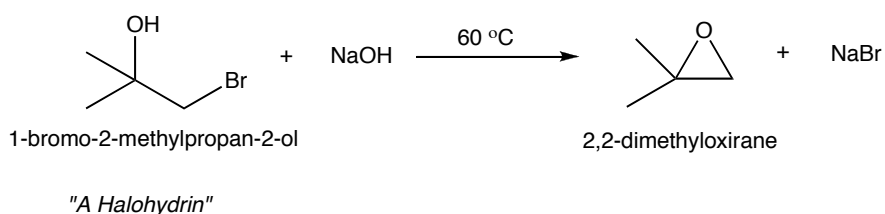
Molecular oxygen is very abundant, as it constitutes about 21% of the content of air in the atmosphere. At standard temperature and pressure, oxygen is a colorless gas with molecular formula O_2 in which the two oxygen atoms are chemically bound together with a spin triplet electron configuration in the ground state.[20] O_2 could be a perfect oxidant but for the fact that molecular oxygen in its triplet state reacts only very slowly with hydrocarbons and consequently this hinders its direct use in oxidation of hydrocarbons, as the more forcing conditions needed for reaction can lead to non-selective reactions.[4,22] As a result of this, O_2 needs to be activated to be most effective. When simple hydrocarbons interact with O_2, the reaction proceeds through free radical chain autoxidation as illustrated in Scheme 1.5.[22] Commonly, initiators are deliberately added to create radical species, however, it is reported that very small amount of impurities can also trigger this reaction.[23]

Scheme 1.5 Autoxidation of Hydrocarbons[22]

Initiation

$$In_2 \xrightarrow{R_1} 2\ In\bullet$$

$$In\bullet\ +\ RH \longrightarrow InH\ +\ R\bullet$$

Propagation

$$R\bullet\ +\ O_2 \longrightarrow RO_2\bullet$$

$$RO_2\bullet\ +\ RH \xrightarrow{k_p} RO_2H\ +\ R\bullet$$

Termination

$$R\bullet\ +\ RO_2\bullet \longrightarrow RO_2R$$

$$2\ RO_2\bullet \xrightarrow{2k_t} RO_4R \longrightarrow \text{Non-radical product}\ +\ O_2$$
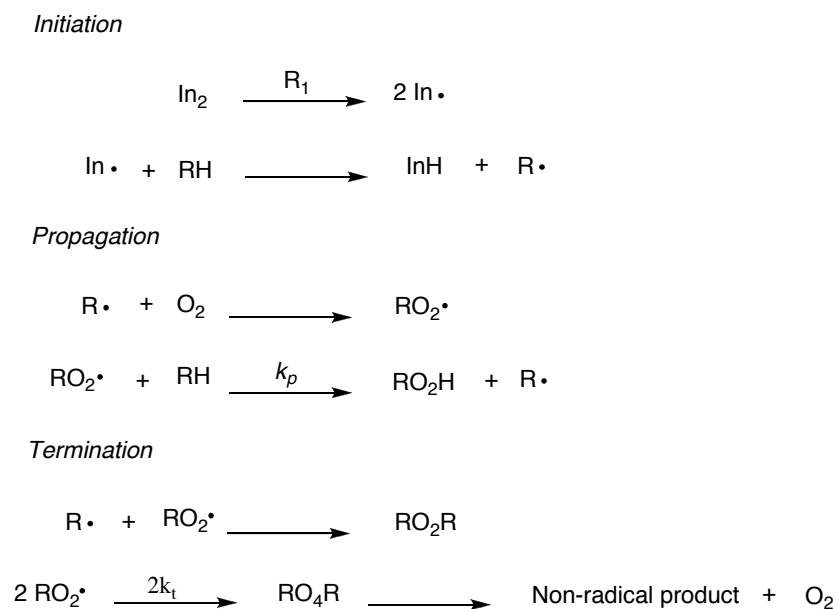
It is worth noting that the initial studies were geared towards preventing

autoxidation. From these studies it was discovered that the controlled oxidation of

hydrocarbons can lead to the production of a variety of oxidized hydrocarbons.[22] In

1944, Hock and Lang developed a commercial route of producing phenol and acetone

from cumene by using O_2 as shown in Scheme 1.6.[23] Another catalyzed industrial route

to oxidized organic compounds that utilizes O_2 as the only oxidant is the Wacker

process.[24] The role of O_2 in the Wacker process is that of proton/electron acceptor as it

facilitates reoxidation of the palladium catalyst through a copper co-catalyst in the

conversion of ethylene to acetaldehyde.[24] In a recent review by Stahl, this type of

oxidation is described as an oxidase-type oxidation reaction.[24] Other industrial oxidation

processes are essentially oxygenase-type oxidation reactions (explained below).

Noteworthy, DuPont is the largest user of O_2 in the commercial production of maleic acid

from butane.[25]

Scheme 1.6 Conversion of Cumene to Phenol and Acetone by O_2
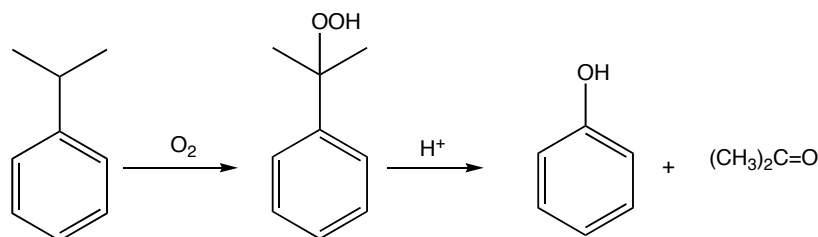
The major difference between the two classes is the fate of oxygen atom from the

molecular oxygen. In an oxygenase-type oxidation, the oxygen atom transfers from

molecular O_2 to the organic substrate, oftentimes through a high valent metal-oxygen

intermediate. In an oxidase pathway, as explained earlier in Wacker process, O_2 acts as electron/proton acceptor in organic substrate oxidation, and no oxygen-atom transfer to the organic substrate occurs.[24]

A very good example of oxygenase-type industrial oxidation mediated by transition metals is that of epoxidation of ethylene and 1, 3-butadiene to produce ethylene oxide (EO) and butadiene monoepoxide (BME) in the presence of molecular O_2. These processes use heterogeneous Ag-based catalysts on low surface area α-Al_2O_3 supports as indicated in Scheme 1.7.[26] In this route, the addition of promoting amounts of modifiers such as alkali metal salts, organic chlorides and transition metal oxoanions has increased the selectivity of EO in the commercial reactors to ~90% based on ethylene.[26-34]

Scheme 1.7 Direct Epoxidations Using Heterogeneous Catalysts[26]
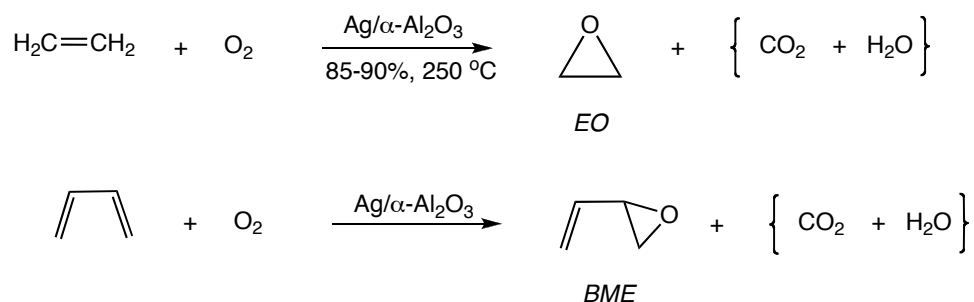
However, as pointed out earlier in the Introduction, simple alkenes such as propylene which possess allylic hydrogens cannot be directly epoxidized using O_2 and a Ag-based heterogeneous catalyst. [35] [36] Total combustion of propylene to CO_2 and H_2O occurs rather than producing the desired PO, as shown in Scheme 1.8. This is believed to be due to a long-lived allylic radical or anion that is formed and stabilized by the Ag surface, leading

eventually to total combustion products rather than the epoxide.[37] This can be attributed to the fact that the allylic C-H bond strength in propylene is approximately 77 kcal/mole while the bond strength of a vinylic C-H bond in ethylene is about 112 kcal/mole, thus favoring C-H attack over O-atom transfer.[38]

Scheme 1.8 Attempted Epoxidation of Propylene
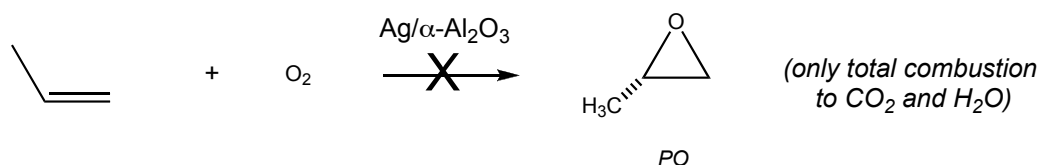
There have been efforts over the past few years to produce PO directly with O_2 using heterogeneous Ag catalysts, Ag/Au catalysts, or Au catalysts and molecular H_2.[39-47] However, none of these systems has led to sufficient understanding to give a successful breakthrough. It is worth noting, however, that these systems studies have been very important for the fundamental knowledge gained in the study of these reactions on solid surfaces. There have also been attempts to produce PO via homogeneous routes based on heteropolyacids,[48] europium salts,[31,49] or directly using ozone as oxidant.[50] As well, these attempts suffer greatly due to selectivity, conversion, and/or lifetime issues on the catalysts.

Essentially all the routes to epoxides discussed in this section have some shortcomings either by producing undesired products, issues with selectivity, or expense. Thus, it would be very useful commercially to utilize more atom-efficient reactions to produce alkene epoxides. More importantly for this work, it would be of interest to explore fundamentally the preparative chemistry of a homogenous, organometallic-based route to

12

partial oxidation catalysts. For this reason we proposed a possible catalytic cycle that will utilize O_2 as oxidant.

1.3   Proposed Catalytic Cycle for Making Epoxides

The two cycles shown in Scheme 1.9 have been proposed as possible routes to selective alkene oxidation using O_2 as the oxidant. Key to the design of these cycles is the identification of an efficient means of activating molecular oxygen for the subsequent reaction with the alkene. Recent work, including a study from the Goldberg and Kemp groups, has documented the direct reactions of metal hydrides (specifically Pd^{2+}) with O_2 to form metal hydroperoxide species.[51] This type of reactivity is particularly promising for our purposes as a number of alkene oxidations are proposed to proceed via metal hydroperoxide intermediates. The two cycles shown in Scheme 1.9 are characterized by identical steps leading up to alkene oxidation. The postulated cycle begins with a pre-formed metal hydride M-H **1** inserting O_2 to form a metal hydroperoxide, M-OOH **2**. The next step in the proposed cycle is transfer of one of the oxygen atoms to an organic substrate from the metal hydroperoxide, resulting in an oxidized organic substrate and metal hydroxide, M-OH **3**. The cycles then diverge in the possible regeneration of the metal hydride catalyst from the metal hydroxide. In one path, carbon monoxide (CO) inserts into the metal hydroxide bond to form a metal hydroxycarbonyl species, M-COOH **4a**. The metal hydride would then be regenerated upon the thermodynamically-favored release of carbon dioxide (CO_2).

Scheme 1.9 Proposed Catalytic Cycles for Making Oxidized Substrate
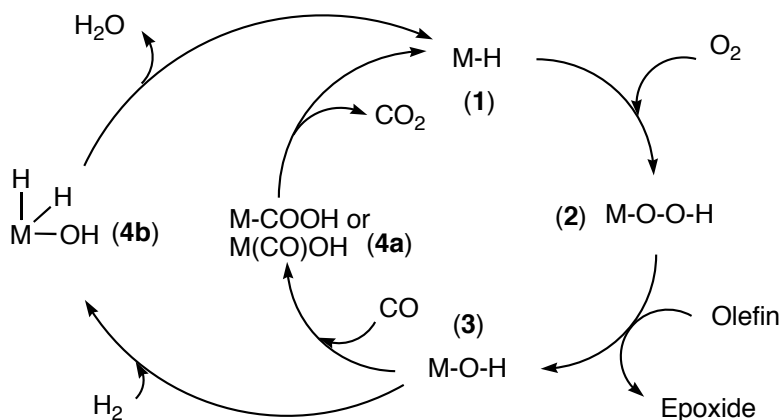
Both of these reactions, insertion of CO into a M-OH bond and decarboxylation of

M-COOH, have been reported in the literature for late transition metal systems.[52]

However, a possible problem with this route is the undesired re-insertion of CO_2 into the

newly-formed M-H bond to generate a metal formyl complex. Johansson and his group

observed this type of reactivity when they reacted ^{tBu}PCP-Pd-H **5** with CO_2 in which they

produced a palladium formate complex instead of palladium hydroxycabonate complex.[52]

Therefore, we were interested in finding alternatives to CO. An alternative regeneration

cycle proposed adds H_2 via an oxidative addition reaction to the metal hydroxide,

resulting in intermediate **4b**. Subsequent release of the thermodynamically-favored water

product allows regeneration of the metal hydride. Again, there is precedence in the

literature of each of these individual steps in the late transition metal chemistry. As well,

the reaction step to generate water would not be reversible.

M-H complexes are known for every transition metal beginning in 1930 with the

discovery of the unstable hydridocarbonyls, $H_2Fe(CO)_4$ and $HCo(CO)_4$.[53] Transition

metal hydrides have long been recognized as intermediates or catalysts in reactions such as hydroformylation, olefin isomerization, and hydrogen exchange.[54] Fortunately for our purposes the general preparative chemistry of metal hydrides is well-developed and can serve as useful background material. However the reaction chemistry of these M-H complexes with O_2 is much less developed. It is worth noting that M-OOH complexes have primarily been prepared by using hydrogen peroxide (H_2O_2), and only a few M-OOH complexes have been prepared by the direct insertion of O_2 into M-H bonds. In this project we are interested in using the middle to late transition metals as possible catalysts due to the less oxophilic nature of these metals. This lowered oxophilicity should avoid the thermodyanamically-driven formation of metal oxides as can be observed in early transition metals. This is particularly relevant to our proposed cycle in that we must regenerate a M-H complex (species **1**) from a M-OH complex (species **3**) and so the M-O complex cannot be so stable as to not allow this reaction to occur. The insertion of O_2 directly into a metal hydride bond (conversion of **1** to **2** in Scheme 1.9 has previously been reported in cobalt, rhodium, iridium and platinum systems.[51,55-57]

Scheme 1.10 Reaction of ^{tBu}PCP-Pd-H with O_2[51]
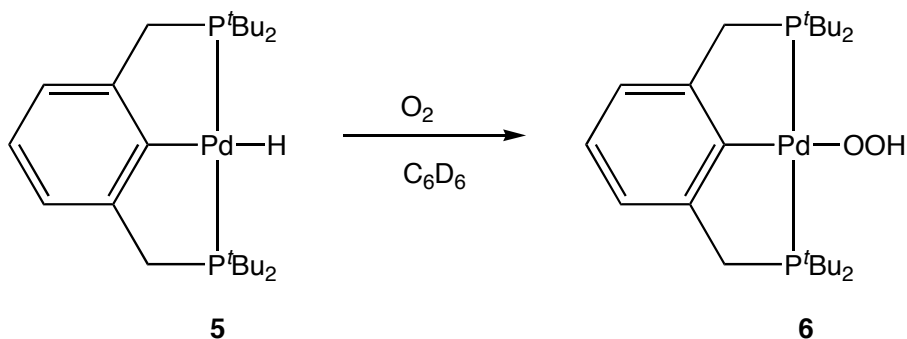
It is also noteworthy in this regard that the reactivity of O_2 and Pd-H recently reported by

Goldberg and Kemp constitutes the first unambiguous example of direct oxygen

reactivity at Pd^{2+}, and is shown in Scheme 1.10.[51] ^{tBu}PCP-Pd-OOH was formed by

reaction of the pincer complex ^{tBu}PCP-Pd-H with O_2 at 70 psig. This result supports a

different mechanism than the radical pathways proposed for similar reactions at Pt^{2+} and

Pt^{2+} centers. [55-57] ^{tBu}PCP-Pd-OOH **6** in Figure 1.2 was completely characterized by ^{1}H

NMR, ^{31}P NMR, and by single crystal X-ray diffraction.

Our group's collaborators at Sandia National Laboratories and the California

Institute of Technology performed density functional theory (DFT) computational studies

to examine the mechanism involved in O_2 insertion into Pd-H.[58] Their results resulted in

the proposed mechanism shown in Figure 1.3. In the proposed mechanism, PCP-Pd-H

reacts with triplet O_2 to form a weakly bound van der Waals complex with O_2 attaching to

the hydride and not directly to the metal.

Figure 1.2 X-Ray Structure of (^{tBu}PCP)PdOOH[59]
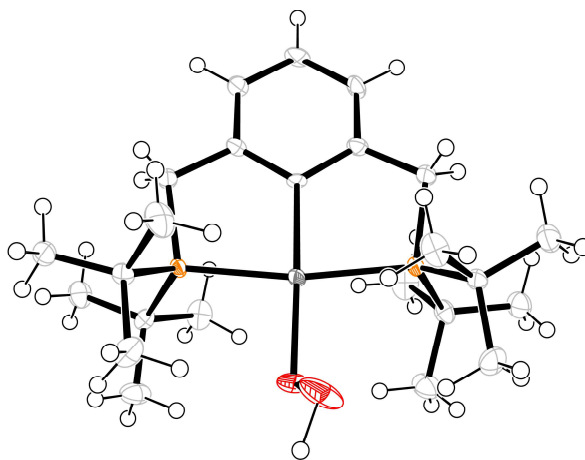
Computational attempts to initially interact O_2 with the metal center in a direct fashion failed, and this can be attributed to unfavorable interactions between the electron-rich oxygen molecule and the filled d orbitals on the metal. From intermediate **2** in Figure 1.3 the O_2 insertion mechanism proceeds to transition state TS1 ($\Delta H^\ddagger = 12.9$ kcal/mol) in which the triplet O_2 abstracts the hydrogen from the palladium center, resulting in a shorter O-H bond distance. From this point the reaction proceeds to intermediate state **3**, a triplet species Pd^+ T-complex (which is a radical at palladium center) with a closely associated HO_2 radical. The calculated O-H bond length of 1.01 Å is similar to that calculated for free HO_2, and the lengthened Pd-H bond distance of 2.36 Å signifies complete bond breakage. The Pd^+ T-complex has an overall ΔH of 8.2 kcal/mol. HO_2 coordinates to palladium in an agostic fashion in which one of the spins resides on palladium in an orbital previously bonded to hydrogen. The singlet η^1-hydroperoxo palladium(II) product **4** is then achieved by rotation of the HO_2 fragment in a triplet-singlet conversion through the minimum energy crossing point (MECP1), also shown in Figure 1.3. This triplet-single conversion has a calculated ΔH of -27.3 kcal/mol. Computationally, the triplet version of η^1-hydroperoxo Pd^{2+} can possibly occur, although at such high energy it would be expected to have a significantly short life. By using the method of Harvey and co workers[60-62] it was possible to establish the MECP1 between the singlet and triplet potential energy leading to the final product.

Figure 1.3 DFT Calculations for Mechanism for O$_2$ Insertion[58]
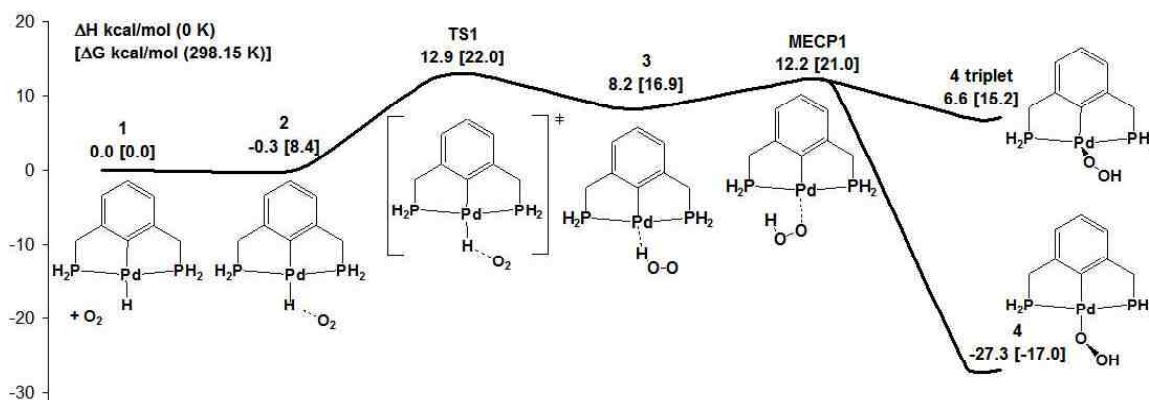
The MECP1 has a calculated ΔH of 12.2 kcal/mol. In their computational studies, these authors also considered a dissociative process in which the PCP-Pd and -OOH moieties separate in the solution of radical species. Computationally, reassociation with a radical of the appropriate spin could then generate the singlet **4** because of the fact that the dissociative process is less favored than the concerted process. The calculated ΔH for this process was found to be 13.1 kcal/mol. However, the ΔG is uncertain, therefore it cannot be concluded that it is a preferred mechanism. In order to ascertain whether their computational results were realistic, the authors studied various possible ligand formations as illustrated in Figure 1.4, so as to rule out the possibility that O$_2$ inserts through Pd^0 pathways. Ligand deformation species **5** was found to be the product of intramolecular reductive elimination of the hydride with the neighboring phosphorus atom; however, this species was not found despite many trials. Instead, it collapsed to either **7** or **8**. Noteworthy, **6** was found to be a stable linear Pd^0 species with calculated ΔH of -14.7 kcal/mol.

18

Figure 1.4 Potential Candidates Examined Along the Theoretical Pd^0 Pathway[58]

5   6   7   8
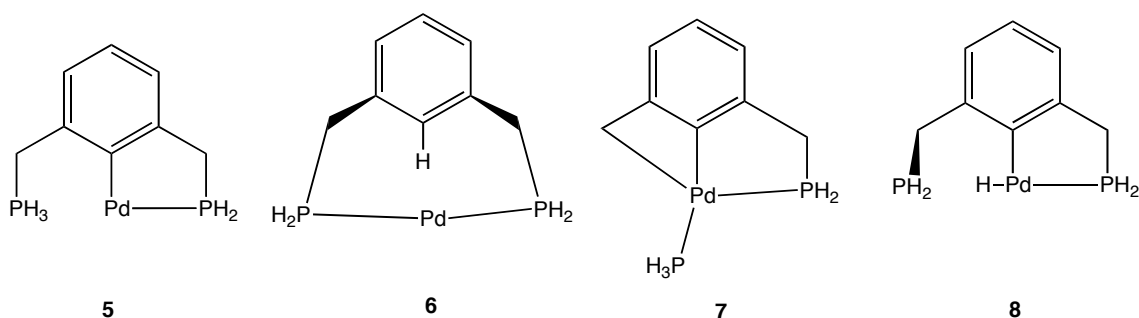
1.4   Pincer Ligands

Pincer ligands are tridentate 6e$^-$ chelating agents that generally bind to a metal in a co-planar fashion, and this topic has been the subject of several reviews and a recent monograph.[63,64] There is a wide variety of pincer ligands, varying in both backbone structure as well as donor atoms, and these donors can include carbene, phosphorus, nitrogen, and sulfur-based ligands as shown in Figure 1.5. As is traditional, these ligands are abbreviated by the combination of atoms that are bound to the metal as shown in Figure 1.5. Fortunately, it appears that essentially all pincer metal complexes display pronounced stabilities toward high temperatures, relatively-high tolerances towards O_2, and increased water stabilities due to the chelate effect when compared to their monodentate analogues. It should be noted that the possible modifications of electronic and steric factors on pincer ligands that can be envisioned are virtually limitless. As a result of this functionality, a wide range of pincer-ligated transition metal complexes have been prepared.

Figure 1.5 Forms of Pincer Ligands

Carbene-Based Pincer Ligands

X, C, N

CNC **7** or CCC **8**

CNC **9** or CCC **10**

PCP **11**
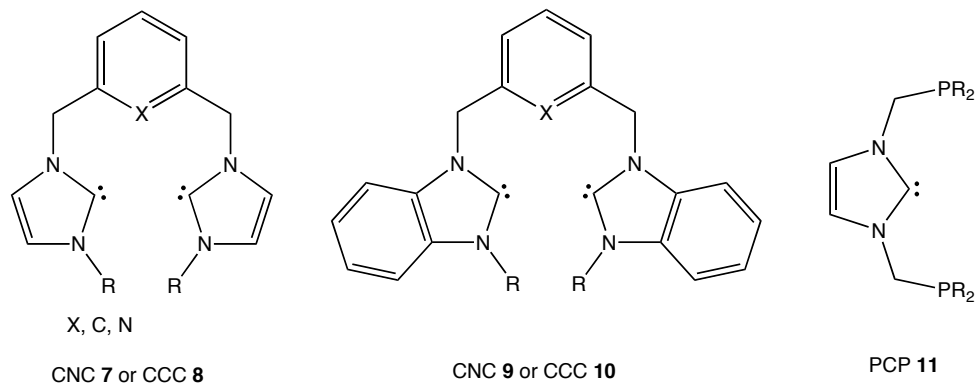
Phosphorus-Based Pincer Ligands

Anthracene PCP
12

Ozerov PNP
13

Phosphinito PCP
14

X = C, N

PCP **14** or
PNP **16**
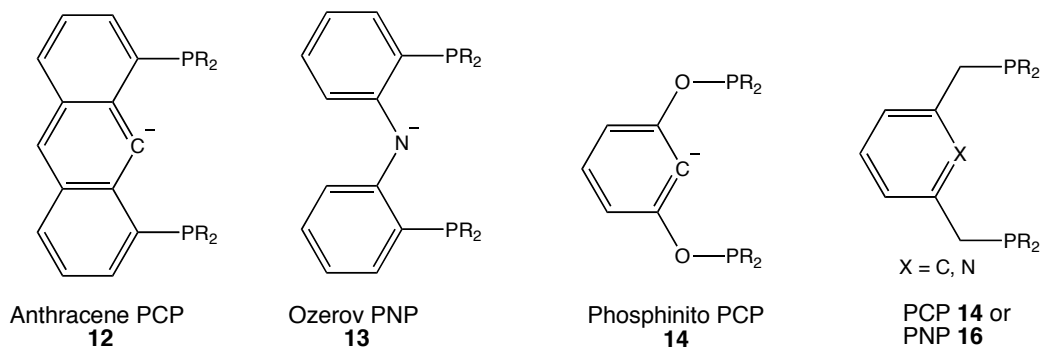
Sulfur and Nitrogen-Based Pincer Ligands

SCS **17**

NCN **18**
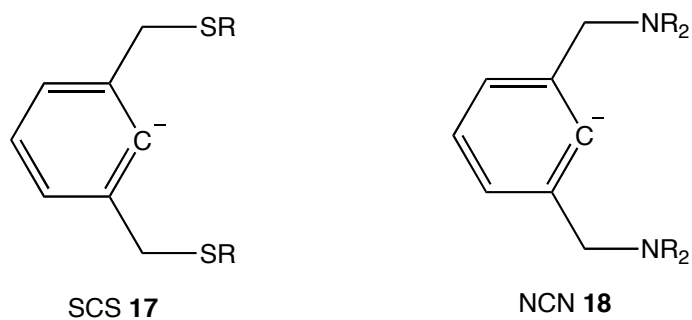
One major advantage of the pincer ligand system is that due to prior successful

applications of such ligands in numerous catalytic transformations, sufficient literature

exists on making modifications to the pincer ligand and ligand precursors. The electronics

are largely influenced by the nature of the X groups, the bridge atoms, and Y group on the

aryl or pyridyl ring (Figure 1.6). The X-group can be donor atoms such P, S, N, or carbene.

Changing R groups attached to X can easily modify the sterics around the metal center.

Figure 1.6 Pincer Ligand Modification

Bridge: none, -CH$_2$-, -CRR'

M - Ir, Ru, Rh, Ni, Pd, Pt

Y: C, N, P (changes charge on ligand)

R: Size, electronics
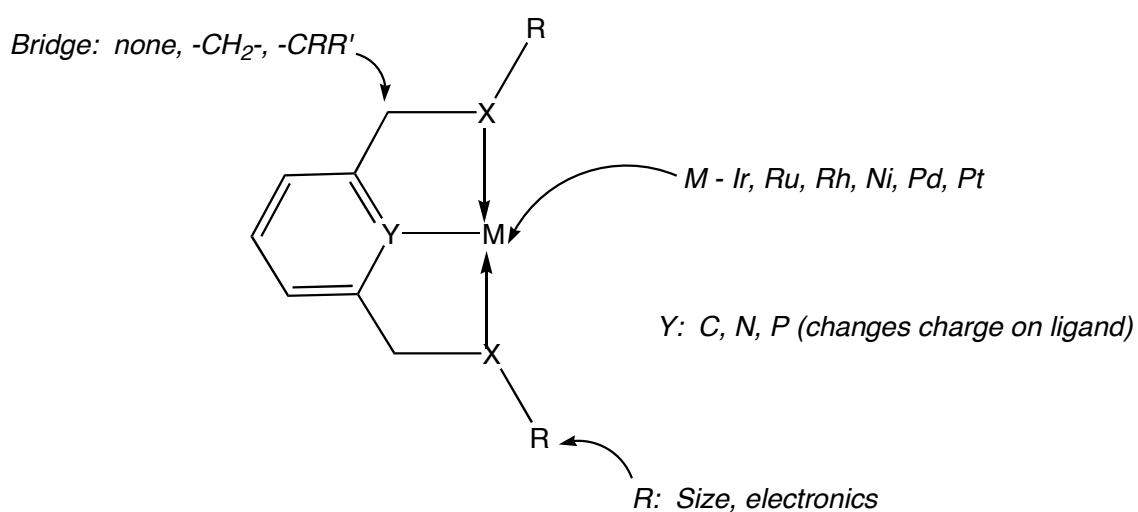
Despite the wide variety of pincer ligands, our focus in this particular project is on

the pincers that incorporate stabilized N-heterocyclic carbenes as donor atoms. Since

their discovery in 1991 by Arduengo,[65] these pincer carbenes have become ubiquitous

ligands in inorganic coordination and organometallic chemistry.[66] The research interest

in metal pincer carbene complexes is expanding to the study of multifaceted ligand

geometries that have shown pincer carbenes to be widely effective spectator ligands in

catalysis.[66,67] One of these geometries is the "pincer" design that provides an arrangement

capable of binding to meridional coordination sites of the metal; hence, allowing the

remaining sites to be available for catalysis.[68] In fact, due to the relatively-recent

invention of these pincer carbene ligands in 1991, the evolution of this field has been

slow when compared to the well-studied area of classic phosphine ligands.[67] These

pincer carbenes are evidently effective in a wide range of catalytic reactions, including

hydroformylation, hydrogenation, C-C coupling reactions such as Heck, Suzuki,

Kumada, and Stille coupling, alkene metathesis, and C_2H_4/CO copolymerization.[67] In

certain cases, the pincer carbene ligands have proven to be more effective than their

phosphine counterparts. Studies indicate that pincer carbenes have Lewis basicities

towards metal ions comparable to those of phosphines.[69] Furthermore, studies show that

metal-carbene bonds are stronger than metal-phosphine bonds.[70] In addition, carbenes

have higher *trans* effects than do N- or P- donors and are more tightly bound to the

metal.[71] It is worth noting that the strong metal-carbon bond leads to high stabilities of

carbene complexes against heat and moisture.[72] Pincer carbenes have been shown to be

effective ligands for almost any metal center and this is attributed to their excellent donor

ability.[64] Theoretical studies done by various groups in this area suggest possible

secondary interactions such as C_{carb}-M "π-donation" [73,74] Cl-C_{carb} [75] as well as N-C_{carb}

"back-donation" [64] as shown in Figure 1.7. The thermal stability of carbene complexes is

high and lack reactive bonds that might be broken in any decomposition process,[76] and

thus these ligands do not appear to dissociate easily from metal centers. As a result, an

excess of the ligand is not required to prevent clustering of catalyst molecules.[4]

Despite all the advantages of pincer carbenes, studies show that while pincer carbene precursors (bis(imidazolium) or bis(benzimidazolium) salts) are easy to synthesize, once obtained the pincer carbenes can be more challenging to bind to the metal than are phosphines.[67] As with other pincer ligands, pincer carbenes can be categorized into two groups - neutral and anionic. Within their framework the neutral pincer carbene ligands commonly possess an aryl nitrogen atom as a central atom and two imidazole or benzimidazole rings (that contain the carbenic carbon) on the pincer arms. Representatives of this group include carbene-based pincer ligands **7** and **9** in Figure 1.5. In the case of anionic versions of the ligand, the aryl group contains the central atom that possesses a negative charge, and most commonly carbon is used as the central atom (ligands **8** and **10** in Figure 1.5). We have noted earlier that the possible modifications of electronics and sterics factors on pincer ligands that can be envisioned are virtually limitless. As a result of this functionality, a wide range of pincer-ligated transition metal complexes have been prepared.

Figure 1.7 Plausible Secondary Interaction in Pincer Carbene Complexes[64]

$C_{carb} \longrightarrow M$	$Cl \longrightarrow C_{carb}$	$N \longrightarrow C_{carb}$
"π-donation"	"back-donation"	"back-donation"
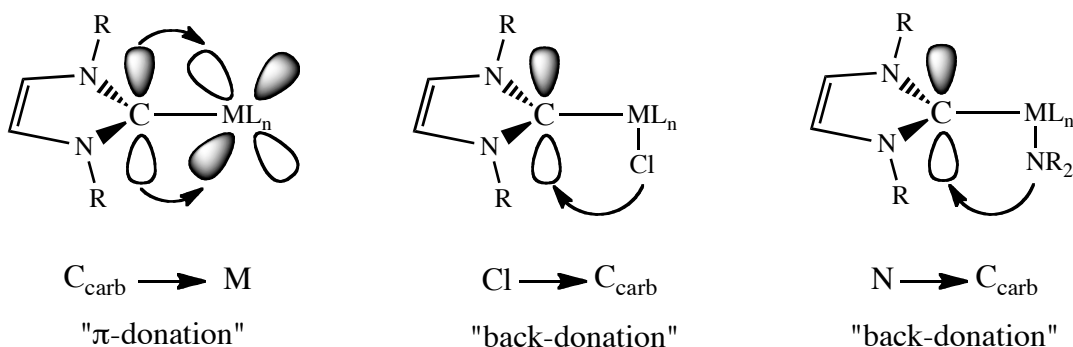
1.4.1 Applications of Pincer Carbene Ligands and Pincer Carbenes Metal Complexes

There are several catalytic applications of pincer carbenes; however, we will limit our discussion to few representative cases in which pincer carbenes have been used in homogeneous catalysis. As well, we begin with a recent novel example in which a carbene can be used directly to catalyze an oxygen transfer reaction.

1.4.1.1 Splitting of CO_2 to CO Mediated by Carbene

Most of the reactions discussed in this section include pincer carbene-transition metal complexes as catalysts for various organic reactions. However, a very recent study by Gu and co-workers indicates that a carbene can split CO_2.[77] Because of its high stability, CO_2 splitting to form CO requires a great deal of energy input.[78] Methods used to effect CO_2 splitting include use of metal complexes to cleave oxygen from CO_2 in order to form CO, [79,80] photoreduction, [81,82] electrochemical reduction,[83] and enzyme-CO dehydrogenase. [84] However, in the recent study by Gu and co-workers, the authors proposed that CO_2 is reduced to CO under milder conditions. Evidently, the carbene reacts with CO_2 to form the imidazolium carboxylate **1** that attacks the 2-position of cinnamaldehyde and results in the proposed intermediate **2**. The nitrogen imidazolium carboxylate **2** then deprotonates the 2-position C-H on cinnamaldehyde. Subsequently, an intermediate is generated by movement of electrons to a newly formed C-O bond by 1,5-hydride shift (Scheme 1.11). In their paper, Gu and co-workers proposed that possible

intermolecular hydrogen interaction N-H—C in **2** could help to stabilize the intermediate

state. Then, the base traps the proton on the nitrogen of the imidazolium ring. This leads

to C-O bond scission (**2**) and formation of cinnamic salt.

Scheme 1.11 Splitting of CO_2 to CO by Aldehyde Catalyzed by Carbene[77]
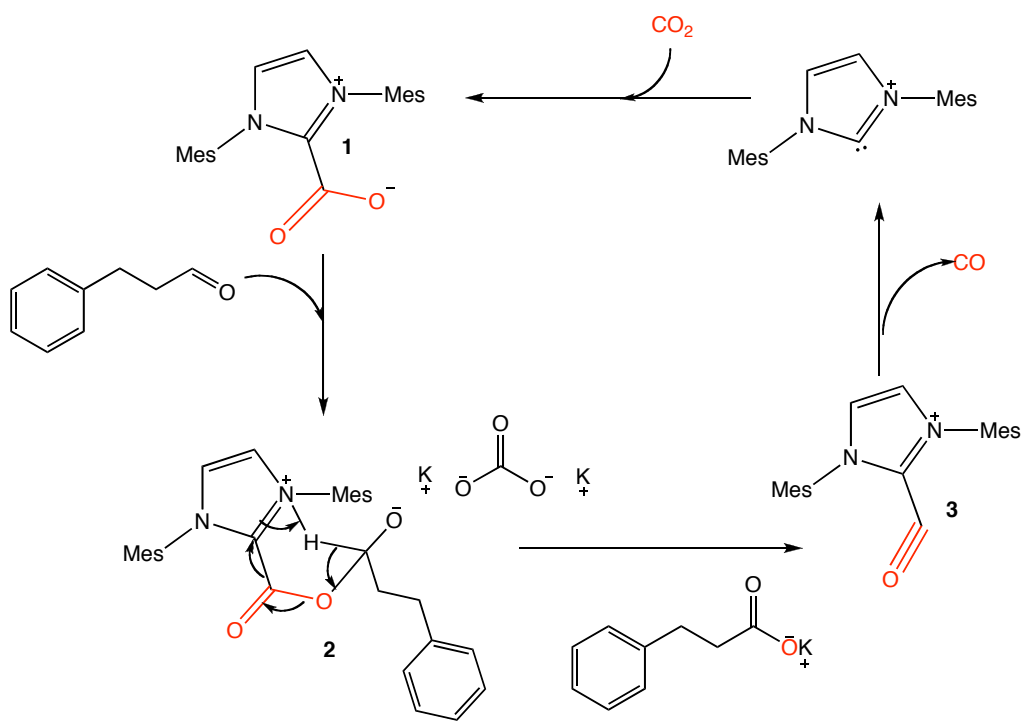
Subsequently, CO is released from the carbene-CO complex **3** and in the presence

of CO_2 the imidazolium carboxylate is formed very rapidly; hence, repeating the catalytic

cycle. In their study, Gu confirmed the production of CO by GC analysis and by the

reduction of $PdCl_2$.[85]

1.4.1.2   Hydrogenation

One catalytic application of pincer carbene metal complexes is hydrogen transfer from isopropanol (*i*PrOH) to a ketone using a base as shown in Scheme 1.12.[86] Albrecht and co-workers reported the first example of a pincer-based rhodium complexes [(Rh^{3+}bis- carbene)I$_2$(OAc)] that catalyzed reduction of various ketones and imines.[87] Peris and co-workers have explained that the mechanism involves the deprotonation of *i*PrOH by a base; in this case, KOH is used to produce an *i*Pr-OM species (Scheme 1.12). *i*PrOH is commonly used as hydrogen source.[88] *i*Pr-OM can undergo β-H elimination to produce a hydride that can attack the ketone substrate (R$_2$C=O) to give R$_2$CH-O-M. Alkoxide exchange with *i*PrOH liberates the product and reforms the *i*Pr-O-M species.

Interestingly, Peris and co-workers noted in their review paper that an intermediate metal hydride (M-H) that forms in this process could be a potential source of problems.[86] Peris suggested that if the carbene reductively eliminates with the hydride, the ligand is lost by formation of an imidazolium salt. However, this type of reductive elimination has not been observed with any of the catalysts described in this section. The hydrogenation catalysts are capable of up to 5 x 10^4 turnovers before deactivating.[86] This high performance can be explained by the fact that the chelating nature of pincer carbenes may help prevent the decomposition by either using the strong chelate effect or by holding the carbene ring in a conformation that prevents reductive elimination.[86]

Scheme 1.12 Proposed Catalytic Cycle for Hydrogenation of Ketone by Iridium(Bis-Carbene) Complexes Involving Monohydride Species[86]
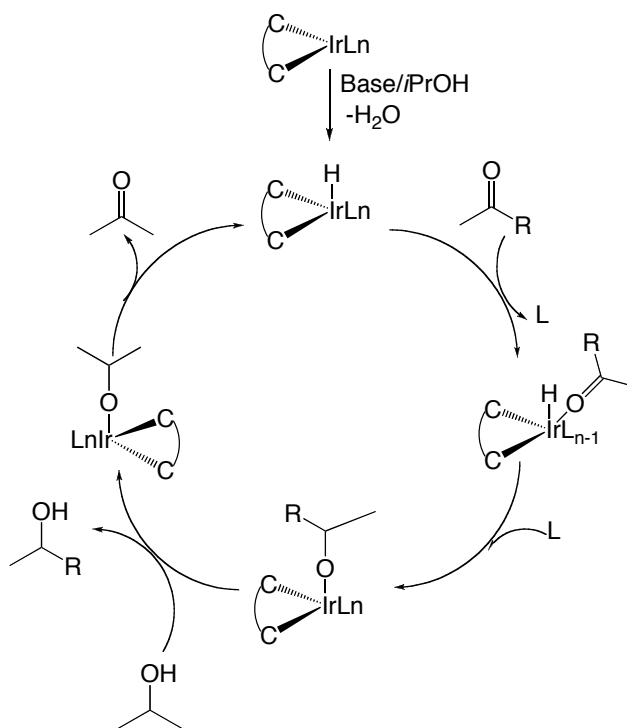
1.4.1.3   C-C Coupling Reactions

1.4.1.3.1   Heck Reaction (Arylation of Alkenes)

Heck reactions are widely used in organic synthesis.[6] Heck reactions require the use of any of a wide variety of Pd^0 or Pd^{2+} complexes as catalysts for coupling of an aryl halide with an alkene to prepare vinylic C-C bonds. Although Ni^{2+} complexes have been reported to catalyze the Heck reaction, palladium-pincer complexes are among the best Heck catalysts known, [89,90] giving extremely-high turnover numbers (TON). Pd complexes with or without phosphine ligands can catalyze these reactions. However,

Singleton reports that these catalysts without phosphines are sensitive to O_2 and not particularly thermally stable, and decompose to palladium black, Pd^0.[88] Phosphine-containing catalysts often give good results in the Heck reaction.[91] It is also worth noting that phosphine ligands are expensive, toxic, and unrecoverable.[86] In addition, most of these catalysts are unable to activate aryl chlorides due to inertness of C-Cl bond, and so high temperatures are required. This has become one of the big challenges in the search for improved catalysts for the Heck reaction. Hermann and co-workers reported pincer carbene-containing palladium complexes with reasonably high TON.[92] It has been argued that the strongly electron-donating nature of the carbene ligand may facilitate oxidative addition. Bis-carbene complexes **19, 20, 22,** and **23** in Figure 1.8 can all withstand high temperatures and are air-stable. However, a disadvantage of **19** is its low solubility in non-polar solvents. To eliminate this problem, **22** was designed with a -CH_2- linker between the imidazole rings for the purpose of enhancing solubility.[67] Moreover, substitution of the methyl group of **19** by *n*-Butyl substituents to produce **20** improved the solubility of the catalyst significantly.[71] Compounds based on complex **24** in Figure 1.8 have shown good catalytic activities in Heck-type reaction catalysis.[72] At elevated temperature, over 24 hours and aerobic conditions, compounds based on **24** catalyzed activated substrates such as 4-bromobenzaldehyde and 4-bromoacetaldehyde in yields of 98-100%. With the same catalysts, Hahn and co-workers reported reasonable catalytic activity, requiring a shorter reaction time of 2 hours, and producing reasonable yields of 55-84% when 4-bromobenzyaldehyde was used as the substrate.[72] Although pincer carbene complexes containing palladium are commonly known to catalyze the Heck reaction, only a few pincer carbene complexes containing Ni have been reported.[93]

Inamoto and coworkers reported the first air and moisture-stable pincer carbene-derived

nickel complex **21** that can catalyze the Heck reaction.[93] Aryl chlorides and aryl iodides

as well as bromides were successfully used with this system.

Scheme 1.13 Heck Activity of 24 with Functionalized Aryl Bromides and Styrene[72]
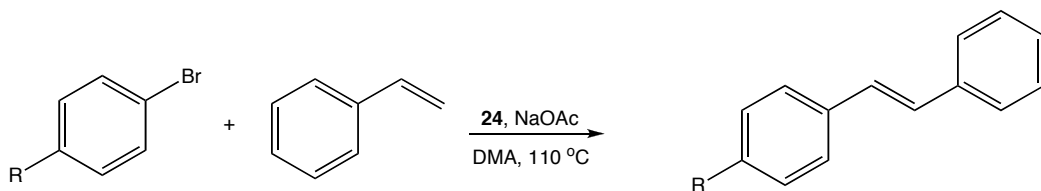
Scheme 1.14 Catalytic Activity of 21 in the Heck Reaction[93]
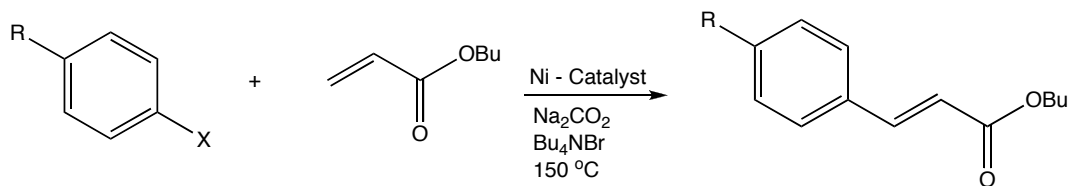
1.4.1.3.2 Suzuki Activity

Suzuki coupling consists of reactions between an aryl- or vinyl- boric acid and an

aryl or vinyl halide and is widely used in organic synthesis. Pd⁰ catalysts are used to give

poly-alkenes, styrenes, and substituted biphenyls.[94]

Scheme 1.15 Suzuki Coupling of 24[72]
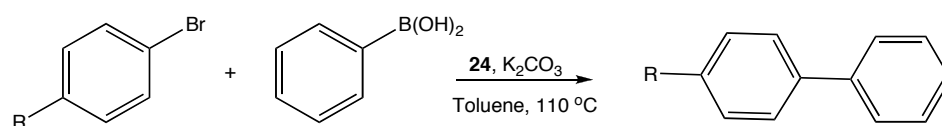
Figure 1.8 Some Pincer Carbene–Containing Pd and Ni Complexes

M = Pd, R = Methyl, **19**; Butyl, **20**

M= Ni, R = Methyl, **21**

22

23

24

25
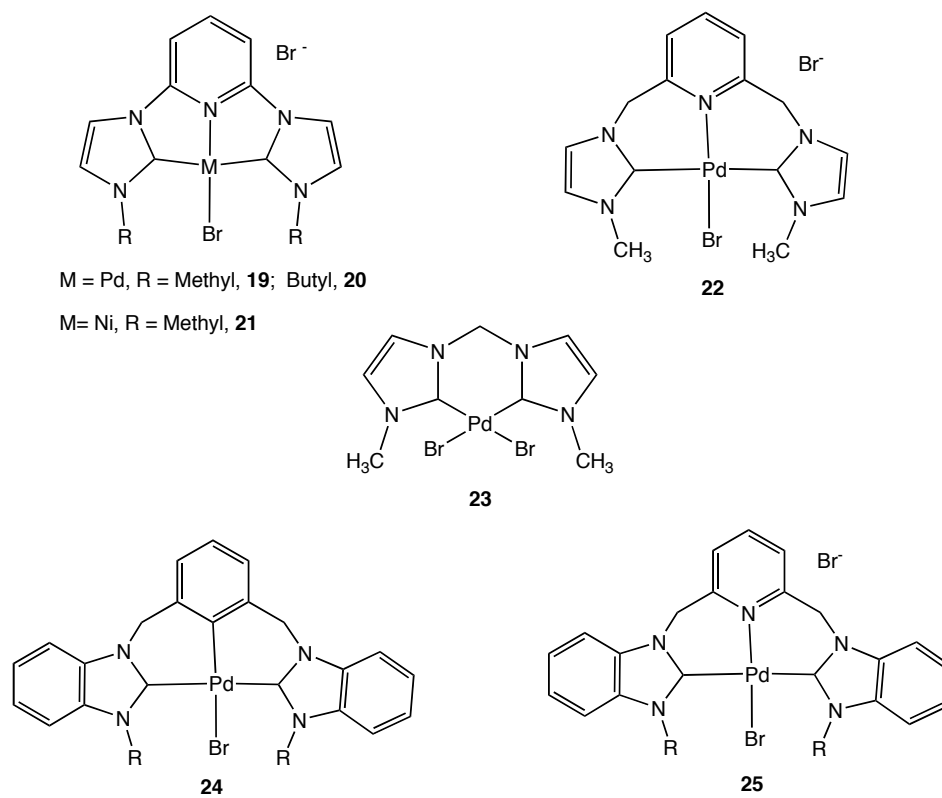
It should be noted that most of the catalysts that are effective for Heck reaction are also effective for the Suzuki reaction. This may be due to similarity in the mechanisms for both Suzuki coupling and the Heck reaction. A good example is the catalyst based on **24** (R = *n*-Butyl) shown (Figure 1.8). Coupling of several aryl bromides with phenylboronic acid over 24 hours, with no optimization of reaction

conditions, can yield biphenyls in up to 80% yield using 0.1 mol % catalyst **24** (R = *n*-

Butyl). However, when activated aryl bromides are used as substrates the reaction results

in 100% conversion.[72]

1.4.2   Syntheses of Pincer Carbene Ligands

Pincer carbene ligand precursors can be prepared in excellent yields in a single step

by various routes. The carbene precursors based on **26** are prepared by directly heating a

mixture of 2,6-dibromopyridine or 2,6-dichloropyridine and two equivalents of N-alkylated

imidazole in a sealed tube.[76] The resulting precipitates are collected by filtration, washed

with $CHCl_3$, and dried *in vacuo* to give white solids in approximately 90% yields.

Scheme 1.16 Generalized Preparation of Bis(imidazolium) Salt 26

R = Alkyl   X = Br, Cl   **26**
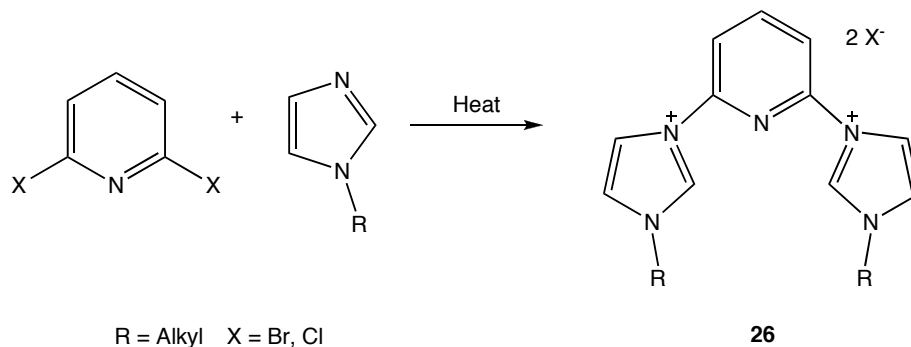
The xylene-bridged bis(imidazolium) salt **27,** and bis(benzimidazolium) salt **28**

are synthesized by reaction of two equivalents of N-alkylated imidazole and

dibenzimidazole derivatives with 1,3-(dibromomethyl)-2-bromophenylene in 1,4-dioxane

solvent. After purification, **27**[71] and **28**[72] are obtained in approximately 90% yields.

NMR spectroscopy is a diagnostic tool used to follow these reactions. The proton spectra

of these pincer carbene precursors exhibit singlets for resonance of the NC*H*N protons at

δ 10.6 ppm for **26**, δ 9.2 ppm for **27**[71], and δ 10.1 ppm for **28**.[72] The resonances of the

methylene protons of the xylene bridge for both **27** and **28** are observed as singlets at δ

5.9 ppm. Again, this resonance is diagnostic for these types of ligands.

Scheme 1.17 Preparation of Bis(imidazolium) Salt 27

R = Alkyl   X = Br, Cl

1,4 - Dioxane
100 °C

2 X⁻

27
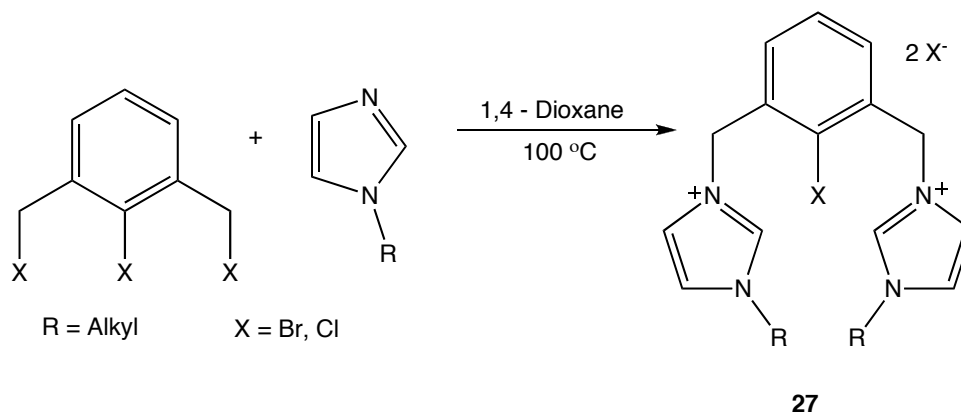
Scheme 1.18 Preparation of the Bis(benzimidazolium) Salt 28

R = Alkyl   X = Cl, Br

1, 4- Dioxane
Reflux
12 h

2 X⁻

28
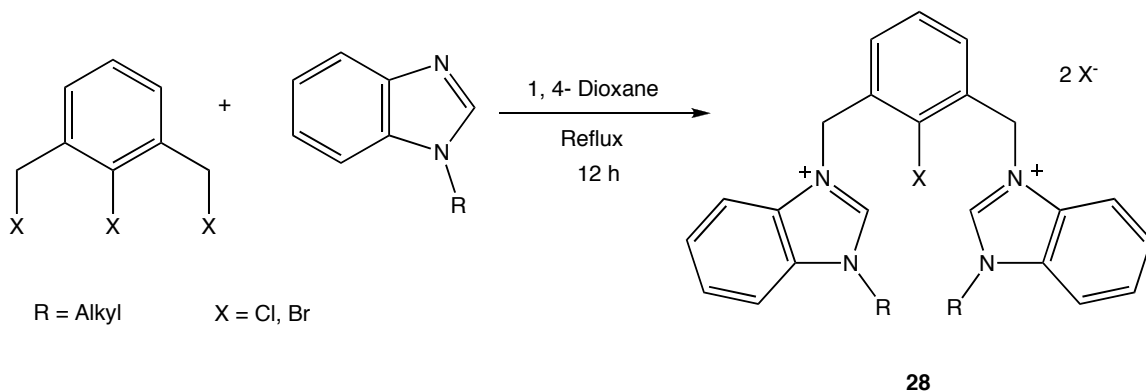
1.4.3 Syntheses of Pincer Carbene Metal Complexes

There are several approaches to the metallation of pincer carbene ligands. The metal precursors that are used generally for Group 10 transition metals are nickel acetate $[Ni(OAc)_2]$, palladium acetate $[Pd(OAc)_2]$ and tris(dibenzylideneacetone)dipalladium(0) $[Pd_2(dba)_3]$. One of the synthetic routes involves the metallation of imidazolium-substituted pyridines using a Pd^{2+} source such as $Pd(OAc)_2$, resulting in loss of acetic acid (AcOH) as shown in Scheme 1.19.[67,76] Peris and co-workers reported the synthesis of the planar complex **19** that had low solubility when compared to $^{n\text{Bu}}$CNC-Pd-Br **20**.[67] Solubility of pincer carbene metal complexes can also be improved by introducing a methylene linker; however, the resulting pincer complex will have a twisted, less-rigid structure. This has been shown crystallographically.[67]

Inamoto and co-workers reported the first pincer carbene-derived Ni-pincer complex that can catalyze the Heck reaction, as was mentioned in Section 1.4.2.1. Similar to the Pd complex, the Ni complex was prepared by cyclometallation of $Ni(OAc)_2$ by the carbene precursor in the presence of tetrabutylammonium bromide (Bu_4NBr) as shown in Scheme 1.19.[93] In these cyclometallation reactions, high boiling solvents such as dimethylsulfoxide (DMSO) are frequently used.

Secondly, metallation of the imidazolium-substituted bromoaryl precursor can be successfully achieved with Pd^0 and not Pd^{2+}. Crabtree and co-workers suggest that Pd^0 binds to the bromoaryl group by oxidative addition, followed by cyclometallation of the imidazole rings with loss of gaseous H_2 in the last step.[67] In these reactions, $[Pd_2(dba)_3]$ is commonly used as the source of Pd^0.

Scheme 1.19 Preparation of Pincer Carbene-Derived Pd Bromide Complexes 19, 20 and 21
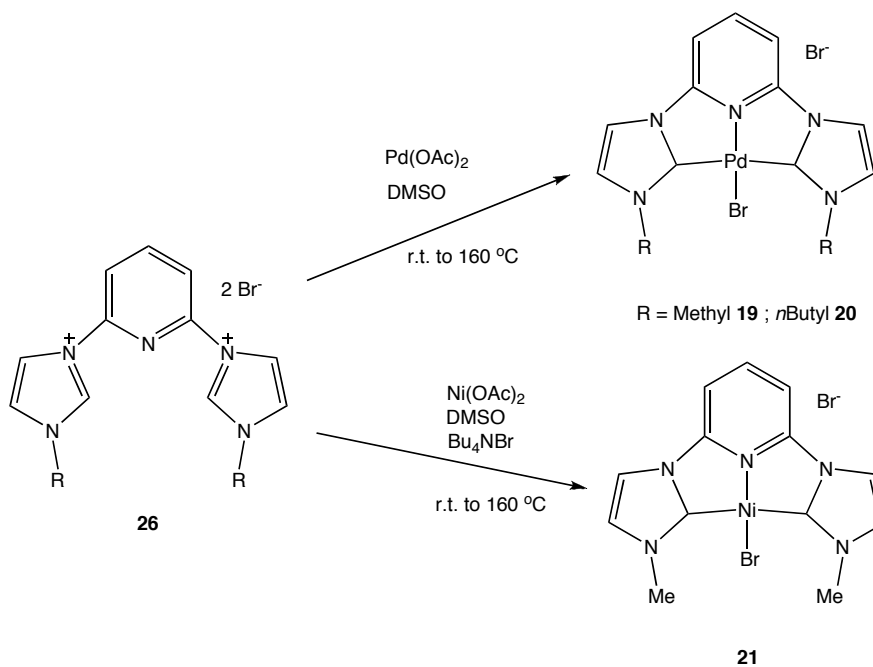
Shown in Scheme 1.20 is a pincer complex reported initially by Loch and co-workers.[95] The imidazolium-substituted bromoaryl precursor **28** reacts with [Pd$_2$(dba)$_3$] to establish the initial M-L bond through oxidative addition and gives the desired product **29** in 43% yield.[95]

Scheme 1.20 Preparation Pincer Carbene-Derived Palladium Pincer Complex 29
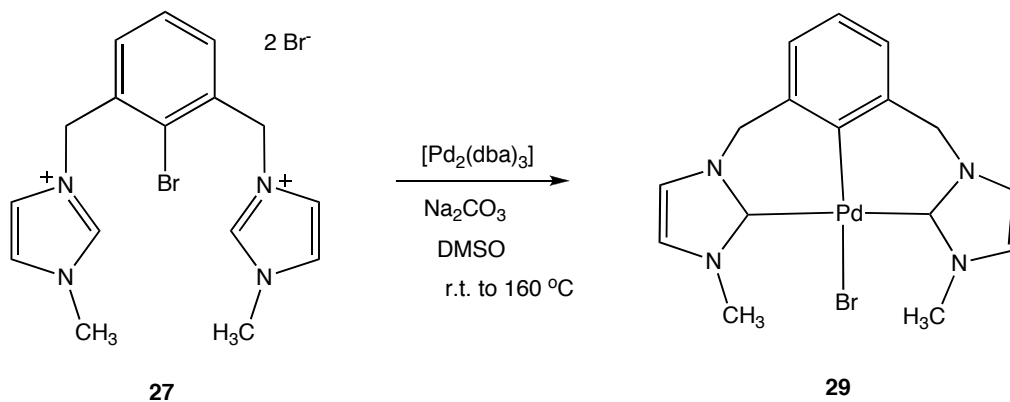
Pincer carbene complexes can also be prepared by transmetallation reactions. In this method, silver-carbene complexes are often used as carbene transfer reagents. This method was first brought to light by Lin and co-workers when they prepared carbene complexes of Pd^{2+} and Au^+.[96] As of today, many metal-carbene complexes of palladium[97] and copper[98] have been prepared using this route. As illustrated in Scheme 1.21, carbene precursor **30** reacts readily with Ag_2O in dichloromethane (CH_2Cl_2) producing the pincer carbene silver complex **31** in 70% yield.[99] In fact, the oxide does the deprotonation of protonic C2 hydrogen of the imidazolium salt and subsequently the Ag^+ ion metallates the C2 position.[100] The silver–carbene complex so formed can then be used to transfer the carbene to various metal salts and organometallic precursors to give a wide range of pincer carbene metal complexes. A representative reaction is shown in Scheme 1.22, in which the pincer carbene silver complex reacts with $(PhCN)_2PdCl_2$ in CH_2Cl_2 to produce in reasonable yield the palladium complex **32** and two equivalents of AgCl.[99] As well, silver carbenes can react with the dirhodium(I) complex ($[Rh(COD)Cl]_2$) in CH_2Cl_2 to provide complex **33** in reasonable yields (Scheme 1.22).[99]

Scheme 1.21 Preparation of Pincer Carbene Silver Complexes

R = *n*-Butyl, X =Cl; **30**   **31**
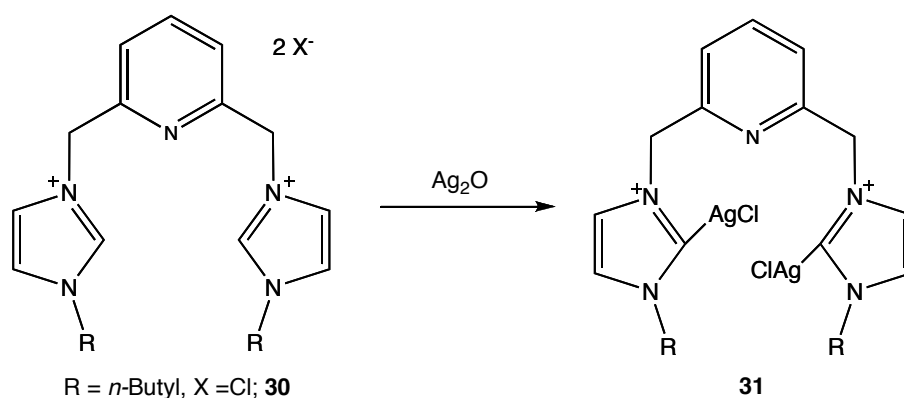
In addition, tungsten-carbene complexes have also been shown to be functional carbene-transfer reagents. Ku and co-workers have reported several complexes containing M-carbene bonds (M = Au, Pd, Pt, Rh) that have been prepared through this route.[101]

Scheme 1.22 Preparation of Pincer Carbene Rh and Pd Complexes via Transmetallation with Ag Carbene
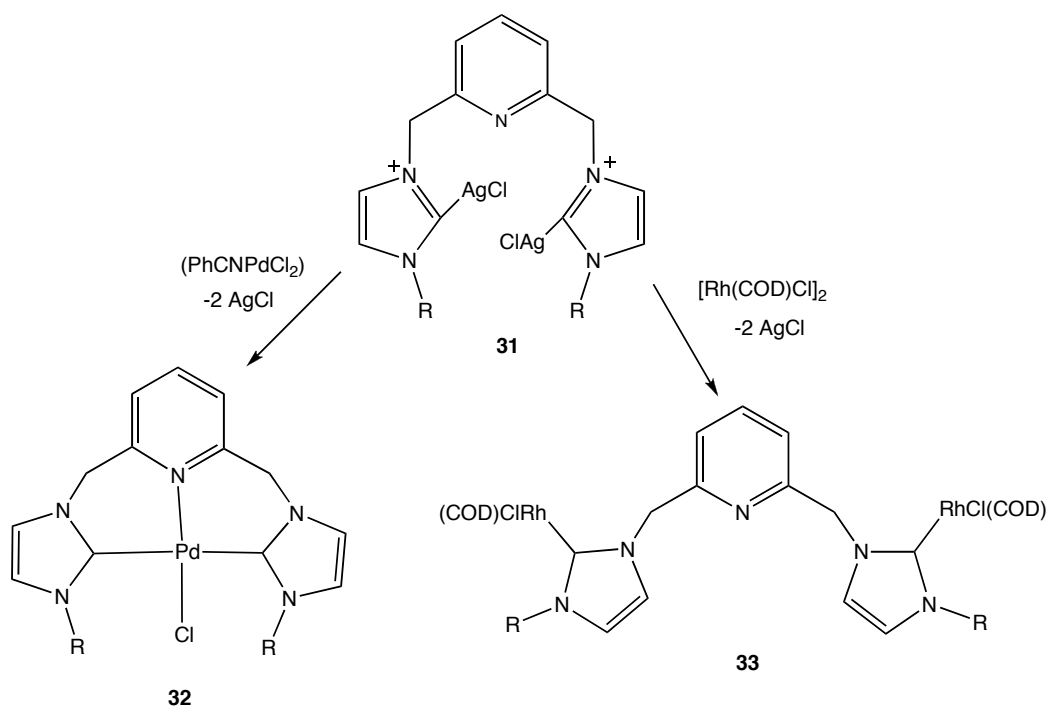
Surprisingly, it has been shown that metallation of an imidazolium carbene precursor such as **34** (R = Me) rapidly reacts with the metal hydride IrH_5L_2 (L = PPh_3) to produce **36**, where metallation has occurred almost completely at the C5 rather than the typical C2 position (Scheme 1.23).[67] This is actually a very unexpected result, and these ligands have been termed "abnormal" carbenes. In the presence of a strong acid,

however, **34** will rearrange to form **35**. In general, the reason for this abnormal binding remains unclear, and fortunately by blocking the 4- and 5-imidazolium positions (*e.g.*, by using benzimidazolium analogues) can prevent formation of this abnormal mode. Interestingly, the formation of abnormal carbenes can deliberately be achieved by blocking the C2 position by a methyl group.[67,100]

Scheme 1.23 Abnormal Binding in Pincer Carbene Complexes[67]
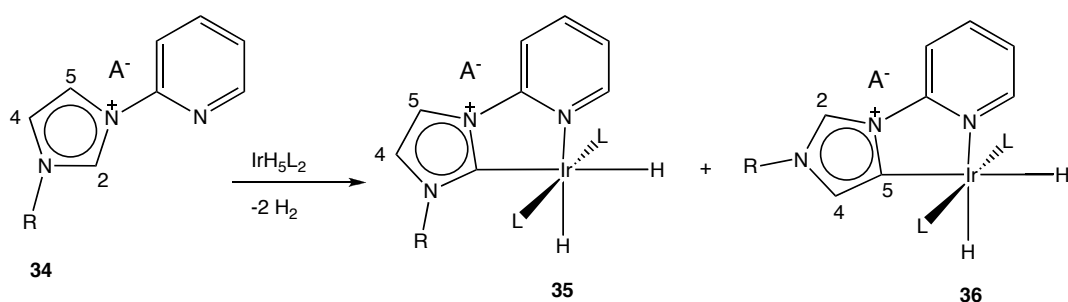
Another route to metallation of pincer carbene precursors is through deprotonation of the carbene precursor at NC*H*N position. However, it is reported that deprotonation of pincer imidazolium-based carbene precursors by strong bases such as *n*-BuLi can lead to the abstraction of protons on undesired sites.[67] Deprotonation works well with benzimidazolium salts because as mentioned above, positions 4 and 5 are protected. Bis(carbene) **37** is prepared by first deprotonating the benzimidazolium salt represented in compound **28** with *n*-BuLi in THF at -78 °C.[72] It seems likely that the carbenes are formed at this temperature and then react with [Pd$_2$(dba)$_3$] to give the desired product **24** by oxidative addition of C-Br bond to the Pd^0 center.[72] After purification by

recrystallization, usually in methanol, the palladium complexes are obtained and are moisture and air-stable.

Scheme 1.24 Preparation of Bis(benzimidazolin-2-ylidene) Palladium Bromide 24
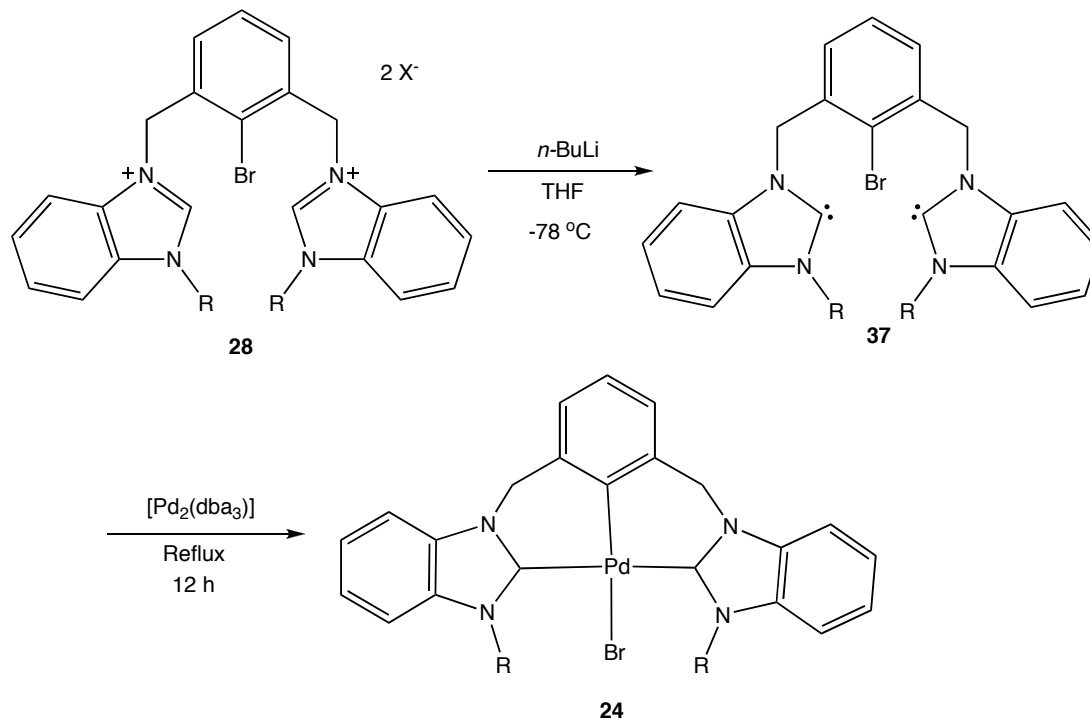
A very recent detailed study on NHC-derived complexes of Group 9 indicates that $[Ir(\mu\text{-}Cl)(COD)_2]_2$ reacts with bis(imidazolium) salts to give Ir^{3+} hydrides.[102] When the base NEt_3 is used in a stoichiometric amount with $[Ir(\mu\text{-}Cl)(COD)_2]_2$, the products iridium(III) pincer hydrides **40** and **41** are formed, but in very low yields. However, replacement of NEt_3 by Cs_2CO_3 or conducting the reaction with excess of NEt_3 (11 equivalents) leads to the pure desired products **40** and **41** in almost 70% yield. The

presence of the Ir-H bond is observed by a ^{1}H NMR resonance as singlet at around -22 ppm, as well as observation of an Ir-H stretch in the IR spectrum (ν_{IrH} at ~2118 cm^{-1}).[102]

Scheme 1.25 Preparation of Pincer Carbene-Derived Iridium Pincer Hydride Complexes 40 and 41[102]
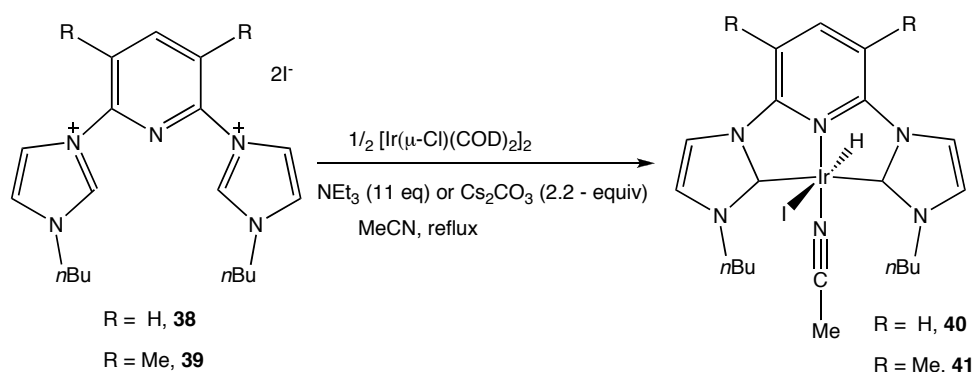
Interestingly, in order to gain further understanding into the formation of pincer hydride complexes, Raynal and co-workers[102] performed detailed labeling experiments. As shown in Scheme 1.26, the carbene precursor was deuterated at the imidazolium C2 position and reacted under the same conditions used in the synthesis route for the pincer hydride **43**. Interestingly, the spectroscopic data indicate that the main product in the analogue of **43** now has a deuterium atom instead of hydride ligand bound to Ir. These results therefore confirm that the hydride in **41** and **43** comes from one imidazolium C2 moiety of the carbene precursor.

Scheme 1.26 Deuterium Labeling Experiment to Determine the Origin of the

Hydride[102]

$1/_2$ [Ir(μ-Cl)(COD)$_2$]$_2$
Cs$_2$CO$_3$ (2.2 - equiv)
MeCN, reflux

42

43
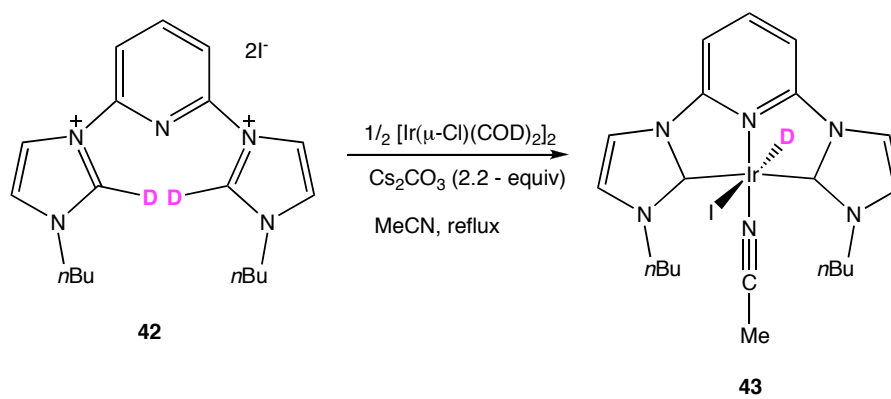
2   CHAPTER TWO

2.1   Preparation of Pincer Carbene-Pd-H Complexes

Transition metals are routinely used in organic synthesis and important new transformations continue to be uncovered.[103]   Quite interestingly, due to its multifunctional nature, palladium has been a widely employed transition metal in organic synthesis,[24] catalyzing both oxidative and non-oxidative transformations.[104,105]   Some of non-oxidative organic reactions catalyzed by palladium include hydrogenation, Heck reactions, Suzuki–Kumada reactions, Stille couplings, olefin metathesis, and CH_2/CO copolymerization.   As explained earlier in Chapter One, oxidation of organic molecules by palladium catalysis is primarily oxygenase-type oxidation in which palladium facilitates the transfer of the oxygen atom from molecular O_2 to the organic substrate.[24]   As proposed in our catalytic route to epoxides shown in Scheme 1.9, the preparation of several carbene pincer-containing M-H's with varied sterics and electronic properties were attempted.   This chapter gives more information on our efforts to prepare these carbene-containing, pincer based Pd-H complexes and the investigation of their potential

to activate molecular oxygen and eventually transfer oxygen atoms to alkenes and other organic substrates. Also, alternative routes to Pd-OOH complexes were investigated and will be discussed in this chapter.

Syntheses of carbene-containing pincer Pd halides (both charged and uncharged) have been widely reported as indicated in Section 1.4.3. In fact, this background has significantly helped us in the syntheses of pincer carbene ligands and, subsequently, their transition metal complexes. The primary difference between the uncharged and charged pincer carbene Pd complexes is the nature of central atom at which the pincer carbene ligand attaches to the metal. The central atom can possess either a negative charge (*e.g.*, CCC ligands **8**, **9** and **10** in Figure 1.5 for the anionic pincer carbene ligands or it can be neutral (*e.g* CNC ligand **7** and PCP ligand **11** in Figure 1.5) for the neutral pincer carbene ligands. The anionic versions of the pincer carbene ligands lead to the formation of uncharged pincer carbene Pd halides while the neutral versions lead to the positively-charged pincer carbene Pd halides. However, the conversion of pincer carbene Pd halides (Pd-X, where X = Cl, Br, or I) to pincer carbene Pd-H's, along with the characterization of these hydrides, has not been not widely reported. According to our recent search in Cambridge Crystallographic Database (CSD version 5.31, May 2010 update), there are very few fully-characterized and reported carbene-containing pincer ligated metal hydrides, none of them Group10 species. Among these are ^{DiPP}CNC-Fe-H[106], ^{DiPP}CNC-Ir-H,[107] and ^{Ph}PCP-Ru-H.[63] It is known that traditional, monodentate carbene metal hydrides can undergo reductive elimination with the complex losing ligand with the formation of the imidazolium salt.[100] However, we decided to prepare the pincer carbene metal hydrides as we hypothesized that the chelating nature of the pincer

carbenes would help prevent decomposition. We believed this for two reasons - first, the chelate effect should stabilize the complex, and second, the pincer holds the carbene rings in an overall conformation that does not favor reductive elimination.[86]

Hydride sources such as NaBH$_4$ have previously been used in converting pincer carbene-based metal halide complexes to metal hydrides.[63] The conversion of **44**, containing a PCP carbene-based ligand, was achieved through the use of NaBH$_4$ in ethanol, forming **45** (Scheme 2.1).[63]

Scheme 2.1 Conversion of 44 to 45 using NaBH$_4$[63]
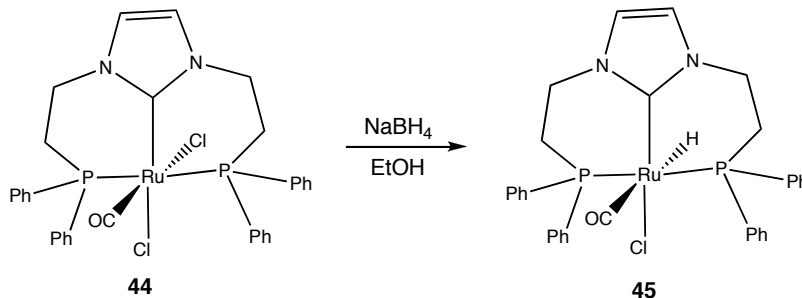
Scheme 2.2. Preparation of ^{DiPP}CCC-Ir-H 48[107]
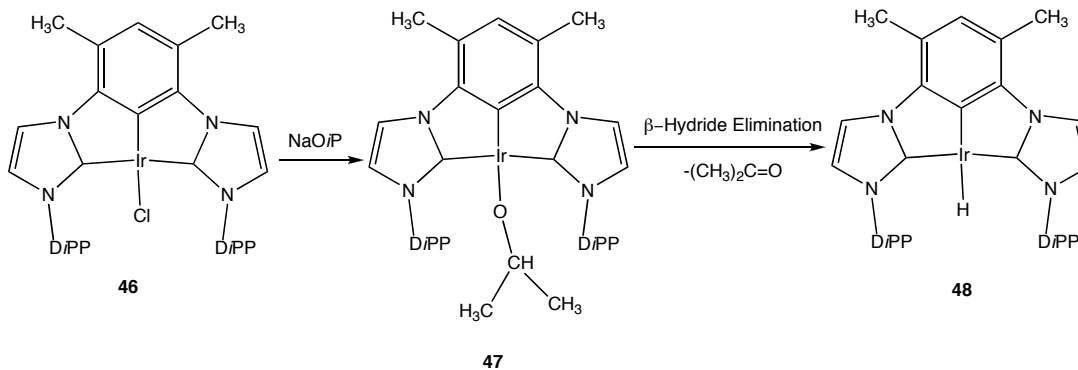
More recently, Danopoulos and co-workers reported the synthesis of a ^{DiPP}CNC-Ir-H species in which they were able to exchange the Cl⁻ in complex **46** with -OiPr to give **47**. Eventually, the Ir-H **48** was formed by the elimination of acetone as shown in Scheme 2.2.[107]

As well, Danopoulos and co-workers reported the related species ^{DiPP}CNC-Fe-H **50** which was obtained by photolysis of ^{DiPP}CNC-Fe-(N₂)₂ and benzaldehyde anilide in THF (Scheme 2.3). The phenyl ring from benzaldehyde anilide and hydride are *cis* to each other, suggesting that a concerted C-H oxidative addition reaction had occurred.[106]

Scheme 2.3 Preparation of ^{DiPP}CNC-Fe-H 50[106]
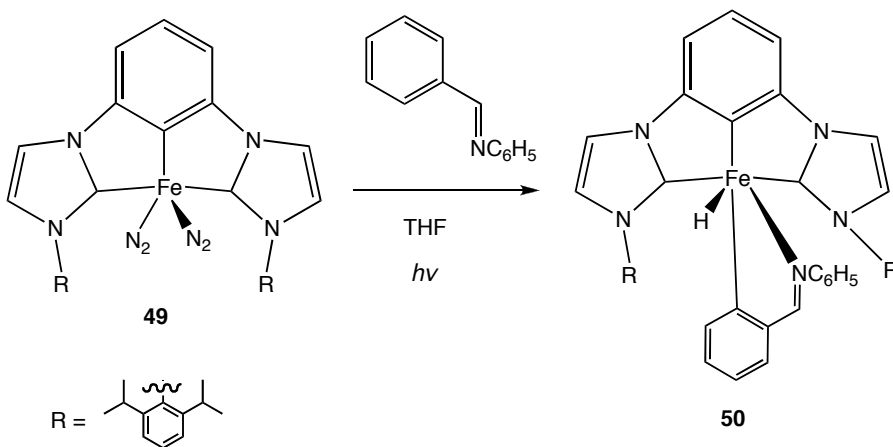
In our attempts to convert uncharged ^{Me}CCC-Pd-Br **29** to ^{Me}CCC-Pd-H **51**, hydride sources such as LiAlH₄, LiEt₃BH (Super-Hydride™ solution), Et₃SiH, and NaBH₄ failed to give the desired product, ^{Me}CCC-Pd-H **51**. Quite interestingly, when K⁺[*sec*-Bu₃BH] in THF (K-Selectride™ solution) was used, the desired product **51** was formed as an oily solid in 80% yield (Scheme 2.4). The palladium hydride **51** was prepared by

suspending ^{Me}CCC-Pd-Br in THF followed by addition of K-Selectride™ solution at -78

°C. Product **51** was characterized by ^{1}H NMR and IR; however, crystals suitable for X-

ray analysis could not be obtained even after trying different combinations of solvents.

The ^{1}H NMR spectrum of **51** in THF-d$_8$ indicated that the ligand remained attached to the

metal. This can be shown by the appearance of two doublets with a $^2J_{H-H}$ coupling

constant of 13.8 Hz, typical for the geminal coupling of diastereotopic protons arising

from the CH$_2$ (methylene) protons of the pincer arms. Fortunately for the analysis, the

methylene protons are equivalent and often appear as a singlet in the free ligands, but in

bound metal complexes these methylene protons are non-equivalent due to the twisted

geomety[71] of the ligand. As well, the appearance of a doublet is often observed in other

pincer carbene Pd halides, also possessing twisted ligand geometries.[72,108] In addition, a

^{1}H NMR signal assigned to the Pd-H was observed at -10.8 ppm. An infrared (IR) band

was observed at 1770 cm^{-1} and could be assigned to the Pd-H stretch.

Scheme 2.4 Preparation of ^{Me}CCC-Pd-H 51
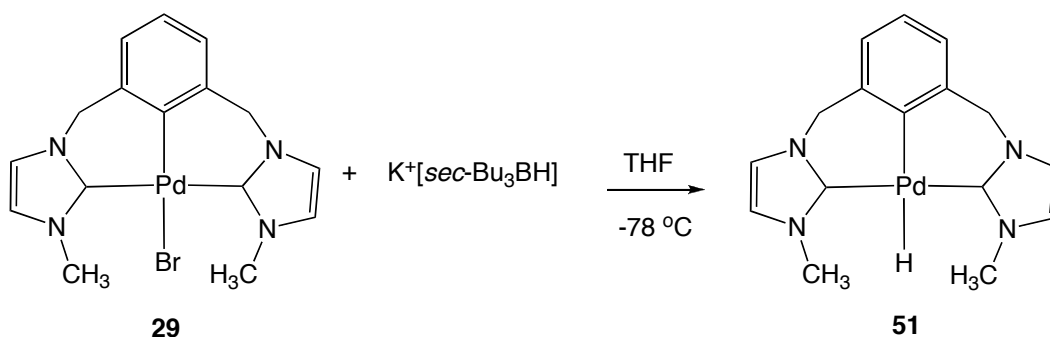
With the aim of preparing pincer carbene palladium complexes that behave

electronically and sterically differently from imidazolin-2-ylidene-based pincer carbene

palladium complexes[108], **53** was prepared from **52** using K-Selectride as a hydride source (Scheme 2.5). Surprisingly, other common hydride sources such as $LiAlH_4$, Super-Hydride, Et_3SiH, and $NaBH_4$ failed to give the desired product **53**. The ^1H NMR spectrum using THF-d_8 as the solvent suggested the formation of Pd-H by the presence of a signal at -8.0 ppm that is consistent with a Pd-H resonance. Similar to ^{Me}CCC-Pd-H **51**, the ^1H NMR spectrum indicated the ligand remained attached to the metal as the CH_2 protons appear as a doublet with $^2J_{H-H}$ of 13.8 Hz.

Scheme 2.5 Preparation of Benzimidazolin-2-ylidene-Based ^{Et}CCC-Pd-H 53

52   **53**
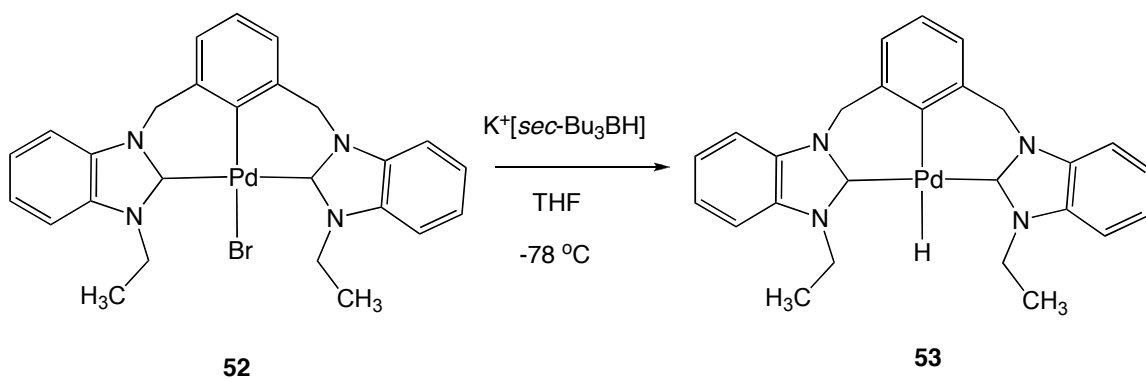
Attempts to isolate benzimidazolin-2-ylidene-based ^{Et}CCC-Pd-H **53** as crystals suitable for single crystal x-ray analysis were unsuccessful.

   Although conversion of benzimidazolin-2-ylidene-based ^{Et}CCC-Pd-H **52** to **53** by K-Selectride reagent was straightforward, when K-Selectride solution was used under the same reaction conditions as those used to convert ^{Me}CCC-Pd-Br **29** to **51**, the conversion of benzimidazolin-2-ylidene-based ^{nBu}CCC-Pd-Br **54** was unsuccessful. This was also the case when hydride sources such as $LiAlH_4$, $NaBH_4$, or Super-Hydride solution were

46

used in attempts to convert **54** and **55** (Figure 2.1) to the Pd-H compounds. This is likely

due to bulkiness of the R group present that may hamper the approach of the hydride-

containing species. It should be noted, however, that although K-Selectride solution was

successful in the conversion of **29** and **52** to palladium hydrides **41** and **53**, respectively,

it was difficult to eliminate the boron by-product impurities associated with the use of K-

Selectride solution even after washing the impure solid repeatedly with pentane and

hexanes.

Figure 2.1 ^{R}CCC-Pd-Br with Bulky R Groups
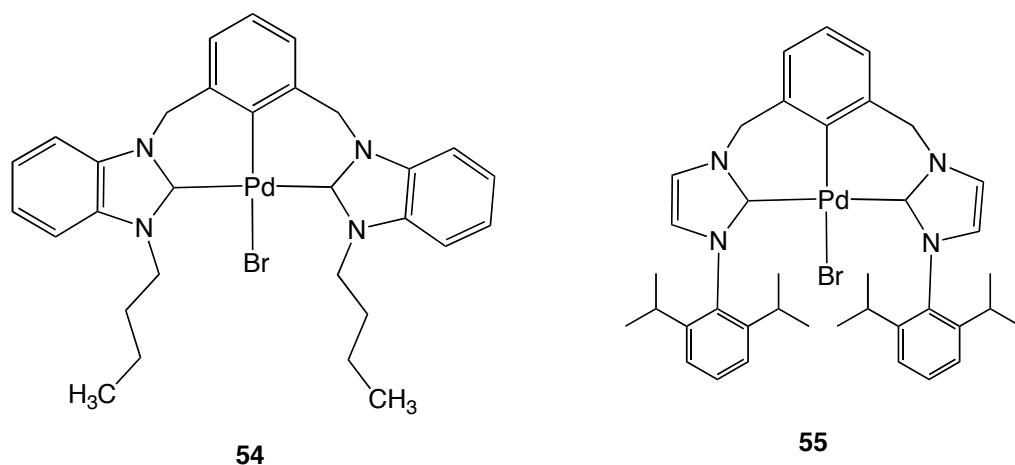
Although we were successful in obtaining a few uncharged pincer carbene Pd- H,

the conversion of the charged pincer-carbene Pd-Br complexes **19** and **20** (shown in

Scheme 2.6) to charged pincer-carbene Pd-H **56** and **57**, respectively, by hydride sources

such as LiAlH$_4$, NaBH$_4$, Super-Hydride solution, K-Selectride solution, and Et$_3$SiH were

unsuccessful. While Et$_3$SiH did not react at all with [^{Me}CNC-Pd-Br]Br **19** and [^{nBu}CNC-

Pd-Br]Br **20**, the hydride sources LiAlH$_4$, NaBH$_4$, Super-Hydride solution and K-

Selectride solution all led to decomposition of the complexes. Although the ligand could not be recovered, a black solid (likely Pd^0) was deposited, suggesting that reductive elimination of the ligand had occurred. The eliminated ligand could possibly react further with the hydride source and form unknown compounds.

Scheme 2.6 Attempted Conversion of Charged Pincer Carbene Pd-Br to Pd-H

R = Methy, **19**
R = *n*-Butyl, **20**

R = Methyl, **56**
R = *n*-Butyl, **57**
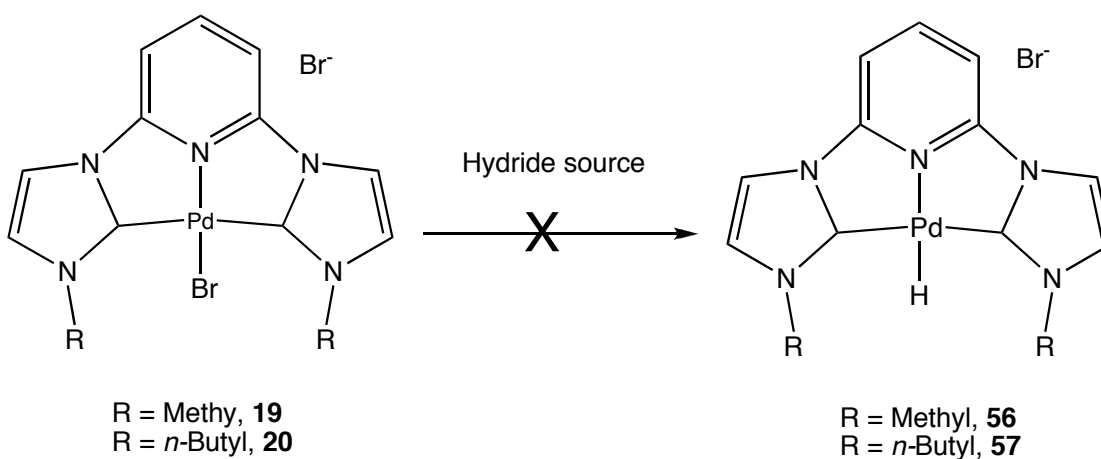
Quite interestingly, attempts to convert the Pd-Br **19** to Pd-H by bubbling hydrogen (H_2) gas while sonicating in methanol (Scheme 2.7) resulted in reductive elimination of the ligand and deposition of Pd^0 as a black solid. Fortunately, this time it was possible to recover the ligand from solution. The ^{1}H NMR spectrum confirmed the presence of the NC*H*N of the ligand proton as a singlet at δ 9.2 ppm.

Scheme 2.7 Reaction of [^{Me}CNC-Pd-Br]Br 19 with H$_2$ Gas
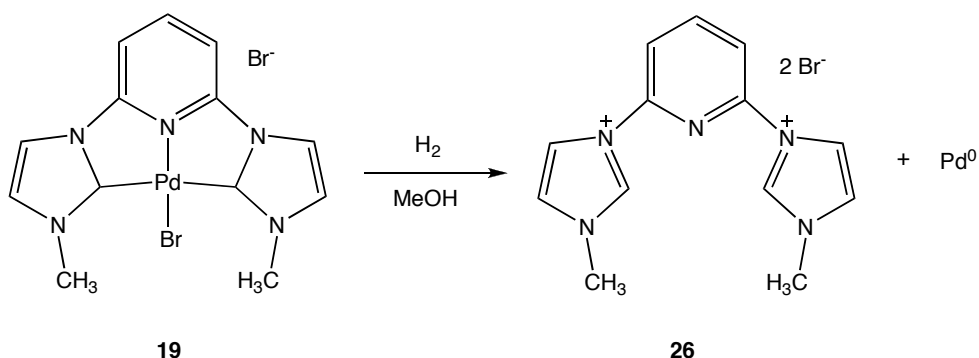
2.2   Attempted Preparation of M-H in a Single Step

In our efforts to prepare M-H species we also hypothesized that M^0 might insert directly into a ligand C-H bond, resulting in M-H complex in a single step. We attempted to cyclometallate the pincer carbene **58** shown in Scheme 2.8 using M(COD)$_2$ (M= Ni, Pd and Pt; COD = cyclooctadiene). Essentially, M(COD)$_2$ acts as a good source of M^0. In this attempt, the ^{Me}CCC carbene ligand was prepared by abstracting protons at NC*H*N positions of the imidazolium rings, and subsequently M(COD)$_2$ was added in the presence of a base. However, this approach proved unsuccessful.

Interestingly, we later learned that Crabtree attempted palladation of **58**, also without success.[67] In his paper, Crabtree argued that palladation of pincer carbene precursors such as **58** fail due to the lack of metal binding site in the *bis*-carbene precursor.[67] More interestingly, as explained earlier in Section 1.4.3, in a very recent report Raynal and co-workers performed labeling experiments aiming at tracing the origin of hydride from pincer carbene iridium hydride complexes that they synthesized.

These workers found that the hydride in complexes **40** and **41** in Scheme 1.25 comes from one of the imidazolium NC*H*N moieties of the carbene precursor.[102]

Scheme 2.8 Attempted Preparation of M-H Bond in Single Step

M = Ni, Pd, Pt
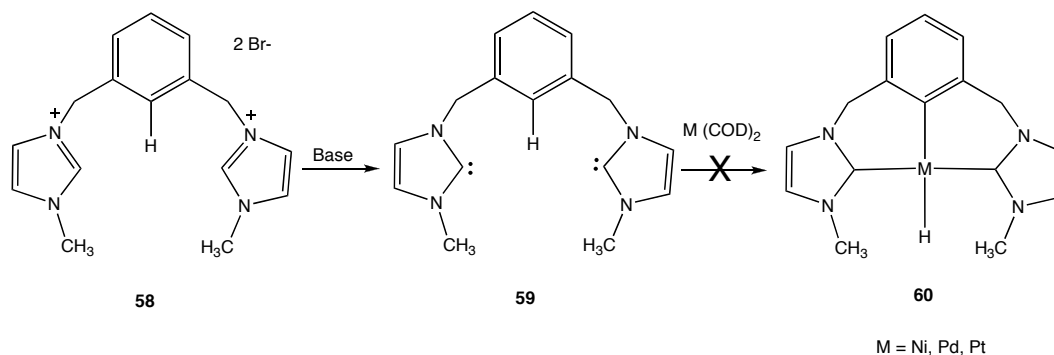
2.3   Alternative Routes to Pincer Carbene Pd-H

Alternatively, we hypothesized that pincer carbene metal bromides should react with silver nitrate (AgNO$_3$) to yield pincer carbene metal nitrates, M-ONO$_2$. If formed, we could then treat the nitrates with sodium methoxide (NaOMe) or sodium isopropoxide (NaO*i*Pr) to give pincer carbenes M-OMe or M-O*i*Pr, respectively, as proposed in Scheme 2.9Via this route we hoped to eventually reductively eliminate formaldehyde or acetone in order to obtain our desired pincer carbene M-H products. We proposed the route in Scheme 2.9 because the M-O bond in M-ONO$_2$ complexes is known to be quite labile; hence, it can dissociate more easily to give a vacant site on the metal complex and thus increase the reactivity. [109-111]

Scheme 2.9 Proposed Alternative Route to Pincer Carbene-M-H

$$L\text{-}M\text{-}Br \quad + \quad AgNO_3 \quad \xrightarrow{\text{- AgBr}} \quad L\text{-}M\text{-}ONO_2$$

$$L\text{-}M\text{-}ONO_2 \quad + \quad NaOMe \; or \; NaOiPr \quad \xrightarrow{\text{- NaNO}_3} \quad L\text{-}M\text{-}OMe \; or \; L\text{-}M\text{-}OiPr$$

$$L\text{-}M\text{-}OMe \; or \; L\text{-}M\text{-}OiPr \quad \xrightarrow{\text{- CH}_2O \; or \; (CH_3)_2CO} \quad L\text{-}M\text{-}H$$
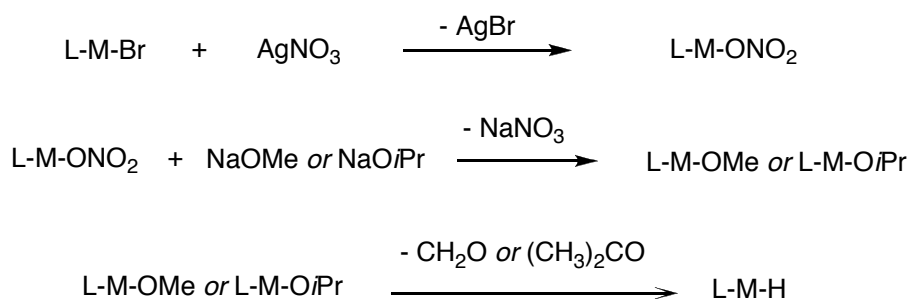
When ^{Me}CCC-Pd-Br **29** was treated with AgNO$_3$ in THF, an off-white solid was obtained in 62% yield (Scheme 2.10). Crystals suitable for single crystal X-ray analysis were obtained. However, the crystals were a mixture of **61** and, surprisingly, ^{Me}CCC-Pd-Cl **62** co-crystallized in a ratio of 4 to 6, respectively. X-ray analysis indicates that both **61** and **62** crystallize in the orthorhombic crystal system and space group Aba2. During refinement it was determined that the best fit of the data occurred with occupancies of the NO$_3$ at 37.1% and Cl at 62.9%, giving a total of 100% occupancy.

Scheme 2.10 Preparation of ^{Me}CCC-Pd-ONO$_2$ 61
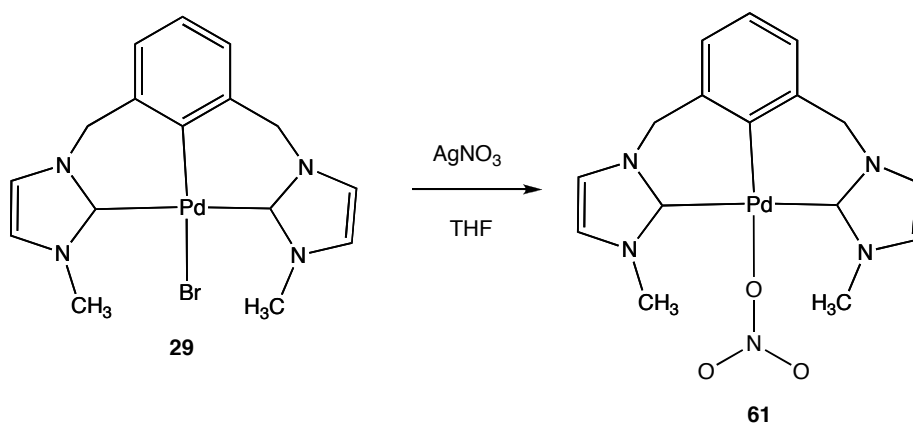
The structure of ^{Me}CCC-Pd-ONO$_2$ is shown in Figure 2.2 and selected bond distances and angles are listed in Table 2.1. The solid-state structure of **61** indicates that the nitrate group is bound in η^1 fashion to the Pd atom. The Pd-C bond in **61** is 2.009(4) Å and is almost identical to that seen in ^{Me}CCC-Pd-Br **29** (2.014(8) Å).[71] Notably, contrary to what we expected, the Pd-ONO$_2$ bond of 2. 084(2) Å in ^{Me}CCC-Pd-ONO$_2$ is significantly shorter than the Pd-Br bond (2.5388(10) Å) in ^{Me}CCC-Pd-Br **29**. The bond distances and angles within the nitrato group are very similar to other characterized pincer-based M-ONO$_2$ complexes and deserve no special remarks. The C1-Pd-ONO$_2$ angle of 167.6(3)° and C9-Pd1-C13 angle of 171.4(2)° show significant deviations from linearity and thus indicates that the complex exhibits a distorted square planar geometry.

Single crystal analysis of **61** indicates that the rings are strongly puckered, as are those of ^{Me}CCC-Pd-Br **29**.[71] For instance, the dihedral angle of **61** (C2-C1-Pd1-C9) is 41.1(4)° is quite similar to the dihedral angle of 42.9(7)° seen in **29**.[71] The ^{1}H NMR spectrum of **61** obtained in deuterated methanol (CD$_3$OD) is as expected very similar to ^{Me}CCC-Pd-Br **29**, with only slightly upfield shifts of the resonances from the CH$_2$ protons of the pincer arms and CH$_3$ protons that are attached to the imidazole ring. Introduction of the NO$_3^-$ group in the complex removed the symmetry that is observed when Br is attached to pincer carbene palladium complex as in **29**.

Figure 2.2 Thermal Ellipsoid Plot of ^{Me}CCC-Pd-ONO₂ 61 Shown at 50% Probability Level with Hydrogens Omitted for Clarity
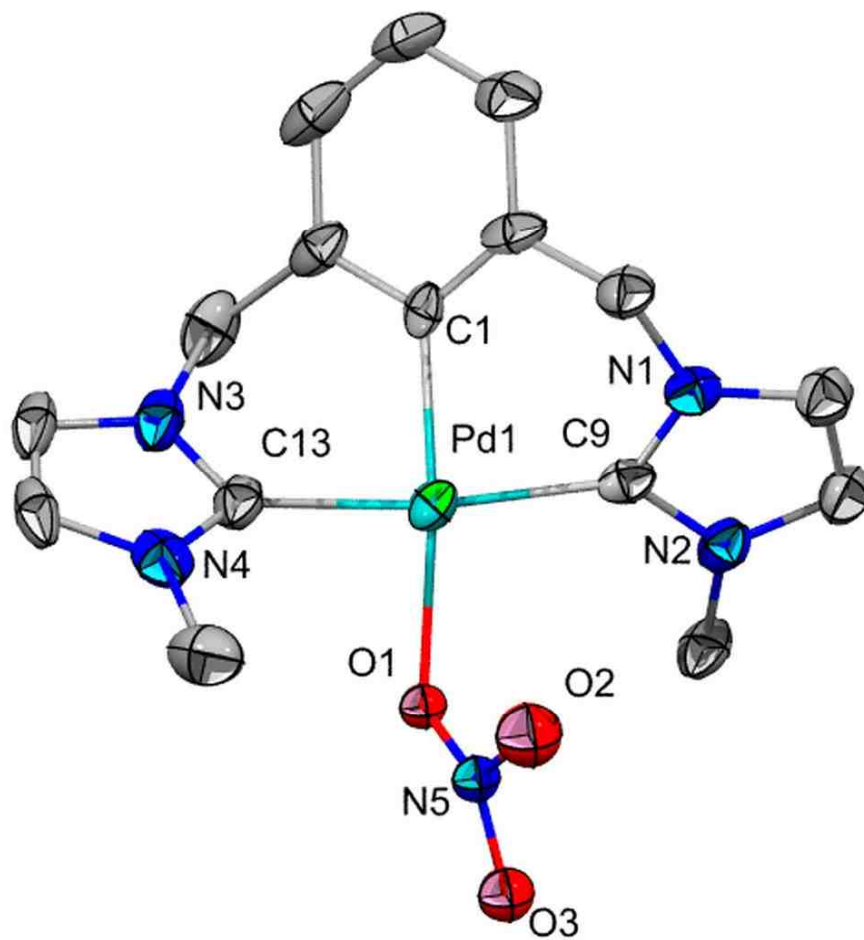
Table 2.1 Selected Bond Lengths and Angles for Compound 61

Bond lengths (Å)

Atom 1	Atom 2	Distances
Pd1	C1	2.009(4)
Pd1	C9	2.014(9)
Pd1	C13	2.022(8)
Pd1	O1	2.084(2)
Pd1	Cl1	2.278(2)
C13	N3	1.350(8)
C13	N4	1.338(9)
C9	N1	1.345(8)
C9	N2	1.378(8)
O1	N5	1.233(11)
N5	O2	1.236(11)
N5	O3	1.276(10)

Bond Angles (º)

Atom 1	Atom 2	Atom 3	Angle
C1	Pd1	O1	167.6(3)
C9	Pd1	C13	171.4(2)
N1	C9	N2	102.5(6)
N3	C13	N4	105.0(6)

Selected bond lengths and angles of compound **62** are listed in Table 2.2. The

structure of ^{Me}CCC-Pd-Cl is shown in Figure 2.2. C1-Pd-Cl1 angle of 178.73(14)° and

C9-Pd1-C13 angle of 171.4(2)° show deviations from linearity and thus indicate that the

complex exhibits a distorted square planar geometry as well.

Figure 2.3 Thermal Ellipsoid Plot of ^{Me}CCC-Pd-Cl 62 Shown at 50% Probability

Level with Hydrogens Omitted for Clarity
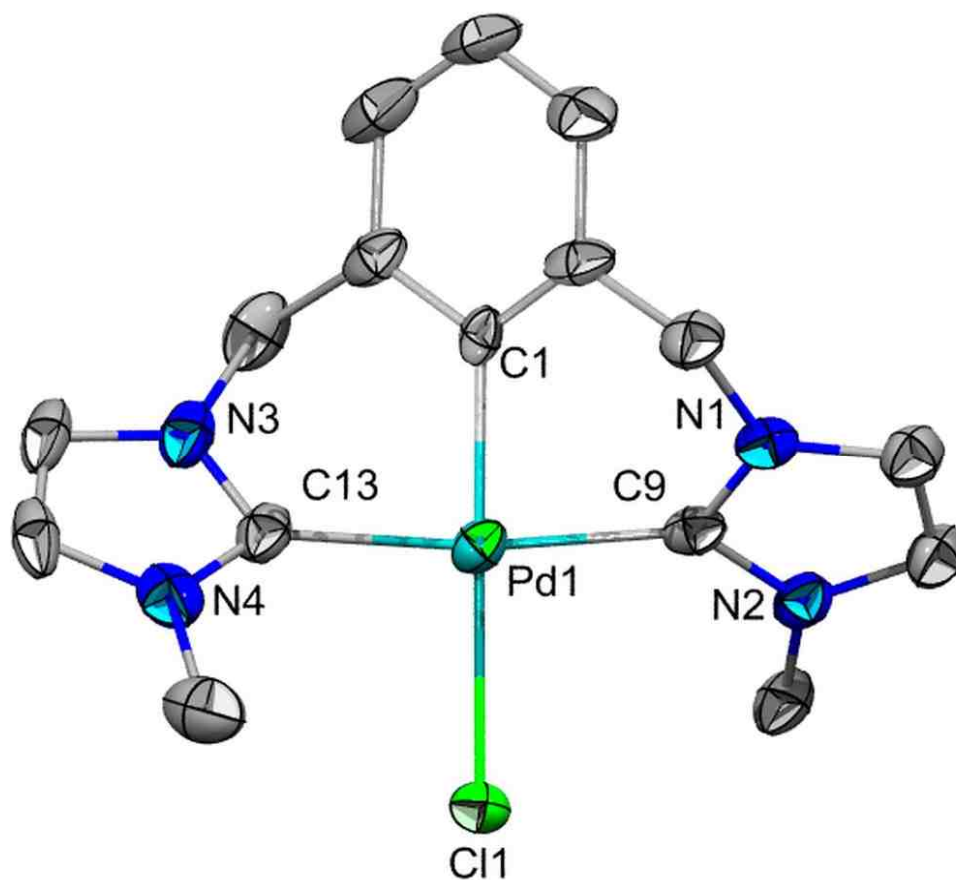
Single crystal analysis of **62** indicates that the rings are also strongly puckered as seen in **29**.[71] For instance, the dihedral angle of **62** (C2-C1-Pd1-C9) 41.1(4)° is similar to that of [Me]CCC-Pd-ONO$_2$ **61** and close to 42.9(7)° of **29**.[71] The Pd1-Cl1 bond distance of 2.278(2) Å is significantly shorter than that of Pd-Br in [Me]CCC-Pd-Br with bond distances of 2.5388(10) Å.[71] As is the case with [Me]CCC-Pd-ONO$_2$ **61** the Pd-C bond distances are within the previously reported values in the literature.[71] Although we started with [Me]CCC-Pd-Br as one of the starting materials, [Me]CCC-Pd-Cl **62** was also obtained unexpectedly. The only source of Cl$^-$ in this reaction is dichloromethane (CH$_2$Cl$_2$) that is used for purification of [Me]CCC-Pd-Br **61** and thus we speculate that to be the origin of the Cl$^-$ ion and the source of the formation of the [Me]CCC-Pd-Cl complex.

Although the crystals obtained were a mixture of [Me]CCC-Pd-ONO$_2$ **61** and [Me]CCC-Pd-Cl **62**, we reacted the mixture with NaOMe or NaO*i*Pr, hoping that **61** would react. However, there was no reaction observed.

Table 2.2 Selected Bond Lengths and Angles for Compound 62

Bond Lengths (Å)

Atom 1	Atom 2	Distances
Pd1	C1	2.009(4)
Pd1	C9	2.014(9)
Pd1	C13	2.022(8)
Pd1	Cl1	2.278(2)

Bond Angles (º)

Atom 1	Atom 2	Atom 3	Angle
C1	Pd1	O1	167.6(3)
C9	Pd1	C13	171.4(2)
N1	C9	N2	102.5(6)
N3	C13	N4	105.0(6)
Pd1	C1	Cl1	178.73(14)

2.4 Attempted Oxygen Insertion Reactions

Ideally, the most appealing route for investigation of the oxygen transfer abilities of metal hydroperoxides would be to first isolate the metal hydroperoxide, followed by reacting hydroperoxide with an organic substrate in the absence of other oxygen sources. Unfortunately, the isolation of carbene-ligated palladium hydroperoxide in proved problematic, experimentally decomposing to the corresponding hydroxides. Therefore, due to this reactivity, we decided to examine oxygen transfer by preparing the hydroperoxides *in situ* prior to the addition of organic substrates or in the presence of organic substrates. The disadvantage of this approach is the recognition that the actual oxygen transfer reagent becomes less clear.

Although it was extremely difficult to get rid of the borane impurities associated with the K-Selectride solution in the reaction shown in Scheme 2.4 which details the preparation of Pd-H **51**, oxygen insertion reactions were attempted despite the presence

of this impurity. We anticipated that while the borane impurity would react easily with

O_2, but we hoped that the M-H bond could also insert O_2 and we might be able to

spectroscopically identify the metal hydroperoxide. The general procedure involved

dissolving the ^{Me}CCC-Pd-H **51** in THF-d_8 solvent (Scheme 2.11), in a medium-walled

NMR tube equipped with 60 psig oxygen for 45 minutes. To ensure thorough mixing,

the tube was periodically shaken. This reaction was monitored by ^{1}H NMR spectroscopy.

^{1}H NMR spectrum indicated appearance of new resonances that can be assigned to

methylene (CH_2) protons as the Pd-H resonance slowly disappeared over a 36 hours

period. This clearly indicates that the Pd-H complex **51** was reacting with O_2. ^{1}H NMR

spectroscopy indicated that the ligand remained attached to the metal as shown by the

appearance of two sets of doublets assigned for the pincer arms' methylene protons at

slightly different chemical shifts (δ 4.71 ppm and δ 5.26 ppm) from the ^{Me}CCC-Pd-H

analog (δ 4.94 ppm and δ 5.14 ppm). However, it was difficult to positively identify the

Pd-OO*H* resonance by ^{1}H NMR and IR that would be seen in **63**. Unfortunately, crystals

suitable for X-ray analysis could not be grown.

Although we could not positively identify or confirm that there was an oxygen

insertion into the Pd-H bond, attempts to perform oxygen transfer reactions by waiting

until there was a complete disappearance of Pd-H resonance upon exposure to O_2 were

performed. To test this, we used cyclohexene, styrene and *t*-Butylisocyanide as the

organic substrates. Unfortunately, no epoxides or isocyanate could be identified as being

formed. These reactions were performed at room temperature and monitored by NMR

and/or GC/MS to determine the identities of the products.

Another approach attempted was to do *in situ* oxygen transfer reaction in which the Pd-H, organic substrate, and O_2 are put together in one flask. To ensure that the Pd-H **51** does not react with organic substrates, we first reacted compound **51** with *t*-Butylisocyanide prior to the addition of O_2 and immediately performed ^1H NMR analysis. Unfortunately, ^1H NMR spectrum indicated that the Pd-H resonance had disappeared. GC/MS also indicated no appearance of peaks associated with *t*-Butylisocyanate. The IR analysis of the crude product showed peaks at 3383 cm^{-1} and 1644 cm^{-1} that could be assigned to the N-H and N=C stretches, respectively. This indicates that *t*-Butylisocyanide has simply inserted into the Pd-H bond. However, when cyclohexene was added to ^{Me}CCC-Pd-H **51** in THF-d_8, NMR analysis indicated no reaction had occurred. The mixture was then pressurized to 60 psig O_2. ^1H NMR and GC/MS analyses did not show any appearance of peaks that could be assigned to cyclohexene oxide. Similar trends were observed with styrene, vinyltrimethylsilane and propylene. Compound **53** exhibited the same reactivity trends and similar spectroscopic results to **51**

Scheme 2.11 Proposed Route to ^{Me}CCC-Pd-OOH 63
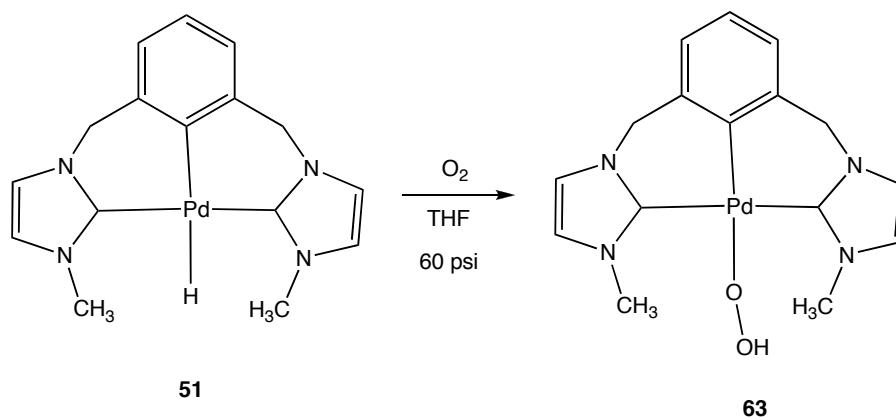
2.5   Alternative Route to ^{Me}CCC-Pd-OOH

Although this route would not use O_2 as oxidant and, hence, not be useful for our proposed catalytic cycle (Scheme 1.9), we decided to investigate the possibility of using H_2O_2 as oxidant in order to learn more about the possible formation and reactivity of ^{Me}CCC-Pd-OOH species. This need was due to our difficulty in preparing and isolating pincer carbene Pd-H species, particularly charged species. If we could prepare the desired hydroperoxide via alternative methods, it might allow the isolation of this new ^{Me}CCC-Pd-OOH species, and more importantly, it would provide means to study the oxygen transfer ability of such a complex. The first step in this alternative method involves the substitution of bromide with a more labile triflate group through reaction of the pincer carbene M-Br with AgOTf. This would then be followed by reaction of the obtained pincer carbene M-OTf with 30% H_2O_2/H_2O to generate the M-OOH complex (Scheme 2.12).

Scheme 2.12 Proposed Generalized Alternative Route to Pd-OOH

L-M-Br   +   AgOTf $\longrightarrow$ L-M-OTf   +   AgBr

L-M-OTf   + H_2O_2/H_2O $\longrightarrow$ L-M-OOH   +   TfOH
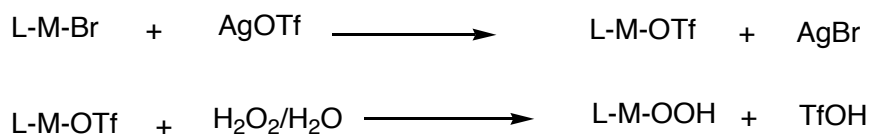
^{Me}CCC-Pd-OTf **64** was prepared by reacting ^{Me}CCC-Pd-Br with silver triflate (AgOTf) as proposed in Scheme 2.13. Compound **64** was obtained in 70% yield, and was obtained as colorless crystals after crystallization from THF.

Scheme 2.13 Preparation of ^{Me}**CCC-Pd-OTf 64**

Scheme 2.13 Preparation of ^{Me}**CCC-Pd-OTf 64**
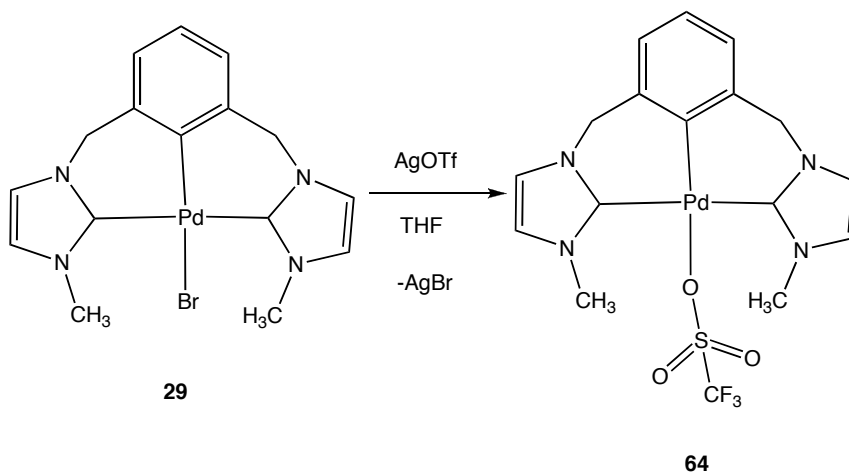
Compound **64** was characterized by ^{1}H NMR, ^{13}C NMR, and single crystal X-ray diffraction. Elemental analysis was also carried out with good results. The ^{1}H NMR spectrum of **64** obtained was similar to that of ^{Me}CCC-Pd-Br **29**. Surprisingly, the benzylic CH$_2$ protons in ^{Me}CCC-Pd-OTf **64** appear as broad singlets at δ 5.22 and δ 4.96 in the ^{1}H NMR spectrum while the benzylic protons in ^{Me}CCC-Pd-Br **29** appear as a sharp AB pattern at δ 5.47 and δ 4.66.

Figure 2.4 Structure of the Atropisomerization Process ^{Me}**CCC-Pd-Br and [**^{Me}**CNC-Pd-Br]Br (E = C, N)**[71]
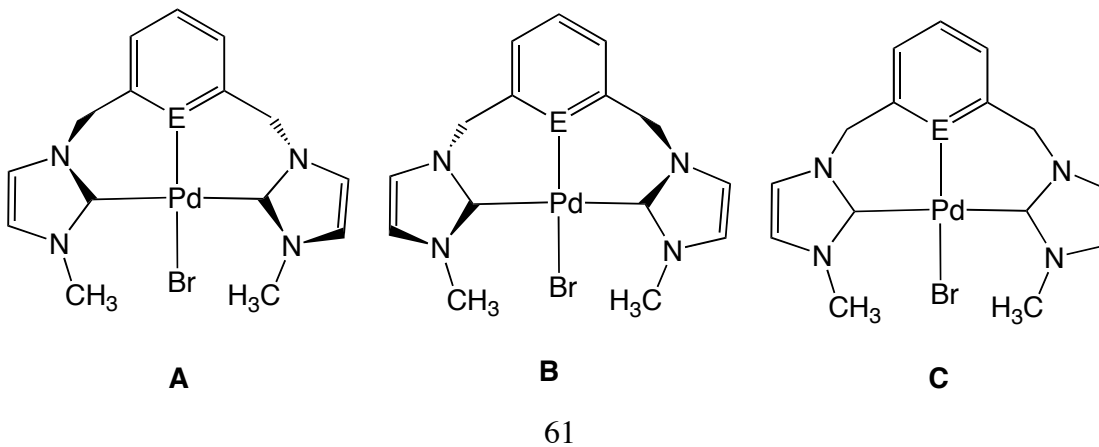
This phenomenon has been reported previously using [^{Me}CNC-Pd-Br]Br **22**.[71] Studies on variable temperature demonstrate that these protons are undergoing a dynamic process. Gründemann and co-workers report the occurrence of interconversion between left and right hand twisted structures with a corresponding chirality change of complex as shown in Figure 2.4.[71] This phenomenon leads to repositioning of all the three rings at the fast exchange limit so that only an averaged structure C is observed. This averaged structure has C_{2v} symmetry with equivalent benzylic protons.[71] The ^{13}C NMR spectrum of **64** is also similar to that of ^{Me}CCC-Pd-Br **29** except that there is now a quartet present with $^1J_{C-F}$ coupling of 321.93 Hz, typical of carbon that is directly attached to a fluorine. We obtained the crystal structure of ^{Me}CCC-Pd-OTf, **64**, and it is shown in Figure 2.5. Analysis shows that **64** crystallizes in the triclinic crystal system and a space group P-1. Selected distances and bond lengths of **64** are listed in Table 2.3.

The solid-state structure of compound **64** shows that the triflate group is attached in η^1 fashion to the Pd atom. The bond distances and angles within the TfO⁻ group are very similar to other characterized pincer ligated Pd-OTf complexes and as such need no special remarks. The angles C1-Pd1-O1 and C10-Pd1-C11 are 176.41(17) and 171.81(19)°, respectively, and show slight deviations from linearity, suggesting that the complex contains a distorted square planar geometry. The angles N1-C11-N2 and N3-C10-N4 are 105.0(4) and 104.1(4)°, respectively.

Figure 2.5 Thermal Ellipsoid Plot of ᴹᵉCCC-Pd-OTf 64 Shown at 50% Probability Level with Hydrogens Omitted for Clarity
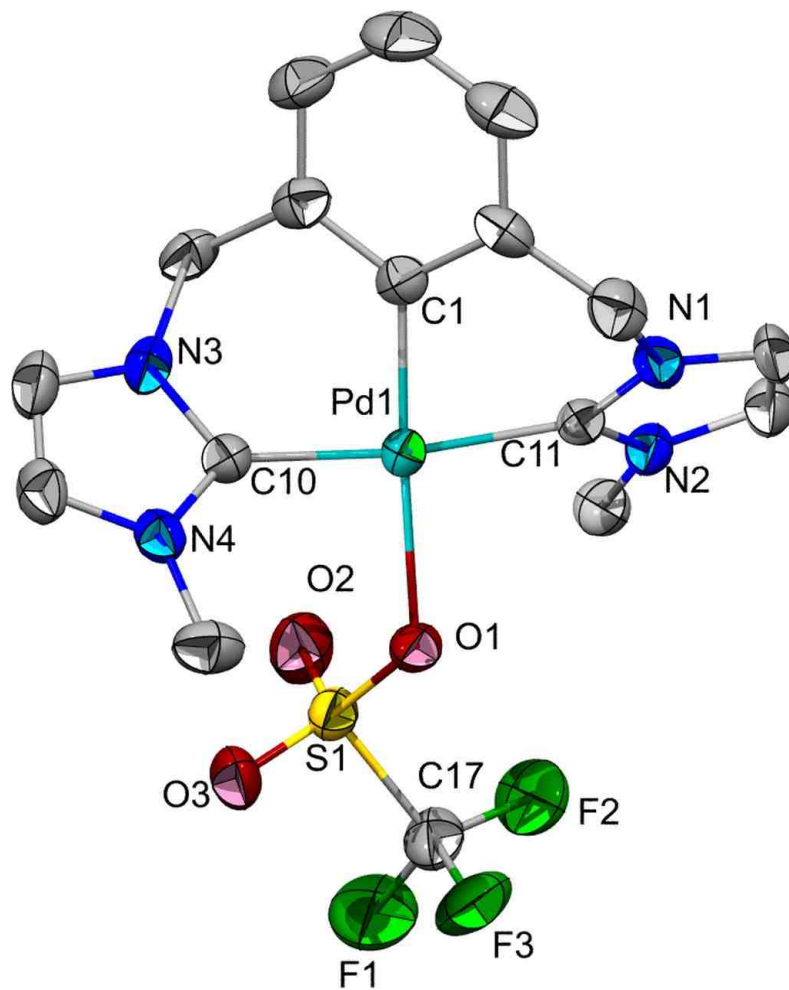
Table 2.3 Selected Bond Lengths and Angles for Compound 64

Bond Lengths (Å)

Atom 1	Atom 2	Distances
Pd1	C1	1.980 (5)
Pd1	C10	2.028(5)
Pd1	C11	2.028(5)
Pd1	O1	2.221(3)
C10	N3	1.354(6)
C10	N4	1.345(7)
C11	N1	1.353(6)
C11	N2	1.347(8)
O1	S1	1.457(3)
S1	O2	1.433(5)
S1	O3	1.433(5)
C17	S1	1.827(6)
C17	F1	1.319(7)
C17	F2	1.322(9)
C17	F3	1.318(8)

Bond Angles (º)

Atom 1	Atom 2	Atom 3	Angle
C1	Pd1	O1	176.41(17)
C10	Pd1	C11	171.81(19)
N1	C11	N2	105.0(4)
N3	C10	N4	104.1(4)

The single crystal X-ray structure of **64** shows that the three rings are strongly puckered, similarly to the reported structure of **29** [71] and our newly isolated ^{Me}CCC-Pd-ONO$_2$ **61** and ^{Me}CCC-Pd-Cl **62** complex. The C1-Pd1 bond is 2.220(3) Å and the Pd-O1 bond length is 1.981(5) Å, while the C10-Pd1 and C11-Pd bond lengths are both 2.028(5) Å. The 41.7(4)° dihedral angle of **64** (C6-C1-Pd1-C10) is very similar to that of **29** containing strongly puckered rings.[71] As well, the solid structure of **64** also indicates that there are two crystallographically-distinct molecules in the asymmetric unit that each contains two THF solvent molecules.

As proposed in the route shown in Scheme 2.12, a key aspect of this approach is to react ^{Me}CCC-Pd-OTf **64**, with 30% H$_2$O$_2$/H$_2$O in order to prepare the Pd-OOH species. This was achieved by suspending ^{Me}CCC-Pd-OTf **64**, in a 1:1 ratio of THF/ether, followed by the addition of 30% H$_2$O$_2$/H$_2$O. The reaction was very rapid, yielding a colorless solution. Crystals suitable for single crystal X-ray analysis were formed after 1 day. Analysis of crystals by X-ray diffraction yielded structure **65** (^{Me}CCC-Pd-OH) with a molecule of triflic acid (TfOH) also present in the structure. Analysis also shows that **65** crystallizes in the triclinic crystal system and a space group P-1. Unexpectedly, the desired ^{Me}CCC-Pd-OOH **66** complex was not formed in at least a stable state, but rather the hydroxide was isolated. Despite the fact that **66** could not be isolated, it is very likely that it was initially formed slowly decomposed to ^{Me}CCC-Pd-OH **65** by loss of an oxygen atom over the 24 hours period. This loss of O atom has previously been observed in our group in ^{tBu}PCP-Pd-OOH in which decomposition over 24-36 hours slowly formed ^{tBu}PCP-Pd-OH.[59] The cyclohexyl analog (^{cy}PCP-Pd-OOH) also showed a similar

reactivity pattern. In both of these systems, the fate of missing oxygen atom is unknown and warrants further investigation, but is very likely O_2.

Scheme 2.14 Preparation of ^{Me}CCC-Pd-OH 65
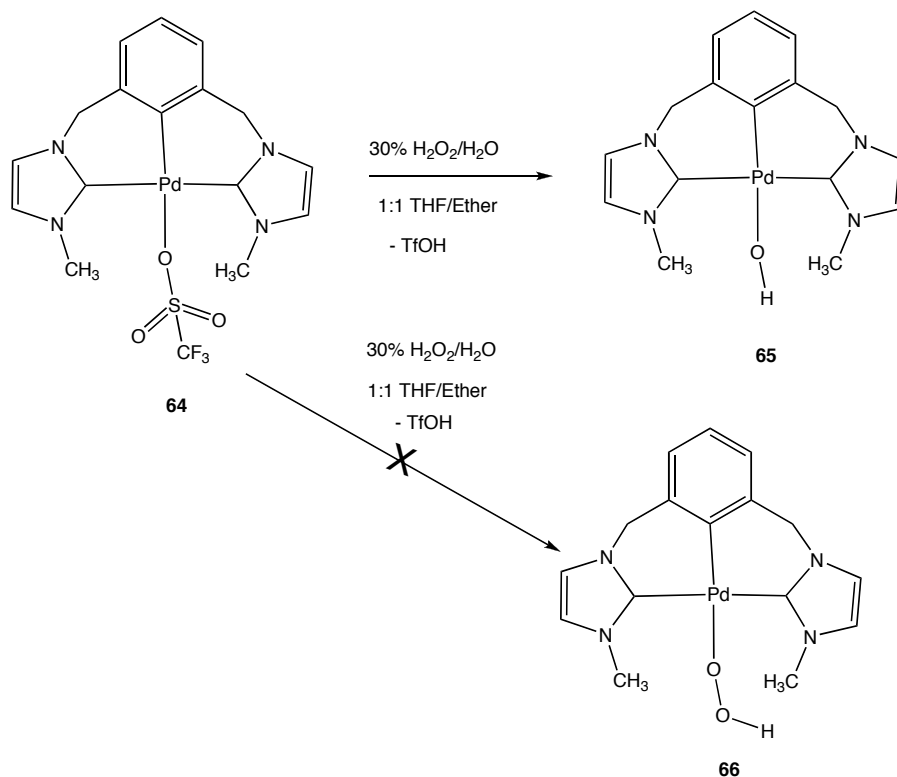
In order to rule out the possibility that ^{Me}CCC-Pd-OTf **64** might react with H_2O to form ^{Me}CCC-Pd-OH **65**, water was deliberately added to a flask containing ^{Me}CCC-Pd-OTf **63** suspended in a 1:1 ratio of THF/ether. Compound **64** showed no reactivity with H_2O, thus suggesting that the -OH group in Pd-OH is not originating from water.

The ^{1}H NMR spectral analysis of ^{Me}CCC-Pd-OH **65** was very similar to that of ^{Me}CCC-Pd-Br **29**. However, it was difficult to positively identify the Pd-OH resonance in

the ^{1}H NMR spectrum. In an attempt to prepare the Pd-H, we reacted **65** with H$_2$ to try to force elimination of H$_2$O (Scheme 2.15). Furthermore, the attempted preparation of ^{Me}CCC-Pd-OH by deliberate reaction of ^{Me}CCC-Pd-Br **29** with KOH was unsuccessful. There was also no reaction between ^{Me}CCC-Pd-Br **29** and H$_2$O$_2$/H$_2$O. The solid-state structure of ^{Me}CCC-Pd-OH **65** is shown in Figure 2.6 and the selected bond lengths and bond angles are listed in Table 2.4. According to a recent search in Cambridge Crystallographic Database (CSD version 5.31, May 2010 update), there are no reported pincer carbene-containing M-OH complexes, and our complex **65** is the first example. The Pd1-C1, Pd-C10, and Pd1-C12 bond lengths in **65** are 2.009(8) Å, 2.031(7) Å, and 2.022(7) Å, respectively. These bond lengths are similar to those reported for compound **29** and as such deserve no special remarks. Lastly, the Pd1-O1 bond length is 2.194(5) Å with a O1-H1A bond length of 0.830 Å.

Scheme 2.15 Attempt to Prepare ^{Me}CCC-Pd-H 51 by reacting 65 with H$_2$ (g)
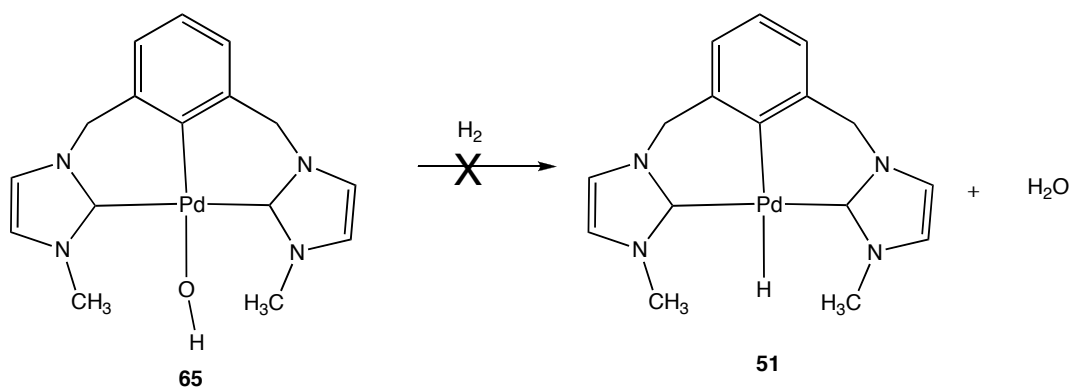
Figure 2.6 Thermal Ellipsoid Plot of ^{Me}CCC-Pd-OH 65 Shown at 50% Probability

Level with Hydrogens Omitted for Clarity
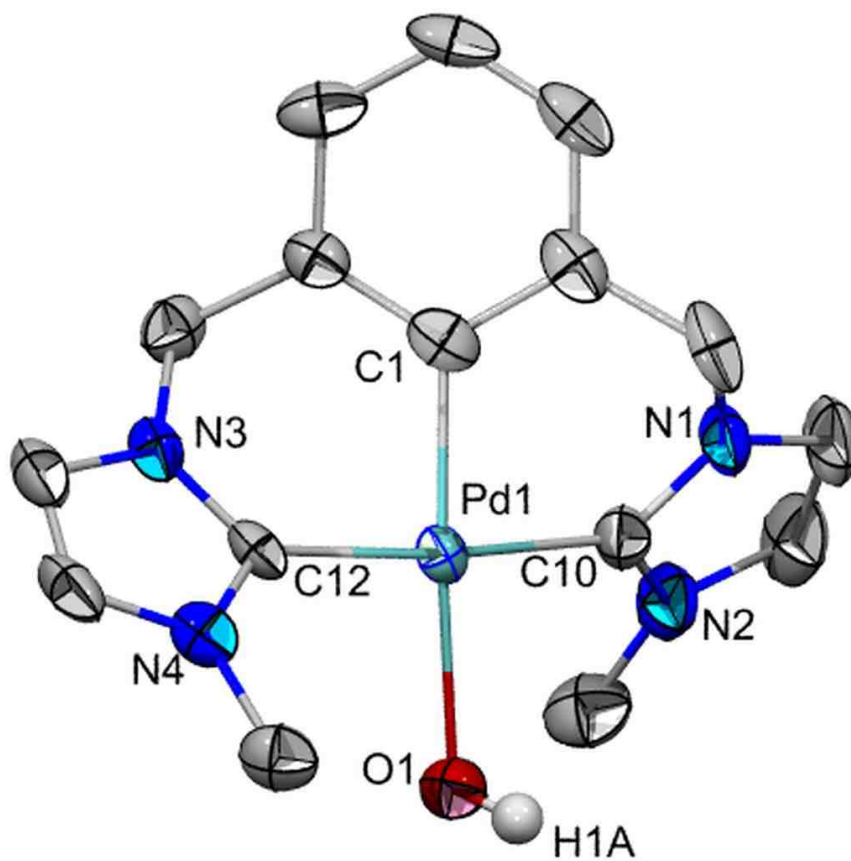
Table 2.4 Selected Bond Lengths and Angles for Compound 65

Bond Lengths (Å)

Atom 1	Atom 2	Distances
Pd1	C1	2.009(8)
Pd1	C10	2.031(7)
Pd1	C12	2.022(7)
Pd1	O1	2.194(5)
C10	N1	1.353(10)
C10	N2	1.368(10)
C12	N3	1.351(9)
C12	N4	1.353(9)
O1	H1A	0.830

Bond Angles (°)

Atom 1	Atom 2	Atom 3	Angle
Pd1	C1	O1	176.7(3)
Pd1	C10	C12	174.1(3)
N3	C12	N4	104.4(6)
N1	C10	N2	104.5(6)

Interestingly, when the charged complex [^{Me}CNC-Pd-Br]Br **19** was reacted with AgOTf in an attempt to replace the two bromides with triflates in order to further react it with 30% H_2O_2/H_2O as shown in Scheme 2.16. However, only the counterion Br⁻ exchanged, forming [^{Me}CNC-Pd-Br]OTf **67**.

Scheme 2.16 Preparation of [CNC-Pd-Br]OTf 67
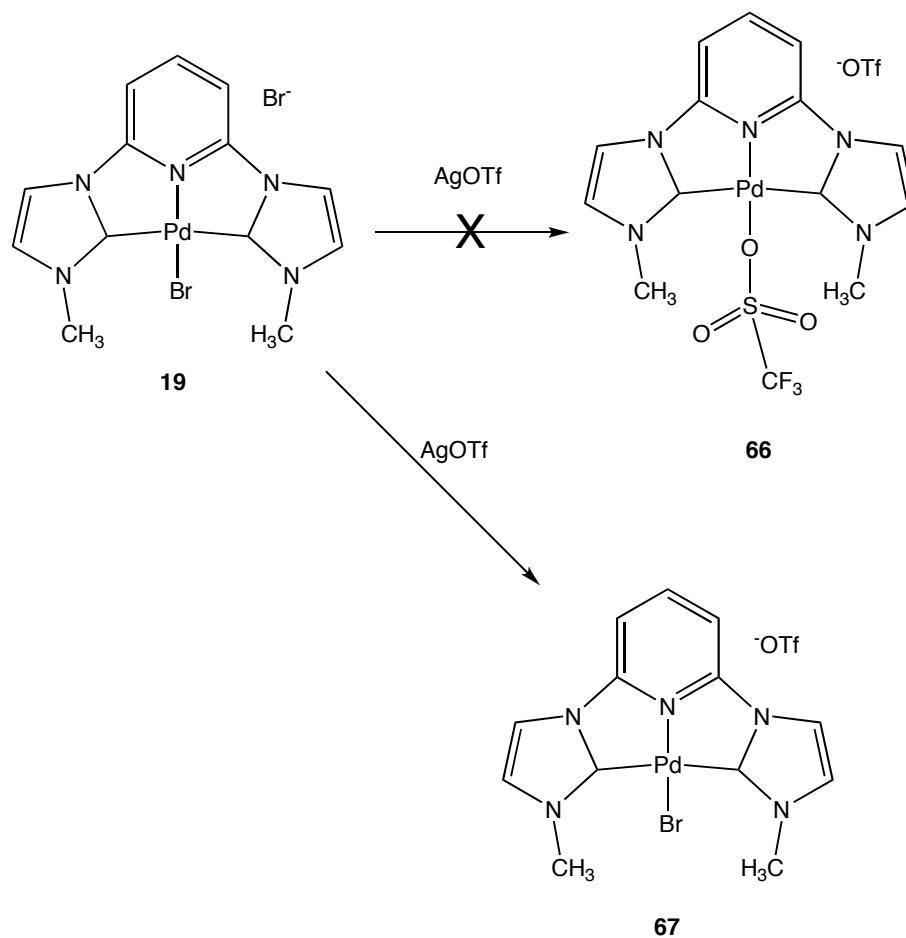
This occurred even after refluxing the reaction mixture overnight. Further reaction of **67** with excess AgOTf never produced the desired product [^{Me}CNC-Pd-OTf]OTf. X-ray analysis indicates that **67** crystallizes in monoclinic crystal system and space group P2(1)/n. Selected bond lengths and angles for compound **67** are listed in Table 2.5. All angles and bonds within the [^{Me}CNC-Pd-Br]$^+$ core are very similar to [^{Me}CNC-Pd-Br]Br and thus deserve no detailed comments. However, having TfO$^-$ as the counterion improved the solubility of the complex significantly.

70

Table 2.5 Selected Bond Lengths and Angles for Compound 67

Bond Lengths (Å)

Atom 1	Atom 2	Distances
Pd1	C13	2.026(5)
Pd1	C12	2.053(5)
Pd1	Br1	2.4165(7)
Pd1	N5	1.983(4)
S1	O1	1.430(5)
S1	C21	1.820(7)
S1	O2	1.433(4)
S1	O3	1.432(5)
C21	F1	1.339(7)
C21	F2	1.329(8)
C21	F3	1.332(8)

Bond Angles (º)

Atom 1	Atom 2	Atom 3	Angle
C13	Pd1	C12	158.26(2)
N5	Pd1	Br1	179.32(11)
N3	C13	N1	104.4(4)
N4	C12	N2	103.9(4)

Figure 2.7 Thermal Ellipsoid Plot of [^{Me}CNC-Pd-Br]OTf 67 Shown at 50%

Probability Level with Hydrogens Omitted for Clarity
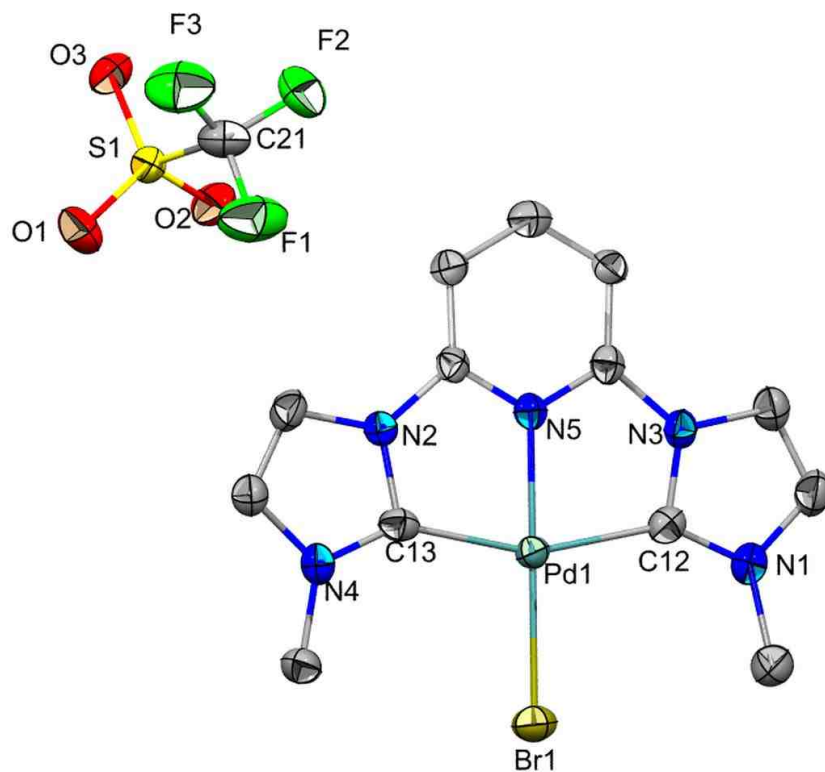
2.6 Summary

The main efforts reported in this chapter were to prepare a variety of pincer carbene Pd-H

complexes and investigate their abilities to activate molecular O_2 for the purpose of

oxidizing alkenes and other organic substrates. Non-pincer carbene Pd-H complexes are

known to reductively eliminate the ligand and form Pd^0. The pincer carbene Pd-H

species were prepared by converting the precursor Pd-Br by using K-Selectride reagent in

THF. Pincer carbene Pd-Br complexes containing large R groups on the imidazole rings

did not convert to Pd-H complexes upon use of various hydride sources. This might be

due to the bulkiness of the R groups that prevents the approach of the hydride reagent.

The problems in converting M-Br to M-H mirrored our group's previous difficulties in

PCP-pincer chemistry.[112] The synthesized hydrides **51** and **53** appear to react with O_2;

however, it was difficult to isolate and conclusively identify the products. *In situ* oxygen

atom transfer attempts proved unsuccessful. Alternative routes to the generation of M-H

complexes were also attempted and resulted in isolation of the previously-unknown

complex ^{Me}CCC-Pd-ONO$_2$ **61**. Unfortunately, this species did not react further with

either NaOMe and NaOiPr in attempts to produce Pd-H complexes by elimination route.

In addition, an alternative route to Pd-OOH also did not result in the desired pincer

carbene Pd-OOH complex. Unexpectedly, yet quite interestingly, the complex ^{Me}CCC-

Pd-OH **65** was isolated. ^{Me}CCC-Pd-OH is a new compound and is the first example of a

pincer carbene metal hydroxide. **65** was completely characterized by ^{1}H NMR and X-ray

diffraction. We speculate that ^{Me}CCC-Pd-OOH is likely formed first and then slowly

decomposes to form ^{Me}CCC-Pd-OH **65**, a phenomenon that has been observed in other

pincer Pd-OOH complexes.[59] There were significant synthetic challenges in attempting to convert the charged [CNC-Pd-Br]$^+$ cation to a Pd-H complex. Upon use of multiple hydride sources, in all cases the Pd-Br complexes led to decomposition upon addition of the hydride reagent. Alternative routes to Pd-H relying on elimination of formaldehyde or acetone also gave disappointing results, as did reaction of **65** with H_2. Lastly, the ion exchange reaction shown in Scheme 2.16 led to the exchange of only one Br$^-$ (outer sphere) and not the bound Pd-Br (inner sphere). Based on the multiple routes attempted in the work to prepare these changed hydride species, we can conclude that these species will exist only rarely.

2.7   Experimental

2.7.1 General Experimental Procedures

Chemical manipulations and all procedures were carried out in an Ar-filled dry box or using standard Schlenk inert atmosphere techniques. High-purity anhydrous solvents were either used as received or dried using standard techniques prior to use. Except as noted all reagents were purchased from commercial sources (Aldrich, Alfa, or Acros) and used without further purification. All solvents were purchased as anhydrous grade. Multinuclear NMR spectral data were collected either on a Bruker AMX 250 MHz spectrometer with Tecmag MacSpect upgrade, or on Bruker Avance 500 MHz spectrometer. Infrared spectra were collected on Bruker Vector 22 instrument using

Nujol mulls or KBr plates. Elemental analyses were performed by Columbia Analytical Services, Tucson, AZ.

The imidazolium salts **26**[76] and **27**[71] and the benzimidazolium salt **28**[72] were prepared according to literature routes.

2.7.2 Crystallographic Studies

Crystallographic data were collected on a standard Bruker X8 *APEX* CCD- based X-ray diffractometer using monochromated Mo-K$_\alpha$ radiation ($\lambda = 0.71073$ Å). Dr. Diane Dickie of the Kemp group and Dr. Eileen Duesler of the University of New Mexico provided additional data handling and solving. Crystals were mounted on nylon cryoloops obtained from Hampton Research using Paratone-N® oil. The data were collected and processed using the Bruker *APEX2* suite of programs, and the *SADABS* program was used to correct for Lorentz polarization effect and absorption.[113] Structures were solved by direct method and refined by full matrix least-square method on F^2 with *SHELXTL*.[114] Non-hydrogen atoms were refined anisotropically and hydrogen atoms bound to carbon were fixed in calculated positions. Crystallographic data collection and parameters and refinement data are collected in Appendix 1. The thermal ellipsoid plots were prepared using Diamond software (version 3.2e).[115]

2.7.3 Syntheses of Pincer Carbene Palladium Complexes

[^{Me}CNC-Pd-Br]Br **19**

The synthetic procedure followed that reported by Peris and co-workers[76] using the following quantities of reagents: ligand **26** (X = Br; R = Me) (0.900 g, 2.25 mmol), Pd(OAc)$_2$ (0. 500 g, 2.23 mmol). The yield of **19** as a grey solid was 0.401 g (40%). ^{1}H NMR data matched the previously reported values. [^{Me}CNC-Pd-Br]Br **19** was then used without further purification.

[^{nBu}CNC-Pd-Br]Br, **20**

The synthetic procedure followed that reported by Loch and co-workers[95] using the following quantities of reagents: ligand **26** (X = Br; R = *n*-Butyl) (0.485 g, 1.00 mmol), Pd(OAc)$_2$ (0.224 g, 1.00 mmol). The yield of **20** as a yellow solid was 0.310 g (52%). ^{1}H NMR data matched the previously reported values. [^{nBu}CNC-Pd-Br]Br, **20** was then used without further purification.

^{Me}CCC-Pd-Br **29**

The procedure followed that reported by Gründemann and co-worker[71] using the following quantities of reagents: ligand **27** (2.220 g, 2.18 mmol), [Pd$_2$(dba)$_3$] (0.200 g, 1.09 mmol), and Na$_2$CO$_3$ (0.186 g, 8.74 mmol). The yield of **29** as an off-white solid was

3.90 g (40%). The ^{1}H NMR data matched the previously reported values. Compound **29** was then used without further purification.

Benzimidazolin-2-ylidene-Based CCC-Pd-Br complexes 52 and 54

^{Et}CCC-Pd-Br **52**

A general synthetic procedure followed that reported by Hahn and co-workers[72] using the following quantities of reagents:ligand **28** [X = Br; R = Et], (0.195g, 0.300 mmol), *n*-BuLi, (0.062mL, 0.660 mmol) and [Pd$_2$(dba)$_3$], (0.137g, 0.150 mmol). The yield of **52** was 0.120 g (64%). NMR data matched the previous reported values. Compound **52** was used without further purification.

$^{n\mathrm{Bu}}$CCC-Pd-Br **54**

A general synthetic procedure followed that reported by Hahn and co-workers[72] using the following quantities of reagents:ligand **28** [X = Br; R = *n*Bu], (0.212g, 0.300 mmol), *n*-BuLi, (0.062mL, 0.660 mmol) and [Pd$_2$(dba)$_3$], (0.137g, 0.150 mmol). The yield of **54** was 0.131 g, (69%). NMR data matched the previous reported values. Compound **54** was used without further purification.

^{DiPP}*CCC-Pd-Br* **55**

A general synthetic procedure followed that reported by Danopoulos and co-workers[116] using the following quantities of reagents:ligand **27** [X = Br; R = D*i*PP], (0.16g, 0.200 mmol), NaCOOCH$_3$ (0.25 g, excess) and [Pd$_2$(dba)$_3$], (0.080 g, 0.100 mmol). The yield of **55** was 0.090 g (60%). NMR data matched the previous reported values. Compound **55** was used without further purification.

^{Me}*CCC-Pd-H* **51**

^{Me}CCC-Pd-Br **23** (0.030 g, 0.066 mmol) was placed in a 50 ml Schlenk flask containing THF (20 ml) and cooled to -78 °C. The flask was sealed with a rubber septum. K-Selectride (0.066 ml of a 1M solution in THF) was added via a syringe to the flask. The suspension was allowed to warm to ambient temperature and was stirred for one hour, during which time everything went into solution. The solvent was removed under vacuum to give an oily solid. The solid was washed repeatedly with hexanes (10 ml x 3) and dried *in vacuo*. The yield of the oily solid was 0.021 g (80%). ^{1}H NMR (500 MHz), (THF-d_8): δ -10.8 (s, Pd-H1, 1H), 3.95 (s, N-CH$_3$, 6H), 4.94 (d, $^2J_{\text{H-H}}$ = 14 Hz, Ar-CHHN, 2H) 5.14 (d, $^2J_{\text{H-H}}$ = 14 Hz, Ar-CHHN, 2H), 6.86 (t, $^3J_{\text{H-H}}$ = 7.5 Hz, Ar-H, 1H), 6.96 (s, $^3J_{\text{H-H}}$ = 1.5 Hz, imidazole H, 2H), 7.03 (d, $J_{\text{H-H}}$ = 7.5, Ar-H, 2H), 7.27 (s, $^3J_{\text{H-H}}$ = 1.5 Hz, imidazole H, 2H); IR = 1770 cm^{-1} (Pd-H stretch).

Benzimidazolin-2-ylidene-Based [Et]CCC-Pd-H 53

[Et]CCC-Pd-Br **52** (0.050 g, 0.086 mmol) was placed in 50 ml Schlenk flask containing

THF (20 ml) and cooled at -78 °C. The flask was sealed with a rubber septum. K-

Selectride (0.090 ml of a 1M solution in THF) was added drop wise via a syringe to the

flask. The suspension was left to warm to ambient temperature and allowed to stir for

one hour during which time everything went into solution. All the solvent was removed

in vacuo yielding **53** as orange-brown solid. The solid was then washed repeatedly with

hexane (10 ml x 3) followed by drying *in vacuo*. The yield of yellow solid was 0.035 g

(82%). ^{1}H NMR (500 MHz), (THF-d_8): δ -8.0 (s, Pd-H, 1H) 1.60 (t, N-CH$_2$CH$_3$, 6H),

4.78-4.60 (m, N-CH$_2$CH$_3$, 2H), 5.20 (d, $^3J_{H-H}$ = 13.8 Hz, Ar-CHHN, 2H), 5.50 (d, $^3J_{H-H}$ =

13.8 Hz, Ar-CHHN, 2H), 7.00 – 6.78 (m, Ar-H, 1H), 7.37 - 7.06 (m, Ar-H, 7H), 7.52 -

7.38 (m, Ar-H, 3H).

[Me]CCC-Pd-ONO$_2$ 61

[Me]CCC-Pd-Br **29** (0.030 mg, 0.066 mmol) was placed in 50 ml Schlenk flask containing

THF (20 ml) forming a suspension. This was followed by addition of AgNO$_3$ (0.017 g,

0.099 mmol). The mixture was allowed to stir for 12 hours. AgBr was removed by

filtration through a medium frit. All the solvent was removed *in vacuo* yielding **61** as off-

white solid. Crystals were obtained by recrystallization in mixture of THF and ether.

The yield of the solid was 0.018 g (62%) ^{1}H NMR (250 MHz), (DMSO-d_6): δ 3.92 (s,

NCH$_3$, 6H), 4.96 (d, $^3J_{H-H}$ = 13.8 Hz, Ar-CHHN, 2H), 5.35 (d, $^3J_{H-H}$ = 13.8 Hz, Ar-CHHN,

2H), 6.86 (t, $^3J_{\text{H-H}}$ = 7.55, Ar-H, 1H), 6.99 (d, $^3J_{\text{H-H}}$ = 7.15 Hz, Ar-H, 2H), 7.04 (s, $^3J_{\text{H-H}}$=

1.5 Hz, imidazole H, 2H) 7.32 (s, $^3J_{\text{H-H}}$=1.5 Hz, imidazole H, 2H). ^{13}C NMR: δ 38.13 (N-

CH$_3$) 58.87 (Ar-CH$_2$-N), 122.45 (imidazole C), 123.0 (imidazole C), 123.7 (C$_{\text{para}}$), 126.9

(C$_{\text{meta}}$), 141.1 (C$_{\text{ortho}}$), 143.56 (C$_{\text{ipso}}$) 176.82 (NCN), IR = 1467 cm^{-1}, 1297 cm^{-1}and 931 cm^{-1}

(Pd-ONO$_2$ stretches).

^{Me}CCC-Pd-OTf **64**

^{Me}CCC-Pd-Br (0.100 g, 0.22 mmol) and AgOTf (0.565 g, 0.22 mmol) were added to a

flask containing 15 ml THF. The mixture was stirred for 4 h at room temperature.

Filtration was done to remove AgBr and the filtrate left to crystallize. The yield of

colorless crystals suitable for single crystal analysis was 0.082 g (70%). ^{1}H NMR (250

MHz), (DMSO-d_6): δ 3.82 (s, N-CH$_3$, 6H), 4.96 (broad, Ar-CHHN, 2H), 5.22 (broad, Ar-

CHHN, 2H), 6.82 (t, $^3J_{\text{H-H}}$ = 7.55 Hz, Ar-H, 1H), 6.97(d, $^3J_{\text{H-H}}$ = 7.15 Hz, Ar-H, 2H), 7.23

(s, $^3J_{\text{H-H}}$ = 1.5 Hz, imidazole H, 2H), 7.50 (s, $^3J_{\text{H-H}}$=1.5 Hz, imidazole H, 2H). ^{13}C NMR:

δ 37.13 (N-CH$_3$). 56.99 (Ar-CH$_2$-N), 121.45 (imidazole C), 122.0 (imidazole C), 123.0

(C$_{\text{para}}$), 123.4, q, (CF$_3$) ^{1}J$_{\text{C-F}}$= 321.93 Hz, 125.5 (C$_{\text{meta}}$), 141.1 (C$_{\text{ortho}}$), 144.78 (C$_{\text{ipso}}$), 175.28

(NCN). Anal. Calcd for **64**; C, 39.05; H, 3.66; N, 10.72. Found: C, 38.94; H, 3.30; N,

9.97.

*Me*CCC-Pd-OH **65**

*Me*CCC-Pd-OTf **63** (0.020 g, 0.040 mmol) was suspended in 1:1 THF/ether mixture followed by addition of 30% H_2O_2/H_2O (0.15 ml, 0.045 mmol). The solution was left to stir for 2 hours. The solution was allowed to crystallize at room temperature. The yield of the crystals was (10 mg, 62%). ^{1}H NMR (250 MHz), (CD$_3$OD): δ 3.95 (s, N-CH$_3$, 6H), 4.99 ((broad), Ar-CHHN, 2H), 5.32((broad) Ar-CHHN, 2H), 6.79 (d, $^3J_{H-H}$ = 7.15 Hz, Ar-H, 2H), 6.89 (t, $^3J_{H-H}$ = 7.55, Ar-H, 1H,) 7.23 (s, $^3J_{H-H}$= 1.5 Hz, imidazole H, 2H), 7.50 (s, $^3J_{H-H}$ = 1.5 Hz, imidazole H, 2H).

[*Me*CNC-Pd-Br]OTf **67**

[*Me*CNC-Pd-Br]Br **19** of (0.050 g, 0.098 mmol) and AgOTf (0.053 g, 0.206 mmol) were added to a flask containing MeOH (15 ml). The flask was then fitted with a reflux condenser and allowed to reflux overnight. AgBr was removed by filtration through a medium filter frit. The solvent was removed *in vacuo*, to obtain a yellow solid. Yellow block-shaped crystals suitable for single crystal analysis were obtained after recrystallization of **67** in MeOH. The yield of the solid was 0.052 g (93%). ^{1}H NMR (250 MHz), (CD$_3$OD): δ 3.99 (s, N-CH$_3$, 6H), 7.53 (d, $^3J_{H-H}$ -1.5 Hz, imidazole H, 2H), 7.83, (d, $^3J_{H-H}$ = 8.34 Hz, Ar-H, 2H,), 8.18 (d, $^3J_{H-H}$ = 1.5 Hz, imidazole H, 2H), 8.46 (t, $^3J_{H-H}$ = 8.30 Hz, Ar-H, 1H). ^{13}C NMR, CD$_3$OD: δ 38.00 (NCH$_3$) 110.20 (imidazole-C), 119.22 (imidazole C), 123.12, q, (CF$_3$) $^1J_{C-F}$ = 327.49 Hz, 126.21 (C$_{para}$), 148.70 (C$_{meta}$), 153.14 (C$_{ortho}$), 168.13 (NCN).

3   CHAPTER THREE

3.1   Charged Pincer Carbene Nickel Complexes

There are relatively few pincer carbene Ni-halide complexes known in the literature when compared to Pd-halide pincer carbene complexes. As explained earlier in Chapter 1, Section 1.4.3, Inamoto and co-workers reported the first complex [^{Me}CNC-Ni-Br]Br **21** that was fully characterized and tested for catalytic activity for the Heck and Suzuki reactions. Compound **21** showed moderate to high yields of desired coupling products.[93] There are other pincer carbene Ni complexes in the literature; however, they have not been tested for catalytic activity; *e.g.*, [^{DiPP}CNC-Ni-Br]Br reported by Pugh and co-workers[117] in 2007 did not report any studies on catalytic activity.

Similar to Chapter 2, Chapter 3 attempts to provide information on our efforts directed towards preparation of pincer carbene-based Ni hydrides in order to investigate their potential to activate molecular O_2 and eventually transfer oxygen atom to alkenes and other organic substrates. As well, alternative routes to pincer carbene Ni-H's or pincer carbene Ni-OOH's were also investigated, and will be discussed in this chapter. Similarly to the Pd pincer carbenes (Pd-X, X = Cl, Br), syntheses of pincer carbene Ni

halides exist in the literature, this background has significantly aided us in the syntheses of pincer carbene ligands and their transition metal complexes.

3.1.1 Attempted Preparation of Ni-H Complexes

According to a recent search in the Cambridge Crystallographic Database (CSD version 5.31, May 2010 update) there are no known crystallographically-studied pincer carbene-containing Ni hydrides. Our first approach in preparing a pincer carbene Ni-H was to directly use hydride sources in attempts to convert the pincer carbene Ni-Br cation to Ni-H. If successful, we could then insert O_2 to obtain a Ni-OOH species, as proposed in our catalytic cycle for making oxidized substrates (Scheme 1.9). Similarly to what we observed in attempts to convert charged [^{R}CNC-Pd-Br]Br (R = Methyl **19**; R = *n*-Butyl **20**) to [^{R}CNC-Pd-H]Br (R = Me **56;** R = *n*-Butyl **57)**, the conversion of [^{Me}CNC-Ni-Br]Br **21** to **68** was unsuccessful. Hydride sources such as Et_3SiH, $LiAlH_4$, K-Selectride, $NaBH_4$, and Super-Hydride were utilized. These reactions were monitored by ^{1}H NMR and none of them showed the presence of a Ni-H resonance in the ^{1}H NMR spectrum. The Ni complex **21**, shown in Scheme 3.1, appeared to decompose in the presence of these hydride sources. The ligand could not be recovered and a dark brown solid (possibly Ni^0) was deposited, suggesting that reductive elimination of the ligand occurred. The eliminated ligand, however, could very likely react further with the hydride source and form unknown compounds. Attempted syntheses of uncharged ^{R}CCC-Ni-Br (R = Methyl, *n*-Butyl) were unsuccessful. The difficulties that we faced in the attempts to prepare [^{Me}CNC-Ni-H]$^+$ are similar to the difficulties that other members of the group observed when worked with ^{R}PCP-Ni-H complexes. In general, ^{R}PCP-Ni-H

complexes are even more problematic than [R]PCP-Pd-H complexes in their preparations.[118] The synthetic challenges that we faced during the attempted preparations of Ni-H using various hydride sources led us pursue alternative routes to Ni-H. This will be discussed in detail in Section 3.2.

Scheme 3.1 Attempted Preparation of a Pincer Carbene Ni-H
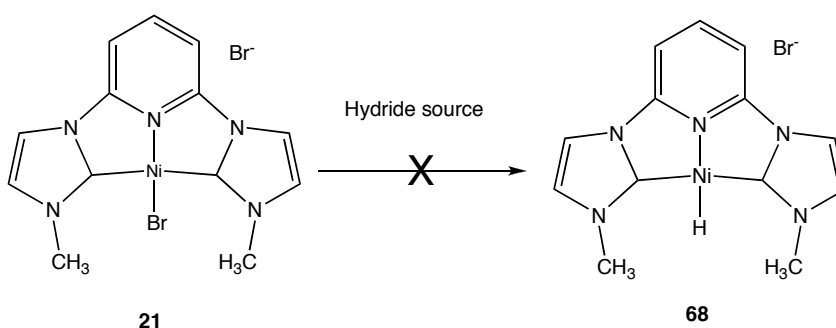
3.1.2 Dinuclear Ni Complex Containing a Bridging [Me]CNC Pincer Ligand

In the course of preparing a known [[Me]CNC-Ni-Br]Br complex **21** first reported by Inamoto and co-workers[93] with the aim of converting it to a pincer carbene Ni-H, an interesting and novel dinuclear Ni complex with the bridging pincer [Me]CNC ligand **69** shown in Scheme 3.2 was unexpectedly isolated. It should be noted that, [[Me]CNC-Ni-Br]Br is a precursor for [[Me]CNC-Ni-H]Br **68**. As was mentioned earlier in Chapter 1, CNC-pincer complexes are typically prepared as monometallic species in which the CNC ligand acts as a tridentate donor towards a single metal atom, taking advantage of the entropy-driven chelate effect. Recently, there have been examples prepared using metals from Group 9 (Rh), Group 11 (Ag, Au), and Group 12 (Hg) in which the CNC ligand acts

not as a tricoordinate chelating ligand, but rather as a bridging ligand via the two carbene donors toward two separate metals. These complexes have been crystallographically-characterized, a requirement for unambiguous confirmation of the bridging nature of the CNC ligand. In 2000, Chen and co-workers prepared and structurally characterized $[\{^{Me}CNC\text{-}Hg\}_2]^{2+}[PF_6]_2$, the first example of a double helical $[Hg_2]^{2+}$ complex containing the ^{Me}CNC ligand in which only the carbenes act as donor atoms, and not the pyridinyl N atom of the central ring. [119] At approximately the same time, the group of Tejada prepared a similar $[Ag_2]^{2+}$ double helical complex containing the $^{PhCH2}CNC$ ligand and triflate anions. [120,121] Since that time, there have been crystallographic reports of other $[Ag_2]^{2+}$ salts that contain different ^RCNC ligands ($^{DiPP}CNC^{117}$, benzimidazolin-2-ylidene $^{nBu}CNC^{122}$). As well, there has been a recent report of a $^{HOCH2CH2}CNC$-containing $[Au_2]^{2+}$ complex, again obtained in the solid state in the double helical form.[117] All compounds that result in the double helix form have a M:L ratio of 1 (Fig. 3.1a). Peris and co-workers have obtained the only crystallographically-characterized complexes in which the M:L ratio is 2, these being the Rh^I species$\{[Rh(COD)Br]_2(^RCNC)\}$, where R = Methyl or n-Butyl.[122,123] These complexes adopt the structure shown in Fig. 3.1b and have been shown to be effective catalysts for hydrosilylation, hydroformylation, and catalytic hydrogen transfer.

Figure 3.1 CNC Ligand – Metal Complexes as a Function of Metal/Ligand Ratio

a) M:L = 1:1; *M = Hg⁺, Au⁺, Ag⁺*   b) M:L = 2:1.
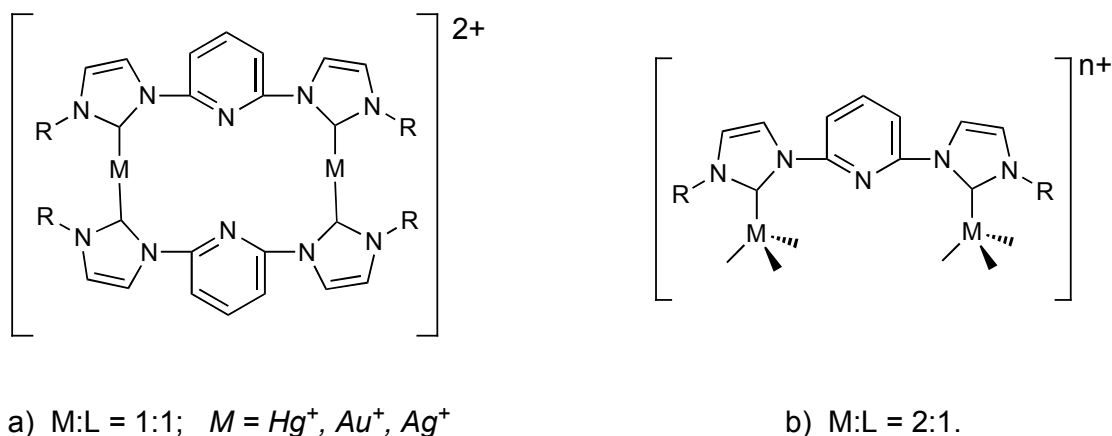
We then deliberately synthesized the dinuclear Ni ^{Me}CNC bridged complex **69,** by utilizing the known ^{Me}CNC ligand precursor **26** (R = Me) as the starting material as shown in Scheme 3.2.[124] It is known that treatment of ligand **26** with Ni or Pd salts at elevated temperatures of 160 °C produces the monometallic, tris-chelating ^{Me}CNC complex of the metal.[76,93] However, when the imidazolium salt **26** (R = Methyl) was treated with Ni(OAc)$_2$ and Bu$_4$NBr in DMSO for 12 hours at room temperature followed by heating at 130 °C for one hour, we did not see formation of the expected cation **21** but rather observed formation of **69** in 32% yield. Product **69** is structurally related to **21** in that three of the four coordination sites on Ni are complexed with the ^{Me}CNC ligand, but the fourth site is filled not with a Br⁻ but rather with a bridging ^{Me}CNC ligand. The unique coordination geometry around Ni in which the ^{Me}CNC ligand complexes to the metal in two entirely different modes has not been seen previously and is a novel feature of our work. Due to its highly insoluble nature we could not recrystallize and grow X-ray quality crystals of **69**, but the ^{1}H NMR spectrum of **69** was consistent with the structure shown in Scheme 3.2. The characteristic proton resonances for the N-CH$_3$ groups on the

^{Me}CNC ligands indicate that there are two types of CNC ligands present in a ratio of 2:1. As well, the distinctive vinyl protons on the imidazole backbones are also present in 2:1 ratios. A ^{13}C NMR spectrum could not be obtained due to poor solubility. Again, due to its lack of solubility as the tetrabromide salt, **69** was not prepared in analytically-pure form as the primary method for purification was simple washing. In order to be confident of the unique structure of **69** we performed an anion exchange on impure **69** using AgOTf to prepare a more soluble version that could then be recrystallized and characterized by single-crystal X-ray diffraction. A sample of **69** was treated with 4 equivalents of AgOTf in methanol at room temperature for 2 hours (Scheme 3.2).

Scheme 3.2 Synthesis of Dinuclear Ni Containing a Bridging ^{Me}CNC Ligand 69[124]
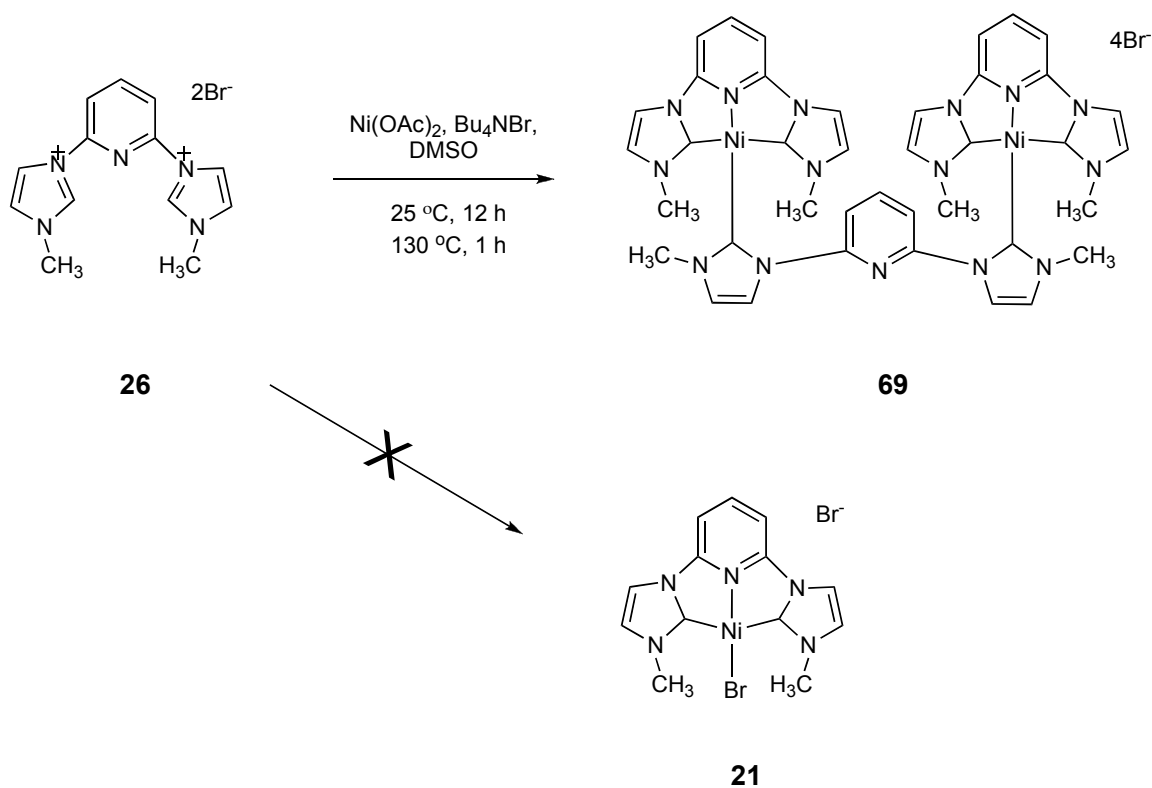
The AgBr formed was removed by filtration and the filtrate was cooled to -32 °C. After 3 days, orange crystals of **70** were obtained. The ^{1}H NMR spectrum of **70** was essentially unchanged from **69**, thus indicating that only simple anion exchange had occurred. As well, the elemental analysis matched the formula for **70** shown in Scheme 2, $[(^{Me}CNC)_3Ni_2]^{4+}[OTf]_4$. The ^{13}C NMR spectrum obtained on **70** was also consistent with the proposed structure, and in addition clearly showed the presence of the triflate anion by F coupling to the methyl group. The Ni-*C* resonances from the carbene donors were also present in the characteristic downfield region at δ 165.56 and δ 166.85 ppm. However, in order to confirm the structure, we performed a single-crystal X-ray analysis upon **70**. Orange crystals of **70** suitable for X-ray diffraction studies were grown at low temperature (-32 °C) from a concentrated solution of **70** in CH_3OH solvent. Analysis indicates that **70** crystallizes in the orthorhombic crystal system, space group Pnma, and contains a mirror plane of symmetry bisecting the central pyridine ring (through N6-C14) of the bridging ^{Me}CNC ligand as shown in Figure 3.2 (without the triflate counterions). Briefly, the structure consists of two symmetry-equivalent $[^{Me}CNC-Ni]^{2+}$ fragments that are bridged by a neutral ^{Me}CNC ligand. The two $[^{Me}CNC-Ni]^{2+}$ fragments exhibit the tridentate, chelating bonding mode typically shown by typical monometallic ^{R}CNC pincer complexes. The Ni^{2+} ion has a distorted square-planar geometry, and the local environment around Ni is similar to the $[^{Me}CNC-Ni-Br]Br$ **21** complex structurally-characterized by Inamoto.[93] Selected bond lengths and angles for **70** are shown in Table 3.1. The two *trans* Ni-C bonds have virtually identical lengths in **70** of 1.915(3) and 1.916(3) Å, again similar to the Ni-C bond lengths found in [^{Me}CNC-Ni-

Br]Br **21** (1.932(4) and 1.920(5) Å). [93] As well, the distortion from idealized square-planar geometry in both complexes is similar. The N6-Ni1-C17 bond angle in **70** (Figure 3.2) is linear (179.76(12)° and the N-Ni-Br angle in [^{Me}CNC-Ni-Br]Br is nearly so (176.36(11)°). The C6-Ni-C10 bond angle in **70** is 162.66(11)°, identical to the 163.02(19)° C-Ni-C angle seen in [^{Me}CNC-Ni-Br]Br. [93]

Scheme 3.3 Preparation of [(^{Me}CNC)$_3$Ni$_2$]$^{4+}$[OTf]$_4$ 70 [124]

69   **70**
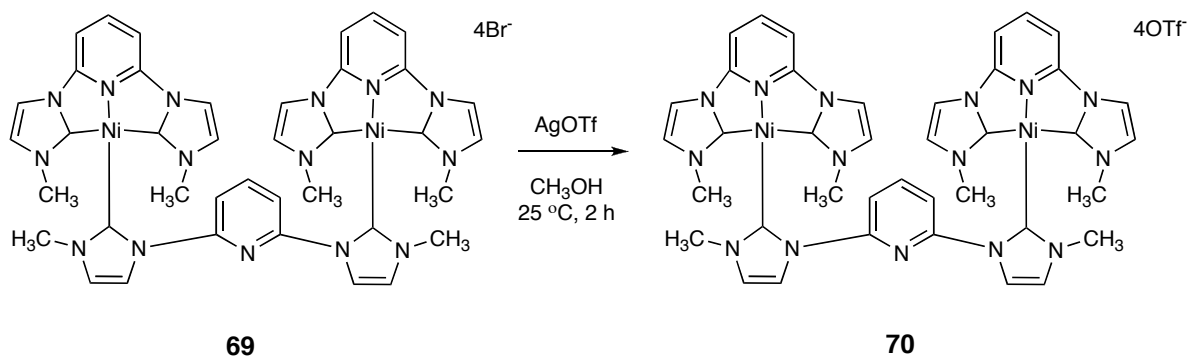
Figure 3.2 Thermal Ellipsoid Plot of 70 Shown at 50% Probability Level with Hydrogens and Triflate Counterions Omitted for Clarity[124]
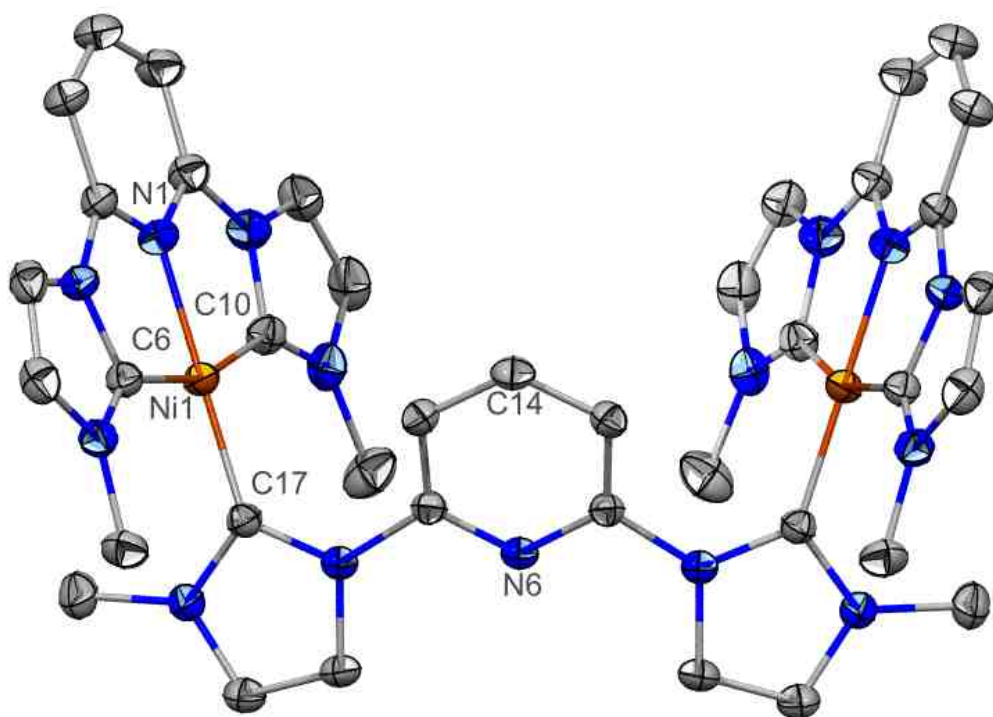
It should be noted that the most highly unusual and novel structural feature found in **70** is that the ^{Me}CNC ligand that bridges the two Ni^{2+} ions via the carbene donors provides the fourth ligand to satisfy the distorted square-planar geometry. This third ^{Me}CNC ligand accomplishes this by utilizing the carbene fragment on each end as a monodentate donor to each of the two Ni^{2+} ions. The bond lengths of the two chelating Ni-carbene bonds (Ni1-C6 (1.915(3) Å) and (Ni1-C10 (1.916(3) Å) are both noticeably longer than the Ni-carbene (Ni1-C17 (1.870(2) Å) bond length for the bridging carbene-Ni bond. This is likely due to the weaker *trans*-influence of the N ligand (pyridine) relative to carbene ligands. Similarly to that seen in the di-Rh complexes, the N6 atom of

the central pyridine ring of the bridging ^{Me}CNC ligand remains uncoordinated. A further interesting feature of **70** is that the two [^{Me}CNC-Ni]$^{2+}$ fragments in the solid state form a cleft, or pocket, with an angle of ~61°, bisected by the molecular mirror plane. One of the triflate counteranions sits on this symmetry plane inside of this pocket. As well, there are two CH_3OH solvent molecules present in the structure of **70** that H-bond to the O atoms in one of the triflate counteranions.

The concept of pincer carbene ligands as bridging ligands via two carbene donors towards separate metals is relatively new and there are only a few examples of metal complexes of Group 9 (Rh), Group 11(Ag, Au), and Group 12 (Hg) that have been crystallographically-characterized.[119-123,125] Our unique and novel dinuclear Ni complex **70** gives a clear and first example of the bridging ability of the pincer carbene ligands in Group 10 chemistry exhibiting a unique M:L ratio of 2:3 rather than 1:1 or 2:1 ratios exhibited by previously-crystallized analogues. Complex **70** contains the ^{Me}CNC ligand both as a traditional chelating ligand and as bridging ligand via two carbene donors to separate two Ni^{2+} ions. Although complex **70** has not been tested for catalytic activity, it might be a potential catalyst for C-C coupling reactions. As well, studying **70** via electrochemical techniques may reveal interesting redox properties for this electron rich molecule.

Table 3.1 Selected Bond Lengths and Angles for Compound 70

Bond Lengths (Å)

Atom 1	Atom 2	Distances
Ni1	N1	1.880(2)
Ni1	C6	1.915(3)
Ni1	C10	1.916(3)
Ni1	C17	1.870(2)

Bond Angles (º)

Atom 1	Atom 2	Atom 3	Angle
N1	Ni1	C17	179.76(12)
C6	Ni1	C10	162.66(11)
N2	C6	N3	104.0(2)
N4	C10	N5	103.7(2)

3.2   Dinuclear Ni Complex - Counterion Changes

We hypothesized that [^{Me}CNC-Ni-Br]Br **21** should react with AgNO$_3$ to yield

[^{Me}CNC-Ni-ONO$_2$]NO$_3$ **71** as proposed generally in Scheme 2.9. If formed, we could

then treat the nitrates with NaOMe or NaOiPr to give the pincer carbenes Ni-OMe/OiPr,

and eventually eliminate formaldehyde or acetone in order to form the Ni-H. We pursued

this approach after the synthetic challenges that we encountered during attempted

conversion of [^{Me}CNC-Ni-Br]Br **21** to [^{Me}CNC-Ni-Br]Br **68.** Quite unexpectedly, yet

very interestingly, when 2 equivalents of AgNO$_3$ were used the intended [^{Me}CNC-Ni-

ONO$_2$]NO$_3$ complex **71** was not formed, but rather **72** was formed in reasonable yields

(67%). ^{1}H NMR, ^{13}C NMR and X-ray analysis confirmed the formation of a pincer

carbene-bridged dinuclear Ni complex **72**, similar in structure to **70**. Orange crystals of

72 suitable for X-ray diffraction studies were grown at room temperature by slow

evaporation of the solvent.

Scheme 3.4 Preparation of [(^{Me}CNC)$_3$Ni$_2$]$^{4+}$[NO$_3^-$]$_{3.75}$Cl$_{0.25}$ 72
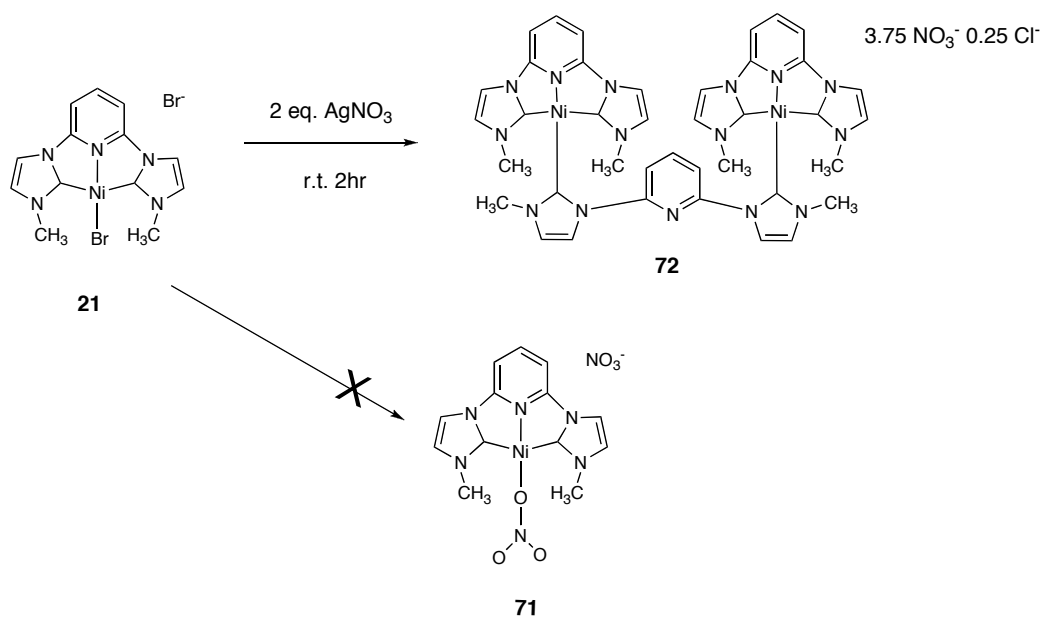
As seen earlier with the crystal structure of complex **70**, the solid-state structure of

72 also consists of two symmetry-equivalent [^{Me}CNC-Ni]$^{2+}$ fragments that are bridged by

a neutral ^{Me}CNC ligand. However, the major difference between **72** and the previously

synthesized pincer carbene bridged dinuclear Ni complexes **69** and **70** is the counterions.

While **69** and **70** have 4Br$^-$ and 4OTf$^-$ as counterions respectively, complex **72** has

3.75NO$_3^-$ and 0.25Cl$^-$ as counterions. During refinement, it was determined that the best

fit of the data occurred with site occupancies of NO_3^- at 75% and Cl^- at 25%, giving a total of 100% occupancy. The origin of the Cl^- is likely from the chloroform ($CHCl_3$) that was used during the purification of complex **21**, which is one of the starting materials in the preparation of complex **69** (Scheme 3.2), this was the only time the complex saw chlorine during the preparation. The ^1H and ^{13}C NMR spectra of **72** are very similar to those of compounds **69** and **70**. The major difference leading to the variety in complexes **69**, **70** and **72** is in the preparative route. Complex **69** was synthesized by using 3 equivalents of ^{Me}CNC ligand and 2 equivalents of $Ni(OAc)_2$ in the presence of Bu_4NBr (Scheme 3.2). Complex **70** was prepared using anion exchange with AgOTf (Scheme 3.3) whereas complex **72** was obtained by a reaction between complex **21** and 2 equivalents of $AgNO_3$ in methanol for 12 hours at room temperature.

Similarly to complex **70**, X-ray analysis of complex **72** also indicates that **72** crystallizes in the orthorhombic crystal system, space group Pnma and contains a mirror plane bisecting the central pyridine ring that passes through N6-C14 of the bridging ^{Me}CNC ligand as shown in Figure 3.3. As in complex **70**, the solid-state structure of **72** consists of two symmetry-equivalent $[^{Me}CNC\text{-}Ni]^{2+}$ fragments that are bridged by a neutral ^{Me}CNC ligand. The two $[^{Me}CNC\text{-}Ni]^{2+}$ fragments exhibit the tridentate chelating bonding mode. As we saw in complex **70** and Inamoto found in monometallic $[^{Me}CNC\text{-}Ni\text{-}Br]Br$ **21**[93], the Ni^{2+} ion has a distorted square planar geometry.

Selected bond lengths and angles found for **72** are shown in Table 3.2. Similar to complex **70**, the two *trans* Ni-C bonds in complex **72** have very similar bond lengths (Ni1-C6 1.920(8) Å and Ni1-C10 (1.908(9) Å). Again, this is very close to the Ni-C bond length found in $[^{Me}CNC\text{-}Ni\text{-}Br]Br$ (1.932(4) Å) and 1.920(5) Å). As well, the Ni-C bond

lengths of **72** are virtually identical to those found in complex **70** (1.915(3) Å and

1.916(3) Å). The N1-Ni1-C17 bond angle in **72** is almost linear 179.9(4)°, also similar to

the N-Ni-Br angle in complex **70** (179.76(12))° and in [^{Me}CNC-Ni-Br]Br **21**

(179.36(11)°). Moreover, the C6-Ni1-C10 bond angle in **72** is 163.4(4)°, closely related

to the C-Ni-C bond angle found in **70** (162.66(11)°) and [^{Me}CNC-Ni-Br]Br **21**

(163.02(19)°).

Figure 3.3 Thermal Ellipsoid Plot of 72 shown at 50% Probability Level with

Hydrogens and Nitrates Omitted for Clarity
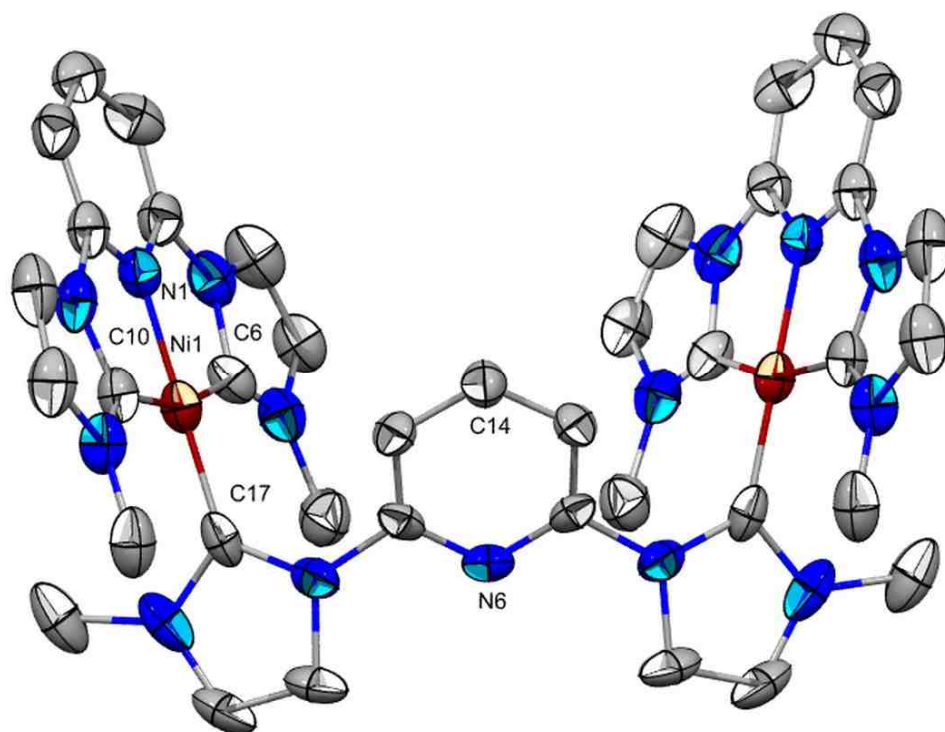
One of the unique features of complex **72** is that ^{Me}CNC ligand bridges the two

Ni^{2+} ions through the carbene donors by providing the fourth ligand to accomplish the

distorted square-planar geometry. As was seen in complex **70**, the bond lengths of the

two Ni-carbene bonds in **72**, Ni1-C6 (1.907(3) Å) and Ni1-C10 (1.921(3) Å) are both

significantly longer than the Ni-C17 (1.835(2) Å) bond length of the bridging carbene-Ni

bond. As explained earlier, this can be attributed to the weaker *trans*-influence of the N

ligand (pyridine) relative to carbene ligands. Surprisingly, the two [^{Me}CNC-Ni]$^{2+}$

fragments in the solid state form a cleft with an angle of (~61°) bisected by mirror plane,

exactly the same cleft angle seen in **70**. Two of the nitrate counterions and a molecule of

methanol solvent sit on this symmetry plane inside of this cleft. As well, there are two

nitrates, one chloride and a methanol solvent found outside this cleft. Another unique

feature of **72** arises from route in which it was obtained. A simple anion exchange

reaction resulted in rearrangement of [^{Me}CNC-Ni-Br]Br **21** to produce **72**. Again,

complexes **70** and **72** are novel and this confirms the bridging ability of pincer carbene

ligand in Group 10 metals.

Table 3.2 Selected Bond Lengths and Angles for Compound 72

Bond Lengths (Å)

Atom 1	Atom 2	Distances
Ni1	N1	1.867(7)
Ni1	C6	1.920(8)
Ni1	C10	1.908(9)
Ni1	C17	1.836(9)

Bond Angles (º)

Atom 1	Atom 2	Atom 3	Angle
N1	Ni1	C17	179.9(4)
C6	Ni1	C10	163.4(4)
N2	C6	N3	104.5(7)
N4	C10	N5	104.4(7)

3.3   Novel 3-Dimensional Silver Carbene Coordination Cluster

As discussed earlier in Section 3.2, in an attempt to prepare the pincer carbene Ni-H species through the route proposed in generalized Scheme 2.9, we instead prepared pincer carbene bridged Ni complex **72** when two equivalents of $AgNO_3$ were added. However, when excess $AgNO_3$ (7 equivalents) was reacted with [^{Me}CNC-Ni-Br]Br **21** in methanol at room temperature for 2 hours, we unexpectedly obtained an interesting mixture of products. One of these products is a unique and novel Ag_7 carbene

coordination polymer **74** that will be explained in detailed later in this section. According to the literature, there are very few known Ag_7 clusters that been reported. Silver cluster chemistry have attracted a lot of attention recently because these clusters have shown to possess interesting spectral properties such as fluoresence,[126] optical absorption[127] and circular dichroism,[128] among others. However, what is not known in these clusters with certainty is the actual composition of these clusters. Recently, Wu and his group have reported a high-yield preparation of the silver cluster $[Ag_7(DMSA)_4]^-$, where DMSA is *meso*-2,3-dimercaptosuccinic acid.[129] Unfortunately, the exact structure of $[Ag_7(DMSA)_4]^-$ is not known due to difficulty in growing single crystals for X-ray analysis. Interestingly, Xiang and his co-workers utilized their newly developed generic algorithm and DFT to predict the structure of the $[Ag_7(DMSA)_4]^-$.[130] Very fortunately, we were able to grow crystals for our coordination polymer **74** and that has enabled us to know the exact structure of the coordination polymer. To our knowledge, there are numerous Ag-carbene based clusters reported in the literature; however, none has unusual features of **74**. In 2004, Melaiye and co-workers prepared and structurally-characterized a Ag-carbene complex.[131] According to their report, the Ag-carbene complex is polymeric in the solid-state as determined crystallographically; however, it exists as monomer in solution as suggested by mass spectrometry results. At approximately the same time, Catalano and co-workers reported pyridine-substituted pincer carbene Ag^+ and Au^+ coordination aggregates.[132] In their paper Catalano and co-workers reported an unusual triangulo-Ag_3 cluster that has photoluminescent characteristics (Figure 3.4).[132] Very interestingly, Catalano and co-workers have since extended this chemistry and have

reported clusters containing mixed metal systems such as Ag-Au and investigated similar chemistry with other pyridyl-substituted pincer carbenes.[132]

Figure 3.4 Unusual Triangulo-Ag$_3$ Cluster[132]
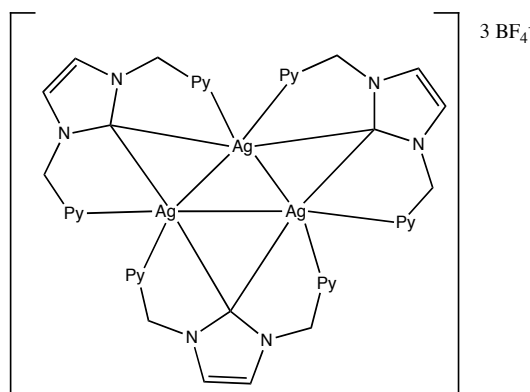
In 2007, Liu's group prepared and reported a variety of structurally-characterized Ag clusters.[133] Interestingly, Lui suggested that pyridyl-functionalized bis-carbene ligands would be expected to be suitable ligands for connecting transition metals into coordination polymers primarily due to the strong σ-donating ability of carbenes.[132] In 2010, Rit and co-workers utilized various pyridyl-functionalized pincer carbene ligands and Ag and/or Au to prepare a variety of Ag clusters or Ag-Au clusters.[132] However, a distinguishing characteristic of the Ag carbene cluster that we have prepared is the novel structure that leads it to exist as a 3-dimensional (3D) coordination polymer.

In a simple attempt to exchange Br$^-$ for NO$_3$$^-$, [^{Me}CNC-Ni-Br]Br **21** was reacted with excess AgNO$_3$ (7 equivalents) in methanol at room temperature for 2 hours. Unreacted AgNO$_3$ was removed by filtration through medium a filter frit. While our goal was anion exchange, we obtained products consistent with new modes of reactivity.

Scheme 3.5 Reaction of [^{Me}CNC-Ni-Br]Br 21 and Excess AgNO$_3$
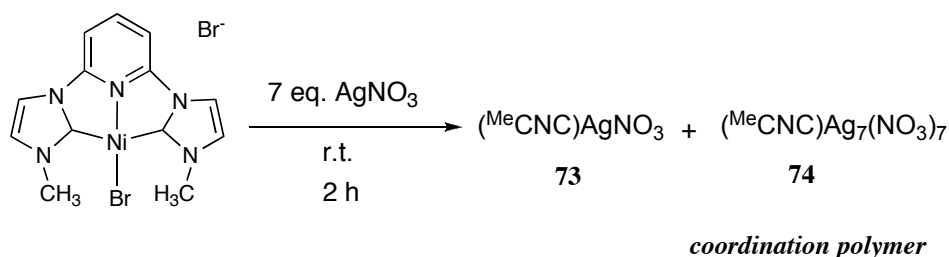
Crystals were grown at room temperature in CH$_3$OH solvent from a concentrated solution of the product mixture. However, the crystals formed displayed two types of morphologies. The first type **73** did not diffract very well and was unsuitable for single crystal X-ray analysis, and so we could not positively identify the actual solid-state structure of the complex. Solubility of these crystals was also a problem, and thus we were not able to get useful information from either ^{1}H NMR or ^{13}C NMR spectroscopy. Fortunately, the elemental analysis results of these crystals were helpful, and are consistent with the overall formula C$_{13}$H$_{13}$Ag$_1$N$_6$O$_3$ indicating that the complex consists of a 1:1 ^{Me}CNC ligand to Ag metal ratio (alternatively, one can view this formula as (^{Me}CNC)AgNO$_3$). Obviously, without the structure we do not know how the atoms are arranged in **73**. The second set of crystals **74** diffracted well, and X-ray analysis indicated the formation of a Ag-carbene coordination cluster polymer as shown in alternate views in Figures 3.5, 3.6, 3.7, and 3.8. The elemental analyses of **73** and **74**, together with X-ray analysis of **74**, indicate that a virtually unprecedented reverse transmetallation reaction has occurred in which Ag$^+$ replaced Ni$^{2+.}$ This will be discussed in more detail next.

Most interesting in this reaction is the replacement of Ni^{2+} by Ag^+ in the synthesis. Ag-carbenes are well-known to be transfer agents of carbenes to transition metals through transmetallation as explained earlier in Chapter One. To our knowledge, there is only one example reported in the literature of a carbene being transferred to Ag^+ from a Ni^{2+} ion. In a brief paragraph, Pugh first reported the unexpected "reverse transmetallation" transfer of a bound carbene from Ni to Ag.[117] Pugh observed this phenomenon when [^{DiPP}CNC-Ni-Br][AgI$_2$] was reacted with two equivalents of AgOTf in THF solution (Scheme 3.6). Quite surprisingly, they isolated a bridged Ag-carbene dication that was confirmed by X-ray analysis, ^{1}H NMR and ^{13}C NMR spectroscopy. The solid-state structure of this bridged Ag carbene dication indicated that the previously-unknown reverse carbene transmetallation reaction had occurred. [117]Although their reaction was reproducible, the Pugh group was not able to observe that type of reactivity with other pincer carbene Ni complexes.

Very interestingly, we have observed the second example of this unusual reactivity when we unexpectedly prepared our 3D-coordination polymer. Pugh and co-workers pointed out in their paper that reverse transmetallation was unexpected.[117] According to Pugh, reverse transmetallation observed in his dication complex **76** might require the hemilability of the CNC pincer ligand in complex **75**. As well, the determination of the direction of transmetallation would be influenced by the strength of M-carbene bond formed and bond broken during the reaction.[117]

Scheme 3.6 Preparation of a Bridged Ag-Carbene Dication 75[117]
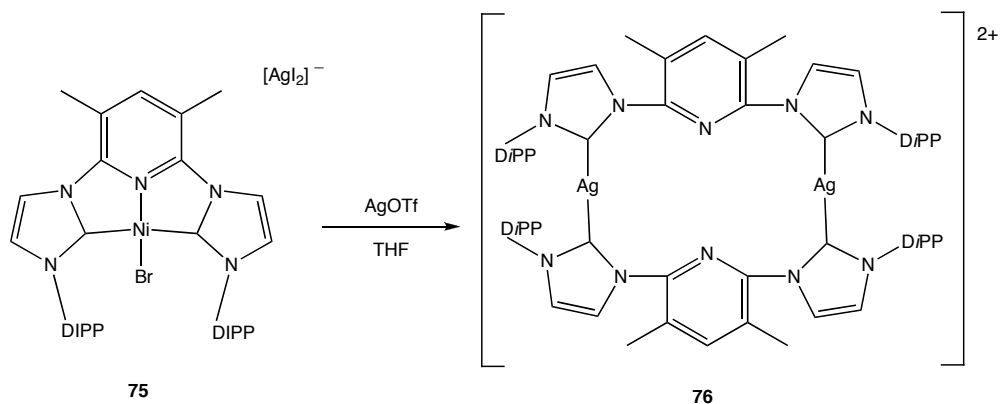
The X-ray analysis of our Ag-carbene cluster indicates that **74** crystallizes in the monoclinic crystal system in space group P2(1)/n. The Ag-carbene cluster consists of repeated units (monomers) with a formula of $C_{26}H_{27}Ag_7N_{17}O_{21.5}$. The solid-state structure of the monomer with the anionic nitrate groups omitted for clarity is shown in Figure 3.5. Interestingly, the monomer contains a Ag_6 core with two neutral, bridging carbene ligands surrounding the Ag_6 core. Ultimately, a seventh Ag^+ ion and nitrate groups connect these Ag_6 cores to each other, eventually forming layers and a 3D-structure. As it can be seen in the structure of the monomer (Figure 3.5), each carbenic carbon from the ^{Me}CNC ligand is essentially bound to two silver atoms. This unusual type of carbene-silver interaction is also referred to as three-centers, two electrons (3c2e), similar to the bonding schemes developed for electron-deficient species.[117,133] As well, each nitrogen from the pyridine rings is essentially symmetrically-connected to two silver atoms, forming an additional 3c2e nitrogen-silver interaction.

The elemental analysis of **74** gave satisfactory results in agreement with the crystal structure of **74**. NMR spectroscopy could not be utilized to characterize the polymer because of the poor solubility of the Ag-carbene coordination polymer.

Figure 3.5 A Monomer of the Ag-Carbene Coordination Polymer, with Nitrates Omitted for Clarity.
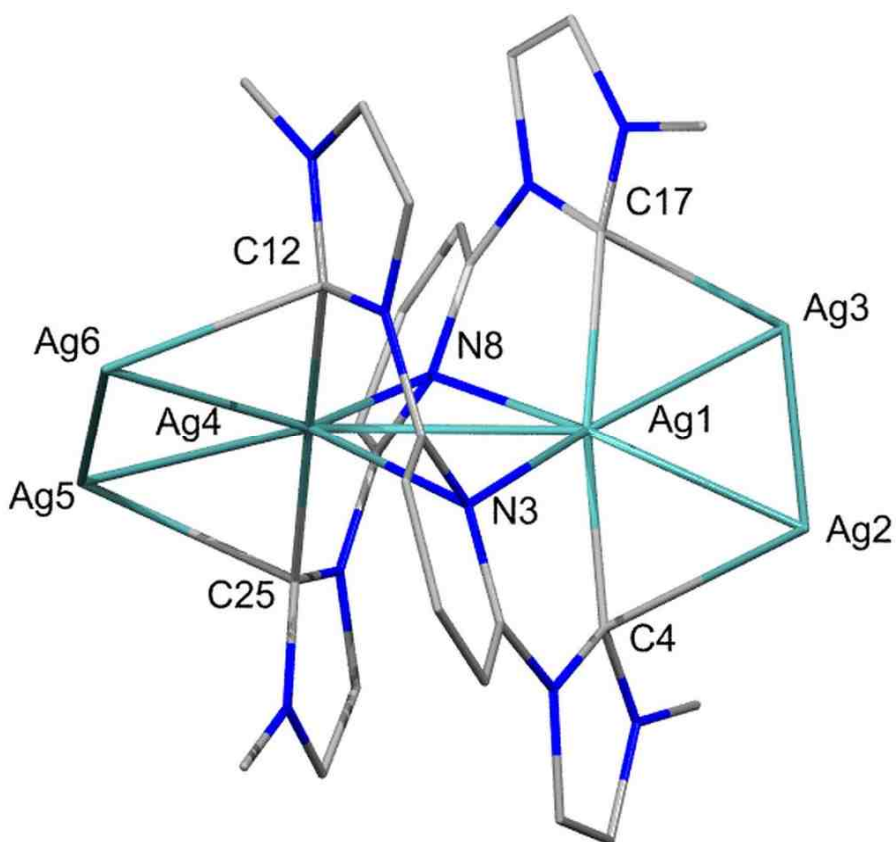
The selected bond lengths and angles of **74** are listed in Table 3.3. The two internal silver atoms (Ag1 and Ag4) within the Ag$_6$ cluster are each dicoordinated by the two unusual bridging carbenic carbons, with Ag4-C12, Ag4-C25, Ag1-C4, Ag1-C17 bond distances of 2.133(6) Å, 2.143(6) Å, 2.146(6) Å and 2.175(6) Å, respectively.

Similar Ag-C bonds lengths have been observed for several Ag-carbene complexes. The geometries of these silver atoms (Ag1 and Ag4) are slightly bent with C17-Ag1-C4 and C12-Ag4-C25 bond angles of 170.3(2)° and 175.7(2)°, respectively. These bond angles are also within C-Ag-C bond angles values previously reported. [117,133] The slightly deviation from linearity can be attributed to Ag-Ag interactions and the twisted fashion in which the ^{Me}CNC ligand is coordinated to the silver ions.

Ag1 and Ag4 are also dicoordinated to two pyridyl nitrogen atoms of the ^{Me}CNC ligand with the Ag-N$_{pyridyl}$ bonds Ag1-N3, Ag1-N8, Ag4-N3, and Ag4-N8 having bond lengths of 2.780(4) Å, 2.714(4) Å, 2.756(5) Å, and 2.788(5) Å, respectively. These observed bond distances are significantly longer than normal Ag-N bond distances.[133,134] This lengthening may be due to overstretch as a result of the rigid structure of the carbene that hampers a closer approach of the pyridine group. This notion of the effect of the rigidity of carbene structure on the Ag-N bond length was first reported by Catalano and his group.[134]

Noteworthy, the two ^{Me}CNC ligand act as bridging ligands spanning four unsymmetrical silver atoms, resulting in four Ag-C-Ag rings. The Ag-C bond lengths between the carbenic carbons and the internal silver atoms in the Ag$_6$ cluster are within the reported normal Ag-C bonds.[117,133-135]

Table 3.3 Selected Bond Lengths and Angles for Compound 74

Bond Lengths (Å)

Atom 1	Atom 2	Bond length (Å)
Ag2	C4	2.527(6)
Ag3	C17	2.330(6)
Ag4	C12	2.133(6)
Ag4	C25	2.143(6)
Ag1	C4	2.141(6)
Ag6	C12	2.493(7)
Ag1	C17	2.175(6)
Ag5	C25	2.502(6)
Ag1	N8	2.714(4)
Ag4	N8	2.788(5)
Ag4	N3	2.756(5)
Ag1	N3	2.780(4)

Bond Angles (º)

Atom 1	Atom 2	Atom 3	Angle
C17	Ag1	C4	170.3(2)
C12	Ag4	C25	175.7(2)
N1	C4	N2	104.79
N4	C12	N5	104.09
N6	C17	N17	103.38
N9	C25	N10	103.13

The Ag-C bond lengths between carbenic carbons and the terminal silver ions -Ag2-C4, Ag3-C17, Ag5-C25, and Ag6-C12- are 2.527(6) Å, 2.350(6) Å, 2.502(6) Å, and

2.493(7) Å, respectively. This range [(2.350(6) Å - 2.527(6) Å] of Ag-C bond distances

show significantly longer bonds for the Ag-carbene lengths. Interestingly, Liu and co-

workers observed this type of bond behavior with the clusters that they reported in their

paper.[133]

Table 3.4 Selected Bond Lengths and Angles For Ag$_6$ Cluster in Compound 74

Bond Lengths (Å)

Atom 1	Atom 2	Bond length (Å)
Ag1	Ag3	2.7208(7)
Ag1	Ag2	2.8317(7)
Ag2	Ag3	3.3567(7)
Ag1	Ag4	2.9736(7)
Ag4	Ag5	2.7701(7)
Ag4	Ag6	2.8589(8)
Ag6	Ag5	3.2154(9)

The Ag-Ag bond lengths for the Ag$_6$ core of the Ag-carbene coordination polymer

are listed in Table 3.4, and are shown in Figure 3.6. The six silver atoms form an

unprecedented structure in Ag cluster chemistry – a twisted bowtie structure. The six

Ag-Ag bonds have bond distances of 2.7208(7) Å, 2.8317(7) Å, 3.3567(7) Å, 2.9736(7)

Å, 2.7701(7) Å, 2.8589(8) Å, and 3.2154(9) Å for Ag1-Ag3, Ag1-Ag2, Ag2-Ag3, Ag1-

Ag4, Ag4-Ag5, Ag4-Ag6, and Ag5-Ag6, respectively. These vary over a wide range,

with some of these Ag-Ag bonds having shorter bond distances of 2.7208(8) Å and

2.7701(7) Å. The Ag2-Ag3 and Ag5-Ag6 bond distances of 3.356(7) Å and 3.2154(9) Å

are notably longer the other Ag-Ag bonds. This signifies a much weaker interaction between Ag2 and Ag3, as well as Ag5 and Ag6. However, Ag-Ag bong lengths are known to vary over a wide range, and these Ag-Ag bond distances within our complex **74** have previously been reported in Ag carbene clusters. [133,134] To our knowledge, only one other twisted bowtie structure is known and crystallographically-determined. Furuya and Gladfelter prepared a $[Fe_4Ru_2(CO)_{22}]^{2-}$ species that had a similar bowtie structure. However, this structure was monomeric in the solid-state, and had no 2D or 3D polymeric structure.[136]

Depicted in Figure 3.7 is a more extended view of the solid-state structure of **74**. In this, the two dimensional layers of the Ag-carbene coordination polymer can be seen, with nitrate groups connecting the Ag_6 bowtie clusters into an extended array. The bond angles and distances within the nitrate group are within the reported values and deserve no special comment. More interestingly, shown in Figure 3.8, is the seventh silver atom that bridges the 2D layers through extensive binding to nitrates and Ag_6 clusters. Addition of this 7th Ag^+ ion forms a 3D coordination polymer. We believe that the stability of this 3D-polymer is a key feature leading to its successful synthesis, and that the ultimate stability of this product is the driving force for the reverse transmetallation reaction. As mentioned, Ag-carbene complexes are known in almost all cases (except the one mentioned by Pugh[117]) for transferring carbenes to other transition metals. In order to reverse this trend, the driving force for transferring carbenes to Ag must be great. We believe that this driving force comes from the ultimate precipitation of this highly-stable, highly insoluble polymeric product.

The by-product nickel bromide after liberation likely stays in solution. Very surprisingly, however, attempts to prepare the 3D Ag carbene coordination cluster directly by utilizing ^{Me}CNC ligand and $AgNO_3$ in a ratio of 2 ligands and 7 $AgNO_3$ did not prove successful.

Figure 3.6 Different Views Of Thermal Ellipsoid Plot Of Ag$_6$ Core of 74 Shown at 50% Probability Level With Nitrates and Pincer Carbene Ligands Omitted for Clarity
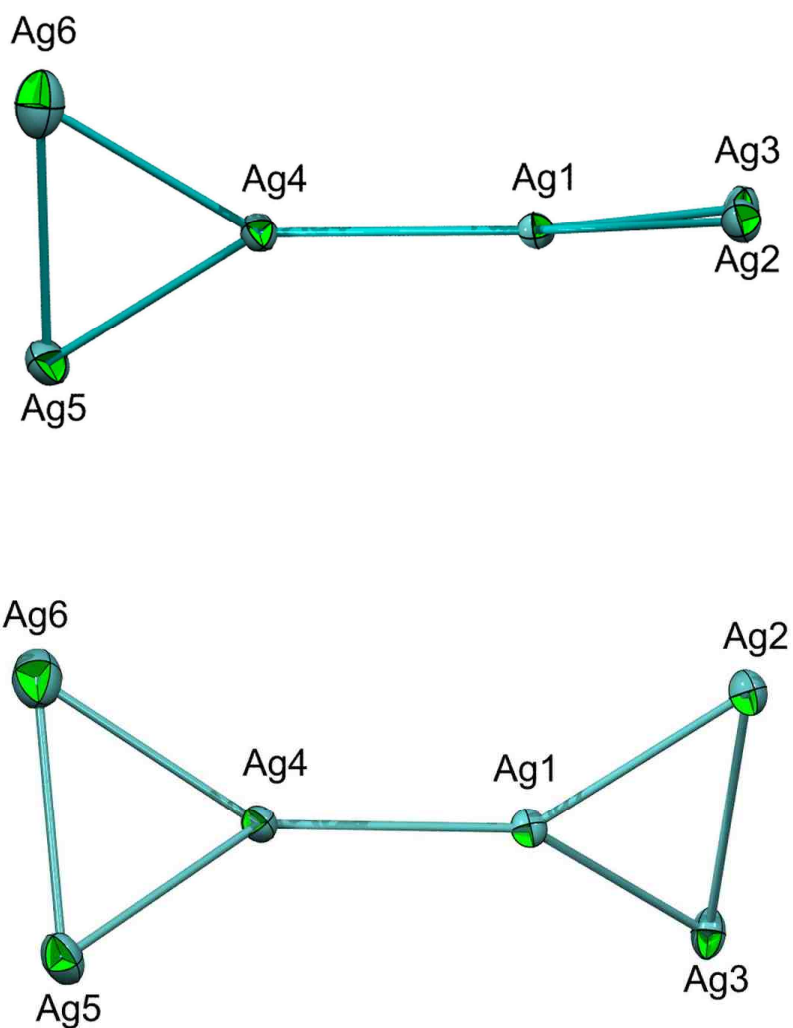
Figure 3.7 2D View of the Ag-Carbene Cluster Layer with Pincer Carbene

Omitted for Clarity.
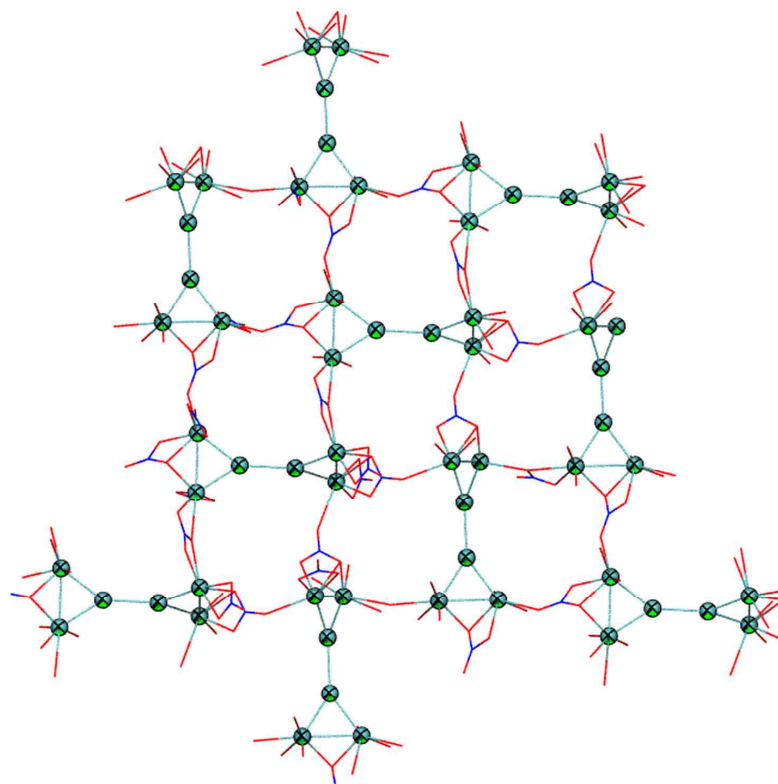
Figure 3.8 7th Ag Connecting Layers of Ag6 Clusters
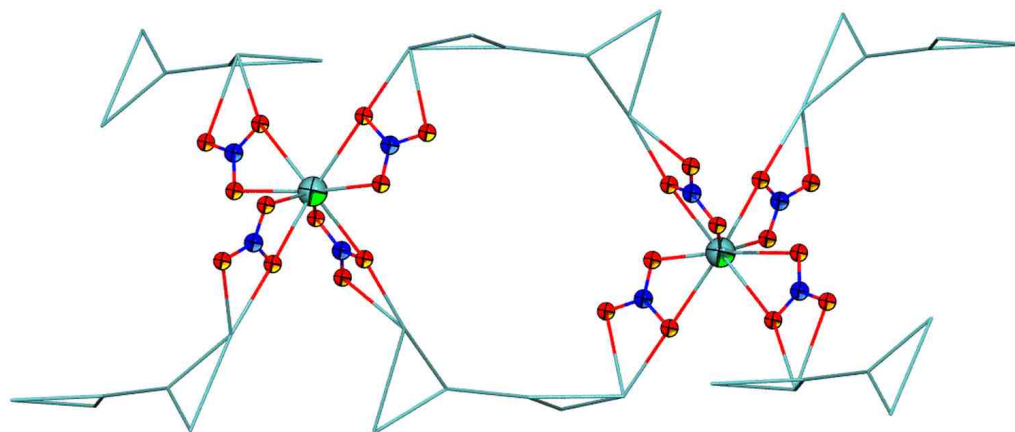
3.4   Summary

In summary, although we have not been successful in achieving our goal of converting ^{Me}CNC-Ni-Br to ^{Me}CNC-Ni-H so as to eventually use the Ni-H to activate molecular O_2 and thus transfer one of the oxygen to olefin or other organic substrate; we however, have prepared and characterized a novel Group 10 complex that contains the ^{Me}CNC ligand both as a traditional chelating ligand and as a bis(monodentate) bridging ligand to two Ni^{2+} ions.[119] The coordinating mode seen in this complex **70** is the first example of a CNC ligand acting as a bridging ligand to the Group 10 metals. The combination of the CNC ligand exhibiting both chelating and bridging modes in a single complex **70**[124] leads to a unique M:L ratio of 2:3 rather than the 1:1 or 2:1 ratio exhibited by previously-crystallized analogues. We plan to continue examining these CNC ligands as bridging ligands towards other metal ions and to utilize this bridging feature in the preparation of new CNC-containing complexes.

We have also prepared and structurally characterized a bridged Ni carbene complex **72**, similar to complex **70**, with the difference being the nature of the counterions. An interesting feature about this complex is the route by which it was obtained. [^{Me}CNC-Ni-Br]Br **21**, one of the starting materials in this reaction, appears to rearrange in the presence of $AgNO_3$ giving rise to a pincer carbene-bridged dinuclear Ni carbene complex **72**. Complex **72** was fully characterized by ^{1}H NMR, ^{13}C NMR and X-ray crystallography.

Lastly, we have also prepared a novel, 3D Ag carbene coordination polymer that contains layers of Ag_6 cores with two ^{Me}CNC ligands that wrap around on each Ag_6

bowtie core. Nitrate groups bridge each of these Ag_6 cores to each other. The seventh

silver connects the 2D layers of Ag_6 cores, forming a unique, 3D Ag carbene coordination

polymer **74**. Noteworthy, the route in which this Ag carbene coordination polymer was

prepared is also very unusual in which Ag^+ replaces Ni^{2+} in what has been explained by

Pugh and co-workers as "reverse transmetallation".[117] We believe this reversal in normal

reactivity is driven by the precipitation of a highly-stable, highly-insoluble polymeric Ag

structure.

3.5 **General Procedures**

   All manipulations were carried out in an Ar-filled glovebox or by using standard

Schlenk techniques. Anhydrous solvents dimethylsulfoxide (DMSO), $CHCl_3$, CH_3CN,

and CH_3OH were purchased from Aldrich and either used immediately upon opening or

stored in the glovebox over 4Å molecular sieves until use. Nickel acetate $Ni(OAc)_2 \cdot 4H_2O$

was obtained from Aldrich and dried by heating at 100 °C for 12 hours under dynamic

vacuum into a separate P_2O_5 collector. Tetrabutylammonium bromide $[(Bu)_4NBr]$, silver

triflate [AgOTf] and silver nitrate $[AgNO_3]$ were purchased from Aldrich and used

without further purification. The imidazolium salt precursor **26,** (X=Br; R= CH_3) for the

^{Me}CNC ligand was prepared according to the literature method.[93,119] ^1H and ^{13}C NMR

spectra were obtained on a Bruker AMX 250 spectrometer using DMSO (d6) as solvents.

Elemental analyses for carbon, hydrogen and nitrogen content were obtained

commercially at Columbia Analytical Services, Tucson, AZ.

3.5.1 Crystallographic Studies

Crystallographic data were collected on a standard Bruker X8 *APEX* CCD- based X-ray diffractometer using monochromated Mo-K∝ radiation ($\lambda = 0.71073\text{Å}$). Dr Diane Dickie of Kemp group and Dr. Eileen Duesler at the University of New Mexico provided additional data handling and solving. Crystals were mounted on nylon cryo-loops obtained from Hampton Research using Paratone-N oil. The data was collected and processed using Bruker *APEX2* suit of programs and *SADABS* program was used to correct for Lorentz polarization effect and absorption.[113] Structures were solved by direct method and refined by full matrix least-square method on F^2 with *SHELXTL*.[114] Non-hydrogen atoms were refined anisotropically and hydrogen atoms bound to carbon were fixed in calculated positions. Crystallographic data collection and parameters and refinement data are collected in Appendix 2. Thermal ellipsoids were prepared using Diamond (version 3.2e) software.[115]

3.5.2 Syntheses of Pincer Carbene Nickel and Silver Complexes

[(Me CNC)NiBr]Br **21**

The procedure followed as that reported by Inamoto and co workers[93] using the following quantities of reagents: ligand **26**, (X = Br; R = Me) (3.200 g, 8.0 mmol), Ni(OAc)$_2$ (1.600 g, 8.8 mmol) and Bu$_4$NBr (2.600 g, 8.0 mmol). The yield of **21** as orange solid was 2.500

g (63%). ^{1}H NMR data matched the previously reported values. The compound **21** was used without further purification.

[([Me]*CNC)$_3$Ni$_2$][Br]$_4$* **69**

Ligand precursor **26,** (X= Br; R= CH$_3$) (1.600 g, 4.0 mmol) was dissolved in DMSO (20 mL) and then treated with Ni(OAc)$_2$ (0.470 g, 2.66 mmol) and Bu$_4$NBr (1.300 g, 4.0 mmol). The mixture was stirred at room temperature for 12 h and then heated to 130 °C for 1 h. The precipitate was collected by filtration. The solid was washed with CHCl$_3$ (10 mL x 3) and CH$_3$CN (10 mL x 3). The solid was then dried *in vacuo*. The yield of **69** as a yellow solid was 1.000 g (32%) based on the limiting reagent Ni(OAc)$_2$). Mp. >260 °C. ^{1}H NMR (DMSO-*d$_6$*): δ 2.81 (s, N-CH$_3$, 12H), 4.21 (s, N-CH$_3$, 6H), 7.64 (d, $^3J_{\text{H-H}}$ = 1.98 Hz, imidazole H, 4H), 7.83 (d, $^3J_{\text{H-H}}$ = 1.95 Hz, imidazole H, 2H), 8.05 (d, $^3J_{\text{H-H}}$ = 8.14 Hz, Ar-H, 4H), 8.17 (d, $^3J_{\text{H-H}}$ = 1.95 Hz, imidazole H, 2H), 8.29 (t, $^3J_{\text{H-H}}$ = 8.14 Hz, Ar-H, 1H), 8.49 (d, $^3J_{\text{H-H}}$ = 1.98 Hz, imidazole H, 4H), 8.62 (t, $^3J_{\text{H-H}}$ = 8.14 Hz, Ar-H, 2H), 8.84 (d, $^3J_{\text{H-H}}$ = 8.14 Hz, Ar-H, 2H). Anal. Calcd for C$_{39}$H$_{39}$Br$_4$N$_{15}$Ni$_2$: C, 40.56; H, 3.40; N, 18.19. Found: C, 38.23; H, 3.71; N, 16.69. No improved elemental analysis could be obtained even after several attempts.

[([Me]*CNC)$_3$Ni$_2$][OTf]$_4$* **70**

To a suspension of **69** (0.800 g, 0.69 mmol) in 20 mL of methanol held at room temperature was added AgOTf (0.712 g, 2.76 mmol). The mixture was left to stir for 2 h.

113

Silver bromide (AgBr) was removed by filtration through a medium frit. The filtrate was left to crystallize at -32 °C. The yield of the analytically-pure, X-ray quality orange crystals of **70** was 0.790 g (80%). Mp. 199-202 °C. ^{1}H NMR (DMSO-d$_6$): δ 2.77 (s, N-CH$_3$, 12H), 4.22 (s, N-CH$_3$, 6H), 7.51 (d, $^3J_{H-H}$ = 1.99 Hz, imidazole H, 4H), 7.77 (d, $^3J_{H-H}$ = 1.94 Hz, imidazole H, 2H), 7.95 (d, $^3J_{H-H}$ = 8.14 Hz, 4H), 8.14 (d, $^3J_{H-H}$ = 1.94 Hz, imidazole H, 2H), 8.27 (t, $^3J_{H-H}$ = 8.12 Hz, Ar-H, 1H), 8.36 (d, $^3J_{H-H}$ = 1.99 Hz, imidazole H, 4H), 8.58 (t, $^3J_{H-H}$ = 8.14 Hz, Ar-H, 2H), 8.80 (d, $^3J_{H-H}$ = 8.12 Hz, Ar-H, 2H). ^{13}C NMR (DMSO-d$_6$): 35.9 (N-CH$_3$), 108.5 (C$_{para}$), 114.4 (C$_{imidazole}$), 117.9 (C$_{imidazole}$), 120.8 (q, C-F on triflate, $^1J_{C-F}$ = 321 Hz), 122.1 (C$_{para}$), 126.8 (C$_{imidazole}$), 127.4 (C$_{imidazole}$), 144.7 (C$_{meta}$), 148.3 (C$_{meta}$), 148.7 (C$_{ortho}$), 150.3 (C$_{ortho}$), 165.6 (C-Ni, carbene trans to N), 166.9 (C-Ni, trans-carbenes). Anal. Calcd for C$_{43}$H$_{39}$F$_{12}$N$_{15}$Ni$_2$O$_{12}$S$_4$: C, 36.08; H, 2.75; N, 14.68. Found: C, 36.20; H, 3.10; N, 14.49.

[(^{Me}CNC)$_3$Ni$_2$][NO$_3$]$_{3.75}$ Cl$_{0.25}$ **72**

[^{Me}CNC-Ni-Br]Br **21** (0.050 g, 0.11 mmol) was dissolved in of methanol (25 mL) was followed by addition of AgOTf (0.033 g, 0.22 mmol). The mixture was left to stir for 12 hours at room temperature. AgBr was removed by filtration through a medium frit. The solvent was removed *in vacuo*, to obtain a yellow solid. The solid was recrystallized in methanol by slow evaporation. Analytically-pure, X-ray quality orange crystals of **72** were obtained. The yield of the solid was 0.080 g (67%). ^{1}H NMR (DMSO-d$_6$): δ 2.79 (s, N-CH$_3$, 12H), 4.22 (s, N-CH$_3$, 6H), 7.53 (d, $^3J_{H-H}$ = 1.99 Hz, imidazole H, 4H), 7.80 (d, $^3J_{H-H}$ = 1.94 Hz, imidazole H, 2H), 7.98 (d, $^3J_{H-H}$ = 8.14 Hz,

Ar-H, 4H), 8.17 (d, $^3J_{\text{H-H}}$ = 1.94 Hz, imidazole H, 2H), 8.27 (t, $^3J_{\text{H-H}}$ = 8.12 Hz, Ar-H,

1H), 8.37 (d, $^3J_{\text{H-H}}$ = 1.99 Hz, imidazole H, 4H), 8.61 (t, $^3J_{\text{H-H}}$ = 8.14 Hz, Ar-H, 2H), 8.85

(d, $^3J_{\text{H-H}}$ = 8.12 Hz, Ar-H, 2H). ^{13}C NMR (DMSO-d$_6$): 35.8 (N-CH$_3$), 108.0 (C$_{\text{para}}$), 114.3

(C$_{\text{imidazole}}$), 118.0 (C$_{\text{imidazole}}$), 121.0 (C$_{\text{para}}$), 126.9 (C$_{\text{imidazole}}$), 127.7 (C$_{\text{imidazole}}$), 144.1 (C$_{\text{meta}}$),

148.9 (C$_{\text{meta}}$), 149.0 (C$_{\text{ortho}}$), 150.9 (C$_{\text{ortho}}$), 165.7 (C-Ni, carbene trans to N), 167.1 (C-Ni,

trans-carbenes).

$[(^{Me}CNC)_2(Ag_7)N_{17}O_{21.5}]$ **(74)**
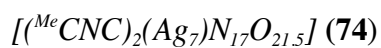
To a suspension of **21** (0.100 g, 0.22 mmol) in methanol (40 mL) held at room

temperature was added AgNO$_3$ (0.260 g, 1.50 mmol). The mixture was left to stir for 2

hours at room temperature. Unreacted AgNO$_3$ was removed by filtration through a

medium frit. The filtrate was left to crystallize at room temperature. The yield of the

analytically-pure, X-ray quality colorless crystals of **74** was 0.069 g (19%). Data for X-

ray analysis have been discussed in Section 3.3. Anal. Calcd for C$_{26}$H$_{27}$Ag$_7$N$_{17}$O$_{21.5}$ **(74)**;

C, 18.62; H, 1.62; N, 14.20. Found: C, 19.32; H, 1.73; N, 14.11. Calcd for C$_{13}$H$_{13}$AgN$_6$O$_3$

(73); C, 38.16; H, 3.20; N, 20.54. Found: C, 37.62; H, 3.22; N, 19.89. IR: 1400 cm^{-1},

814 cm^{-1}, 723 cm^{-1} (NO$_3$$^{-1}$ stretches).

4   CONCLUDING REMARKS

Although the main focus of this project was to accomplish the proposed catalytic cycle in Scheme 1.7 for epoxidation of alkenes using molecular O_2, converting M-X to M-H was more difficult than anticipated. Although few M-H could be prepared, reaction of these M-H and O_2, did not result into transferring of oxygen atom to alkene or organic substrate. However, several new interesting compounds were made. In fact, a major lesson learned in this research work is that conversion of pincer metal halides to pincer metal hydride is synthetically challenging and not straightforward. In addition to that, it is not very clear as to why a certain hydride source would work in conversion of certain M-X while others will not. However in this project, K-Selectride seemed to have worked better than other hydride sources used. In cases where we had charged pincer carbene M-Br such as [^{R}CNC-Pd-Br]Br (R= Me, **19** and R = nBu, **20** and {^{Me}CNC-Ni-Br]Br (**21**)), use of hydride sources in attempts to resulted into decomposition of the complexes. In cases where we had big R group such as in complexes **54** and **55**, the use of hydride sources resulted into no reaction.

Although an alternative route to M-H as shown in generalized Scheme 2.9 did not result into production of M-H at the end; it did allow the isolation of novel ^{Me}CCC-Pd-ONO$_2$ (**61**) that was fully characterized by ^{1}H NMR, X-ray diffraction and IR. In addition, proposed alternative route to M-OOH (Scheme 2.12) also allowed isolation of novel compound ^{Me}CCC-Pd-OTf (**64**) that was also fully characterized. More interestingly, this compound reacted with 30% H_2O_2/H_2O to yield ^{Me}CCC-Pd-OH (**65**) that is also a new compound.

116

Very interestingly, and quite unexpected, charged [^{Me}CNC-Ni-Br]Br reacted differently with AgNO$_3$. When two equivalents of AgNO$_3$ were added, a dication Ni species (**72**) was obtained. A dication Ni species (**69**) very similar to this was also obtained unexpectedly in attempt to [^{Me}CNC-Ni-Br]Br following the reported preparation by Inamoto. Fortunately, the dication Ni complex could deliberately be made following the procedure outlined in Scheme 3.2. Spectroscopically-pure dication Ni species (**70**) was obtained by anion exchange (Scheme 3.3). **70** is also a novel compound and was fully characterized by ^{1}H NMR, ^{13}C NMR and X-ray diffraction.

It is also worth mentioning that a very interesting 3D Ag-carbene coordination polymer (**74**) was isolated when [^{Me}CNC-Ni-Br]Br (**21**) was reacted with 7 equivalents of AgNO$_3$. Normally, Ag-carbene complexes are commonly used to transfer carbene to other metals, but in this case a reverse transmetallation first reported by Pugh and co-workers has been observed, in which Ag$^+$ displaced Ni^{2+} leading to the formation of unique Ag-carbene polymer.

Although we did not achieve our target of preparing pincer carbene M-H's, then insert O$_2$ in M-H bond with an ultimate goal of transferring one of the oxygen to organic substrates, and more specifically alkenes (Scheme 1.9), we have gained significant fundamental knowledge on reactivity pincer carbene metal complexes. While the pincer carbene metal complexes we worked with may not be the optimal catalysts for activation of molecular oxygen, in order to transfer one of the oxygen atom to organic substrates, there is much that is yet to be uncovered about the general reactivity these metal complexes.

5 APPENDIX 1

Compound	61/62	64	65
Empirical Formula	$C_{16}H_{17}Cl_{10\cdot62}N_{4\cdot38}O_{1.12}Pd$	$C_{21}H_{25}F_3N_4O_4PdS$	$C_{17}H_{19}F_3N_4O_{4.50}PdS$
Fw	417.15	592.91	546.82
Cryst Size (mm)	0.10x0.10x0.05	0.14x0.09x0.03	0.16x0.09x0.06
Cryst Syst	Orthorhombic	Triclinic	Triclinic
Space Group	Aba2	P-1	P-1
a, Å	20.2952(7)	8.0788(5)	10.8618(3)
b, Å	12.9264(4)	12.2819(8)	14.4187(4)
c, Å	11.9964(4)	26.0165(17)	14.9206(4)
α, deg	90	76.470(3)	103.741(2)
β, deg	90	84.430(3)	99.665(2)
γ, deg	90	73.597(3)	107.833(
Volume ($Å^3$)	3147.18(18)	2406.3(3)	2086.38(10)
Z	8	4	4
Calc density, g/cm^3	1.761	1.637	1.741
$\mu(MoK_\alpha)$, mm^{-1}	1.297	0.916	1.050
Indep reflecns	3927	9779	7155
T, K	203(2)	228(2)	228(2)
R1, wR2 (all data)	0.0482, 0.0780	0.0861, 0.1436	0.0899, 0.1664
R1, wR2 [I>2σ(I)]	0.0391, 0.0780	0.0455, 0.1087	0.052, 0.1329
GOF on F^2	1.117	1.010	1.074

6   APPENDIX 2

Compound	**67**	**71**
Empirical Formula	$C_{39}H_{39}Br_4F_2N_{15}O_2Pd_2S_2$	$C_{45}H_{47}N_{15}Ni_2O_{14}S_4$
Fw	1384.41	1495.64
Cryst Size (mm)	0.23x0.05x0.05	0.62 x 0.34 x 0.18
Cryst Syst	Monoclinic	Orthorhombic
Space Group	P2(1)/n	Pnma
a, Å	6.9619(3)	13.281(6)
b, Å	11.0620(5)	29.2053(12)
c, Å	23.8015(11)	14.9425(7)
α, deg	90	90
β, deg	94.318	90
γ, deg	90	90
Volume ($Å^3$)	1827.81(14)	5795.9(4)
Z	2	4
Calc density, g/cm^3	2.515	1.714
$\mu(MoK_\alpha)$, mm^{-1}	0.7844	0.910
Indep reflecns	3595	90269 [0.0306]
T, K	188(2)	183(2)
R1, wR2 (all data)	0.0481, 0.1179	0.0737, 0.1734
R1, wR2 [$I>2\sigma(I)$]	0.0368, 0.1039	0.0620, 0.1622
GOF on F^2	1.170	1.032

7   APPENDIX 3

Compound	**72**	**74**
Empirical Formula	$C_{40.50}H_{42}Cl_{1.50}N_{17 \cdot 50}Ni_2O_9$	$C_{26}H_{27}Ag_7N_{17}O_{21.50}$
Fw	1088.51	1676.74
Cryst Size (mm)	0.28x0.07x0.02	0.22x0.12x0.11
Cryst Syst	Orthorhombic	Monoclinic
Space Group	Pnma	P2(1)/n
a, Å	13.0745 (5)	19.964(2)
b, Å	28.439(1)	10.3259(11)
c, Å	13.4313(4)	20.967(2)
α, deg	90	90
β, deg	90	102.277(2)
γ, deg	90	90
Volume (Å^3)	4994.3(3)	4223.4(8)
Z	4	4
Calc density, g/cm^3	1.448	2.637
$\mu(MoK_\alpha)$, mm^{-1}	0.904	3.283
Indep reflecns	5216	7434[0.0262]
T, K	188	110(20)
R1, wR2 (all data)	0.1737, 0.3786	0.0377, 0.0998
R1, wR2 [I>2σ(I)]	0.1095, 0.3233	0.0399, 0.1013
GOF on F^2	1.355	1.141

8 REFERENCES

(1)   White, J. M. *Opportunities for Catalysis in the 21st Century*, Department of Energy, 2002.

(2)   Weskamp, T.; Schattenmann, W. C.; Spiegler, M.; Hermann, W. A. *Angew. Chem. Int. Ed. Engl.* **1998**, *37*, 2490.

(3)   Huang, J.; Stevens, E. D.; Nolan, S. P.; Petersen, J. L. *J. Am. Chem. Soc.* **1999**, *121*, 2674.

(4)   Voges, M. H.; Romming, C.; Tilset, M. *Organometallics* **1999**, *18*, 529.

(5)   Arndtsen, B. A.; Bergman, R. G.; Mobley, T. A.; Peterson, T. H. *Acc. Chem. Res.* **1995**, *28*, 154.

(6)   Smith, M. B. *Organic Synthesis*; McGraw-Hill, Inc., 1994.

(7)   Lewis, S. N. In *Oxidation*; Augustine, R. L., Ed.; Marcel Dekker: New York, 1969, p 213.

(8)   Carlson, G. J.; Skinner, J. R.; Smith, C. W.; Wilcoxen, C. H., Jr.; Epoxidation Using Hydrogen Peroxide and an Acid Salt of a Heavy Metal Peracid. US Patent 2833787, 1958.

(9)   Payne, G. B.; Williams, P. H. *J. Org. Chem.* **1959**, *24*, 54.

(10)   Raciszewski, Z. *J. Am. Chem. Soc.* **1960**, *82*, 1267.

(11)   Kaman, A. J.; Epoxides. GB Patent 837464, 1960.

(12)   Clerici, M. G.; Bellussi, G.; Romano, U. *J. Catal.* **1991**, *129*, 159.

(13)   Prasetyoko, D.; Fansuri, H.; Ramli, Z.; Endud, S.; Nur, H. *Catal. Lett.* **2009**, *128*, 177.

(14)   http://www.dow.com/propyleneoxide/news/20080609a.htm.

(15)   Midland, M. M.; Kazubski, A. *J. Org. Chem.* **1982**, *47*, 2495.

(16)   Soai, K.; Oyamada, H.; Yamanoi, T. *J. Chem. Soc., Chem. Comm.* **1984**, 413.

(17)   Vigneron, J. P.; Bloy, V. *Tetrahedron Lett.* **1979**, 2683.

(18)   Sheldon, R. A. *J. Mol. Cat.* **1980**, *7*, 107.

(19)   Ben-Daniel, R.; Khenkin, A. M.; Neumann, R. *Chem. Eur. J.* **2000**, *6*, 3722.

(20)   Loudon, G. M. *Organic Chemistry*; The Benjamin/Cummings Publishing

        Company, Inc.: Redwoody City, Carlifonia, 1995.

(21)   Morrison, J. D.; Mosher, H. S. *Asymmetric Organic Reaction*; American

        Chemical Society: Washington DC, 1976.

(22)   Sheldon, R. A.; Kochi, J. K. *Metal Catalyzed Oxidation of Organic Compounds*;

        Academic Press: New York, 1981.

(23)   Hock, H.; Lang, B. *Chem. Ber.* **1944**, *77*.

(24)   Stahl, S. S. *Angew. Chem. Int. Ed.* **2004**, *43*, 3400.

(25)   Stadig, W. *Chem. Process.* **1992**, *58*, 26.

(26)   Matar, S.; Hatch, L. F. *Chemistry of Petrochemical Processes*; 2nd ed.; Gulf

        Professional Publishing, 2001.

(27)   Linic, S.; Barteau, M. A. *J. Catal.* **2003**, *214*, 200.

(28)   Linic, S.; Jankowiak, J.; Barteau, M. A. *J. Catal.* **2004**, *224*, 489.

(29)   Linic, S.; Barteau, M. A. *J. Am. Chem. Soc* **2003**, *125*, 4034.

(30)   Linic, S.; Barteau, M. A. *J. Am. Chem. Soc.* **2004**, *126*, 8086.

(31)   Berndt, T.; Boege, O.; Heintzenberg, J.; Claus, P. *Ind. Engr. Chem. Res.* **2003**, *42*,

        2870.

(32)   Van Santen, R. A.; De Groot, C. P. M. *J. Catal.* **1986**, *98*, 530.

(33)   Van Santen, R. A.; Kuipers, H. P. C. E. *Adv. Catal.* **1987**, *35*, 265.

(34)   Kemp, R. A.; Ethylene Oxide Catalysts and Process. US Patent 5663385, 1997.

(35)   Osugi, J.; Kubota, H. *Rev. Phys. Chem.* **1964**, *34*, 19.

(36)   Beran, S. J., P.; Wichterlova, B.; Zahrandik, R. *React. Kinet. Catal. Lett.* **1976**, *5*, 131.

(37)   Nakatsuji, H.; Hu, Z. M.; Nakai, H. *Int. J. Quant. Chem* **1997**, *65*, 839.

(38)   Monnier, J. R. *Appl. Catal. A. Gen.* **2001**, *221*, 2001.

(39)   Choudhary, T. V.; Goodman, D. W. *Top. Catal.* **2002**, *21*, 25.

(40)   Chusuei, C. C.; Lai, X.; Lou, K.; Goodman, D. W. *Top. Catal.* **2001**, *14*, 71.

(41)   Sinha, A. K.; Seelan, S.; Tsubota, S.; Haruta, M. *Top. Cat.* **2004**, *29*, 95.

(42)   Oyama, S. T.; Murata, K.; Haruta, M. *Shokubai* **2004**, *46*, 13.

(43)   Uphade, B. S.; Okumura, M.; Yamada, N.; Tsubota, S.; Haruta, M. *Stud. Surf. Sci. Catal.* **2000**, *130A*, 833.

(44)   Hayashi, T.; Tanaka, K.; Haruta, M. *J. Catal.* **1998**, *178*, 566.

(45)   Kalvachev, Y. A.; Hayashi, T.; Tsubota, S.; Haruta, M. *Stud. Surf. Sci. Catal.* **1997**, *110*, 965.

(46)   Liu, Y.; Murata, K.; Inaba, M. *Chem. Commun.* **2004**, 582.

(47)   Hayashi, T.; Han, L.-B.; Tsubota, S.; Haruta, M. *Ind. Engr. Chem. Res.* **1995**, *34*, 2298.

(48)   Yamanaka, L.; Nakagaki, K.; Otsuka, K. *Appl. Catal. A: Gen.* **1998**, *171*, 309.

(49)   Yamanaka, L.; Nakagaki, K.; Otsuka, K. *Chem. Commun.* **1995**, 1185.

(50)   Bielawski, C. W.; Grubbs, R. H. *Angew. Chem., Int. Ed. Engl.* **2000**, *39*.

(51)   Wick, D. D.; Goldberg, K. I. *J. Am. Chem. Soc.* **1999**, *121*, 11900.

(52)   Johansson, R.; Wendt, O. F. *Organometallics* **2007**, *26*, 2426.

(53)   Kaesz, H. D.; Saillant, R. B. *Chem. Rev.* **1972**, *72*, 231.

(54)   Chatt, J. *Science* **1968**, *160*, 723.

(55)   Bayston, J. H.; Winfield, M. E. *J. Catal.* **1964**, *3*, 123.

(56)   Endicott, J. F.; Wong, C. L.; Inoue, T.; Natarajan, P. *Inorg. Chem.* **1979**, *18*, 450.

(57)   Look, J. L. Dissertation, University of Washington, 2004.

(58)   Keith, J. M.; Muller, R. P.; Kemp, R. A.; Goldberg, K. I.; Goddard, W. A.;

        Oxgaard, J. *Inorg. Chem.* **2006**, *45*, 9631.

(59)   Denney, M. C.; Smythe, N. A.; Cetto, K. L.; Kemp, R. A.; Goldberg, K. I. *J. Am.*

        Chem. Soc. **2006**, *128*, 2508.

(60)   Smith, K.; Poli, R.; Harvey, J. N. *Chem.-Eur. J.* **2003**, *7*, 1679.

(61)   Harvey, J.; Aschi, M.; Schwarz, H.; Koch, W. *Theor. Chem. Acc.* **1998**, *99*, 95.

(62)   Poli, R.; Harvey, J. N. *Coord. Chem. Rev* **2003**, *32*, 1.

(63)   Pugh, D.; Danopoulos, A. A. *Coord. Chem. Rev.* **2007**, *251*, 610.

(64)   Maron, L.; Bourissou, D. *Organometallics* **2009**, *28*, 3686.

(65)   Arduengo, A. J.; Harlow, R. L.; Kline, M. *J. Am. Chem. Soc.* **1991**, *113*, 361.

(66)   Herrmann, W. A. *Angew. Chem. Int. Ed.* **2002**, *41*, 1290.

(67)   Crabtree, R. H. *Pure Appl. Chem.* **2003**, *75*, 435.

(68)   Albretch, M.; van Koten, G. *Angew. Chem. Int. Ed.* **2001**, *40*, 3750.

(69)   Lappert, M. F. *J. Organomet. Chem.* **1988**, *358*, 185.

(70)   Collman, J. P.; Hegedus, L.; Norton, J. R.; Finke, R. G. *Principles and*

        Application of Organotransition Chemistry; 2nd ed. Mill Valley, Carlifornia,

        1987.

(71)   Grundemann, S.; Albrecht, M.; Loch, J. A.; Faller, J. W.; Crabtree, R. H. *Organometallics* **2001**, *20*, 5485.

(72)   Hahn, F. E.; Jahnke, M. C.; Pape, T. *Organometallics* **2007**, *26*, 150.

(73)   Nakai, H.; Hu, X. L.; Zakharov, L. N.; Rheingold, A. L.; Meyer, K. *Inorg. Chem.* **2004**, *43*, 855.

(74)   Hu, X. L.; Tang, Y. J.; Gantzel, P.; Meyer, K. *Organometallics* **2003**, *22*, 612.

(75)   Miqueu, K.; Despagnet-Ayoub, E.; Dyer, P. W.; Bourissou, D.; Bertrand, G. *Chem.-Eur. J.* **2003**, *9*, 5858.

(76)   Peris, E.; Loch, J. A.; Mata, J.; Crabtree, R. H. *Chem. Commun.* **2001**, 201.

(77)   Gu, L.; Zhang, Y. *J. Am. Chem. Soc.* **2010**, *132*, 914.

(78)   Ueno, A. S., T.; Todo, N.; Kotera, Y.; Takasak, S. *Chem. Lett.* **1980**, 1067.

(79)   Yin, X. L.; Moss, J. R. *Coord. Chem. Rev.* **1999**, *181*, 27.

(80)   Leitner, W. *Coord. Chem. Rev.* **1996**, *153*, 257.

(81)   Maidan, R.; Willner, I. *J. Am. Chem. Soc.* **1986**, *108*, 8100.

(82)   Lin, W.; Frei, H. *J. Am. Chem. Soc.* **2005**, *127*, 1610.

(83)   Simon-Manso, E.; Kubiak, C. P. *Organometallics* **2005**, *24*, 96.

(84)   Hegg, E. L. *Acc. Chem. Res.* **2004**, *37*, 775.

(85)   Christman, A. A.; Randall, E. L. *J. Biol. Chem* **1933**, 595.

(86)   Peris, E.; Crabtree, R. H. *Coord. Chem. Rev.* **2004**, *248*, 2239.

(87)   Albrecht, M.; Crabtree, R. H.; Mata, J.; Peris, E. *Chem. Comm.* **2002**, 32.

(88)   Singleton, J. T. *Tetrahedron* **2003**, *59*, 1837.

(89)   Arduengo, A. J. *J. Am. Chem. Soc.* **1999**, *32*, 918.

(90)   Ohff, M.; Ohff, A.; vander Boom, M. E.; Milstein, D. *J. Am. Chem. Soc.* **1997**, *119*, 11687.

(91)   Beletskaya, I. P.; Cheprakov, A. V. *Chem. Rev.* **2000**, *100*, 3009.

(92)   Herrmann, W. A.; Brossmer, C.; Ofele, K.; Reisinger, C. P.; Priermeier, T.; Beller, M.; Fischer, H. *Angew. Chem. Int. Ed.* **1995**, *34*, 1844.

(93)   Inamoto, K.; Kuroda, J.; Hiroya, K.; Noda, Y.; Watanabe, M.; Sakamoto, T. *Organometallics* **2006**, *25*, 3095.

(94)   Miyaura, N.; Suzuki, A. *Chem. Rev.* **1995**, *95*, 2457.

(95)   Loch, J. A.; Albrecht, M.; Peris, E.; Mata, J.; Faller, J. W.; Crabtree, R. H. *Organometallics* **2002**, *21*, 700.

(96)   Lin, I. J. B.; Wang, H. M. J. *Organometallics* **1998**, *17*, 972.

(97)   Nielson, J. D.; Kingsley, J.; Cavell, B. W.; Allan, H. W. *Inorg. Chim. Acta* **2002**, *327*, 116.

(98)   Pytkowicz, J.; Roland, S.; Mangeney, P. *Tetrahedron* **2001**, *12*, 2087.

(99)   Simons, R. S.; Custer, P. D.; Tessier, C. A.; Youngs, W. J. *Organometallics* **2003**, *22*, 1979.

(100)   Crabtree, R. H. *J. Organomet. Chem.* **2005**, *690*, 5451.

(101)   Ku, R.; Huang, J.; Cho, J.; Kiang, F.; Lee, G.; Peng, S.; Liu, S. *Organometallics* **1999**, *18*, 2145.

(102)   Raynal, M.; Pattacini, R.; Cazin, C. S. J.; Vallee, C.; Bourbigou, H. O.; Braunstein, P. *Organometallics* **2009**, *28*, 4028.

(103)   Fairlamb, I. J. S. *Annu. Rep. Prog. Chem., Sect. B*, 2003.

(104)   Tsuji, J. *Palladium Reagent and Catalysis*; Wiley: New York, 1995.

(105) Henry, P. M. *Palladium Catalyzed Oxidation of Hydrocarbons*; Kluwer: Boston, 1980.

(106) Danopoulos, A. A.; Pugh, D.; Smth, H.; Sabmannshausen, J. *Chem. Eur. J.* **2009**, *15*, 5491.

(107) Danopoulos, A. A.; Pugh, D.; Wright, J. A. *Angew. Chem. Int. Ed.* **2008**, *47*, 9765.

(108) Hahn, F. E.; Jahnke, M. C.; Gomez-Benitez, V.; Morales-Morales, D.; Pape, T. *Organometallics* **2005**, *24*, 6458.

(109) Shin, J. A. *J. Ind. Eng. Chem* **2001**, *7*, 337.

(110) Hwang, S. W.; Park, Y. W. *J. Ind. Eng. Chem* **2000**, *6*, 125.

(111) Gretz, E.; Oliver, T. F.; Sen, A. *J. Am. Chem. Soc.* **2003**, *109*, 8109.

(112) Brian, B. J.; Duesler, E. N.; Goldberg, K. I.; Kemp, R. A. *Inorg. Chem.* **2009**, *48*, 5081.

(113) Bruker APEX2; Bruker AXS, Inc.: Madison, WI, 2007.

(114) Sheldrick, G. M. *Acta Crystallogr., Sect. A: Found. Crystallogr.* **2008**, *A64*, 112.

(115) Diamond; Crystal impact GbR: Bonn, Germany, 1999.

(116) Danopoulos, A. A.; Tulloch, A. A. D.; Winston, S.; Eastham, G.; Hursthouse, M. B. *Dalton Trans.* **2003**, 1009.

(117) Pugh, D.; Boyle, A.; Danopoulos, A. A. *Dalton Trans.* **2008**, 1087.

(118) Boro, B. J.; Golberg, K. I.; Kemp, R. A.; Duesler, E. N. *Inorg. Chem.* **2009**, *48*, 5081.

(119) Chen, J. C. C.; Lin, I. J. B. *J. Chem. Soc., Dalton Trans.* **2000**, 839.

(120) Caballero, A.; Diez-Barra, E.; LJalon, F. A.; Merino, S.; Tefjada, J. *J. Organomet. Chem.* **2001**, *617-618*, 395.

(121) Caballero, A.; Diez-Barra, E.; Jalon, F. A.; Merino, S.; Rodriguez, A. M.; Tejeda, J. *J. Organanomet. Chem.* **2001**, *627*, 263.

(122) Poyatos, M.; Uriz, P.; Mata, J. A.; Claver, C.; Fernandez, E.; Peris, E. *Organometallics* **2003**, *22*, 440.

(123) Poyatos, M.; Mas-Marza, E.; Mata, J. A.; Sanau, M.; Peris, E. *Eur. J. Inorg. Chem.* **2003**, 1215.

(124) Mrutu, A.; Goldberg, K. I.; Kemp, R. A. *Inorg. Chim. Acta* **2010**, *in press*.

(125) Brown, D. H.; Nealon, G. L.; Simpson, P. V.; Skelton, B. W.; Wang, Z. S. *Organometallics* **2009**, *28*, 1965.

(126) Yu, J.; Choi, S.; Dickson, R. M. *Angew. Chem. Int. Ed.* **2009**, *48*, 318.

(127) Bakr, O. M.; Amendola, V.; Aikens, C. M.; Wenselers, W.; Li, R.; Negro, L. D.; Schatz, G. C.; Stellaci, F. *Angew. Chem. Int. Ed.* **2009**, *48*, 5921.

(128) Nishida, N.; Yao, H.; Kimura, K. *Langmuir* **2008**, *24*, 2759.

(129) Wu, Z.; Lanni, E.; Chen, W.; Bier, M. E.; Ly, D.; Jin, R. *J. Am. Chem. Soc.* **2009**, *131*, 16672.

(130) Xiang, H.; Wei, S. H.; Gong, X. *J. Am. Chem. Soc.* **2010**, *132*, 7355.

(131) Melaiye, A.; Youngs, W. J. *Expert Opinion on Therapeutic Patents* **2005**, *15*, 125.

(132) Garrison, J. C.; Simons, R. S.; Tessier, C. A.; Youngs, W. J. *J. Organomet. Chem.* **2003**, *673*, 1.

(133) Liu, B.; Chen, W.; Jin, S. *Organometallics* **2007**, *26*, 3660.

(134) Catalano, V. J.; Malwitz, M. A.; Etogo, A. O. *Inorg. Chem.* **2004**, *43*, 5714.

(135)   Rit, A.; Pape, T.; Hahn, F. E. *J. Am. Chem. Soc.* **2010**, *132*, 4572.

(136)   Furuya, F. R.; Gladfelter, W. L. *Chemm. Comm.* **1986**, 129.